ELECTROENCEPHALOGRAPHIC STUDIES OF HUMAN PAIN PERCEPTION

SHAO SHIYUN

(B. Eng. & M. Eng., Xi'an Jiaotong University)

A THESIS SUBMITTED

FOR THE DEGREE OF DOCTOR OF PHILOSOPHY

DEPARTMENT OF MECHANICAL ENGINEERING

NATIONAL UNIVERSITY OF SINGAPORE

2010

Acknowledgments

First and foremost, I am deeply grateful to my main supervisor, Prof. Li Xiaoping, for his constant and patient guidance, inspiration, support during my PhD study. I have appreciated his vast expanse of knowledge and ground-breaking visions on research problems during the past four years. I would also like to express my sincere gratitude to my cosupervisors, Assoc. Prof. Ong Chong Jin and Prof. Einar P. V. Wilder-Smith. Assoc. Prof. Ong guided me on signal processing methods in this research. His selfless sharing of knowledge and experiences on signal processing was invaluable. Prof. Wilder-Smith as an expert in neurology gave me many insightful advices and generously lent me his laboratory equipment, which were critical to this interdisciplinary research.

I would particularly like to thank Dr. Shen Kaiquan for his many precious advices and help on my work. Sincere appreciation is also expressed to the other colleagues in Neurosensors Laboratories, Dr. Fan Jie, Dr. Ning Ning, Mr. Ng Wu Chun, Mr. Khoa Wei Long Geoffrey, Mr. Yu Ke, Mr. Wu Ji, Mr. Rohit Tyagi, Mr. Bui Ha Duc, Miss Wang Yue and Miss Ye Yan, who have more or less helped me.

My deepest thanks go to my parents and my brother, for their unconditional love and support. Sincere thanks to all my friends, especially Miss Fan Dongmei and Miss Zhang Jing, for standing by me through all the good and bad times.

Last but not least, I would like to thank the National University of Singapore for providing me with the research scholarship to support the PhD study.

Table of Contents

Acknowledgments **i**

Summary **vi**

List of Tables **viii**

List of Figures **x**

List of Symbols **xi**

Acronyms **xvi**

1 Introduction **1**

1.1 Motivation 1

1.2 Objectives 7

1.3 Thesis Outline 8

2 Background and Literature Review **9**

2.1 EEG 9

2.1.1 Neurophysiologic Basis of EEG 9

2.1.2 Technological Basis of EEG Recording 11

2.2 EEG Artifact Removal Methods 13

2.2.1 Linear Filtering 14

2.2.2 Regression 14

2.2.3 Blind Source Separation based Methods 16

2.3 EEG Analysis Methods 19

2.3.1 Frequency Analysis 19

2.3.2 EEG Source Localization 21
2.4 Pain Basics 22
2.4.1 Pain: Definition 22
2.4.2 Pain: Classification 24
2.4.3 Experimental Pain Induction Methods 25
2.5 Neurophysiology of Nociceptive Pain Perception 28
2.5.1 Nociceptive Pain Pathways 28
2.5.2 The Pain Matrix 30
2.6 Pain Perception: Measurements 33
2.6.1 Subjective Self-Report Methods 34
2.6.2 Behavioral Measures 37
2.6.3 Performance Measures 37
2.6.4 Physiological Measures 38
2.7 Past Work on EEG Measures of Pain Perception 40
2.7.1 Pain-induced Spontaneous EEG Changes 40
2.7.2 Pain-related Brain Evoked Potentials 44
2.8 Review of Gender Differences in Pain-Related Brain Activations 46

3 General Experimental Methods 49
3.1 EEG Recording 49
3.1.1 Subjects 49
3.1.2 Experimental Setup and Recording Parameters 50
3.2 Experimental Method for Pain Induction 51

4 A Weighted Support-Vector-Machine Approach With Error Correction for Automatic EEG Artifact Removal 54
4.1 Introduction 54
4.2 Overview of the Proposed Automatic Artifact Removal Method 57
4.2.1 ICA Module 58
4.2.2 Feature Extractor 59
4.2.3 IC Classifier 61
4.2.4 EEG Reconstruction 62
4.3 The Proposed Weighted Support-Vector-Machine Approach With Error Correction 63

4.3.1 The Modified Probabilistic Support Vector Machines 64
4.3.2 Error Correction 68
4.4 Numerical Experiments 70
4.4.1 Data Preparation 70
4.4.2 Parameter Selection 71
4.4.3 Quantitative Evaluation 72
4.4.4 Qualitative Evaluation 75
4.5 Results 76
4.5.1 Validation of the Unique Properties of the Learning Problem . . 76
4.5.2 Quantitative Comparison 78
4.5.3 Review of Reconstructed EEG 81
4.6 Discussion 82
4.7 The MATLAB-based Graphical User Interface for Automatic Artifact Removal 85
4.8 Concluding Remarks 86

5 Heartbeat Evoked Potential: A Promising Objective Measure of Pain Perception 87

5.1 Introduction 87
5.2 Methods 90
5.2.1 Subjects 90
5.2.2 Experimental Procedure 90
5.2.3 Data Acquisition 92
5.2.4 Data Preprocessing 92
5.2.5 Data Analysis 93
5.3 Results 94
5.3.1 Subjective Pain Ratings 94
5.3.2 HEP Morphology and Topography 96
5.3.3 HEP and Cold Pain Perception 96
5.3.4 The Potential Effect of Heart Rate Change on the HEP 101
5.4 Discussion 104
5.4.1 The HEP 104
5.4.2 HEP Suppression During Cold Pain Perception 105

5.5 Concluding Remarks 107

6 EEG Source Localization of Gender Differences in Pain Perception 109

6.1 Introduction 109

6.2 Materials and Methods 112

6.2.1 Subjects 112

6.2.2 Experimental Procedure 112

6.2.3 Data Acquisition 113

6.2.4 Data Preprocessing 113

6.2.5 sLORETA Source Localization Analysis 114

6.2.6 Statistical Analysis 115

6.3 Results 116

6.3.1 Subjective Pain Ratings 116

6.3.2 Source Localization Analysis 117

6.4 Discussion 121

6.4.1 Gender Difference in Subjective Pain Ratings 123

6.4.2 Gender Difference in Cerebral Responses to Tonic Cold Pain . 124

6.5 Concluding Remarks 126

7 Conclusions and Recommendations 127

7.1 Conclusions 127

7.2 Recommendations for Future Work 129

Author's Publications 131

Bibliography 133

Summary

Pain, if insufficiently controlled or inadequately treated, may interfere with a person's normal functioning and impair quality of life. The major barriers to effective pain control/treatment include lack of accurate pain assessment and lack of understanding on gender differences in pain perception. This thesis is concerned with exploring objective measures of human pain perception and investigating gender differences in pain perception by using electroencephalogram (EEG) methods. It also includes a novel method to tackle the challenging problem of automatic EEG artifact removal.

EEG signals are susceptible to various artifacts, which are usually much stronger than brain activities and greatly interfere with EEG interpretation. It is necessary to remove the various artifacts from EEG before further analysis. In this thesis, a novel independent component analysis based automatic artifact removal method is proposed. The proposed method has two unique features: a) it uses weighted support vector machine to handle the inherent unbalanced nature of component classification, and b) it accommodates the structural information typically found in component classification. Numerical experiments on real-life EEG show that the proposed method outperforms several benchmark methods and is well suited for EEG artifact removal by achieving a better tradeoff be-

tween removing artifacts and preserving inherent brain activities.

The second contribution of the thesis is in proposing a promising objective measure of acute pain perception — the electrocardiographic R-peak locked brain evoked potential (BEP), i.e. the heartbeat evoked potential (HEP). The HEP is found to be significantly suppressed by tonic cold pain over the right hemisphere which is contralateral to the cold pain stimulation. There is a significant correlation between the suppression of HEP and the level of pain experience. In comparison to the existing pain-related BEPs triggered by external stimuli, the HEP is obtained by using internal triggers, and thus may reveal patterns of endogenous brain activity associated with pain perception.

The last part of the thesis presents a pioneering study of gender differences in pain perception by EEG source localization method. Source analysis shows that during tonic cold pain perception females have significant stronger activations than males in the anterior cingulate cortex (ACC), which likely encodes the affective component of pain. This suggests that females concentrate more on the affective dimension of pain than males, which is consistent with the existing evidence. This study highlights the necessity of incorporating gender differences in clinical pain management. It also demonstrates the possibility of measuring gender differences in pain perception by EEG source localization, which is more portable and affordable than other functional imaging techniques.

The present work adds to the literature on pain assessment and management with a promising objective measure of pain and the evidence on gender difference in central processing of pain. Further works on the causal link between the proposed measure and pain perception are needed to establish the proposed measure as a pain indicator.

List of Tables

4.1 Performance comparison between the proposed method and five benchmark methods 78

4.2 Qualitative evaluation of the proposed artifact removal method 81

5.1 Mean HEP magnitudes in Cold Pain 1, no-pain control, no-task control and Cold Pain 2 conditions 99

5.2 The averaged heart rates and the mean HEP magnitudes over right-central scalp sector in the Cold Pain 1, no-pain control control and no-task control conditions 103

6.1 Brain regions showing significant electrical activity differences between the cold pain and no-pain control conditions 118

6.2 Brodmann areas included in each of the ROIs 120

List of Figures

2.1 Classification of pain by etiology 26

2.2 Schematic of nociceptive pain perception 29

2.3 Schematic of brain areas commonly reported to be involved in pain perception 31

2.4 Common unidimensional pain rating scales 36

3.1 The Neuroscan NuAmps system used for EEG recording. 50

3.2 The electrode arrangement according to the extended 10-20 system. . . 51

3.3 The apparatus used for experimental cold pain induction 52

3.4 The pain rating scales used in the present study 53

4.1 Block diagram of the proposed automatic artifact removal system 57

4.2 A typical example of EEG artifact removal 77

4.3 The MATLAB-based GUI for automatic EEG artifact removal 85

5.1 Subjective pain ratings 95

5.2 The across-subject grand averages of HEP in the Cold Pain 1, no-pain control and no-task control conditions. 97

5.3 Scalp power maps of the across-subject grand averages of HEP 98

5.4 Percent decrease in HEP magnitude in Cold Pain 1 100

5.5 Correlation between the standardized mean HEP magnitude over the midline sector and the normalized mean pain ratings 102

6.1 Pain intensity and unpleasantness ratings for the male and female subjects during the cold pain condition 117

6.2 Brain regions showing significant between-condition (cold pain vs. no-pain control) differences for male subjects. 119

6.3 Brain regions showing significant between-condition (cold pain vs. no-pain control) differences for female subjects. 120

6.4 Scatterplots of the average power changes in pain-related brain activities and the corresponding average pain ratings over the 1-3, 4-7 and 8-10 min of the cold pain condition in all subjects 122

6.5 Gender differences in cerebral response to cold pain localized by sLORETA 123

List of Symbols

A^T	transposed matrix (or vector)
$\lvert\cdot\rvert$	absolute value or modulus
$\lVert\cdot\rVert$	Euclidean norm
$\cup$	the mathematical union operator
α_k^{ij}	the Lagrangian multiplier for the k^{th} sample in the support vector machine (SVM) classifying class i and class j
γ^{ij}	the kernel parameter for the Gaussian kernel used in the SVM classifying class i and class j
$\sigma_{\mathbf{s}_i}$	the standard deviation of $\mathbf{s}_i$
ω	discrete-frequency index
ω_i	the i^{th} class
$\phi^{ij}(\cdot)$	the mapping function in the SVM classifying class i and class j
ξ_k^{ij}	the slack variable for the k^{th} sample in the SVM classifying class i and class j
$\mathbf{A}$	the mixing matrix

$\mathbf{a}_i$	the scalp distribution coefficients of the i^{th} source
A^{ij}, B^{ij}	the sigmoid parameter used in Platt's probabilistic outputs for class i and class j
argmax	the argument of the maximum
b^{ij}	the bias term of the hyperplane in the SVM classifying class i and class j
c	the total number of classes in a classification problem
C_i^{ij}	the regularization parameter for class i in the SVM classifying class i and class j
$\mathbf{c}_p^i$	a series of propagation coefficients for ocular artifact propagating from the reference channel to the i^{th} EEG channel
$C_{\mathbf{x}_1\mathbf{x}_2}$	the coherence between two time series $\mathbf{x}_1$ and $\mathbf{x}_2$
D	dataset
D_{ij}	the subset of D formed by samples from class i and class j
d	the total number of features
$d(\cdot)$	the decision function of a classifier classifying each sample independently
$\mathbf{d}(\cdot)$	the decision function of a classifier classifying the whole dataset collectively
E	mathematical expectation operator
$\mathbf{F}(\mathbf{S})$	the matrix containing the set of feature vectors extracted from $\mathbf{S}$
$\mathbf{f}$	a feature vector or sample

$\mathbf{f}_i$	the i^{th} feature vector or sample
$\mathbf{f}(\mathbf{s}_i)$	the feature vector extracted from $\mathbf{s}_i$
$f_j(\mathbf{s}_i)$	the j^{th} feature extracted from $\mathbf{s}_i$
$g^{ij}(\mathbf{f})$	the output of the SVM classifying class i and class j given a test sample $\mathbf{f}$
$G_{\mathbf{xx}}(\omega)$	auto-spectral density of $\mathbf{x}$ at frequency ω
$G_{\mathbf{x}_1\mathbf{x}_2}(\omega)$	cross-spectral density between $\mathbf{x}_2$ and $\mathbf{x}_2$ at frequency ω
$\mathscr{H}$	Hilbert space
H_I	the prior uncertainty about the class of an unseen input
H_O	the posterior uncertainty about the class of an unseen input
I	the identity matrix
$K^{ij}(\cdot)$	the kernel function used in the SVM classifying class i and class j
l	the length of each EEG epoch subject to independent component analysis (ICA)
l_{ω_i}	the lower bound for the number of source signals corresponding to class ω_i
m	the number of source signals recovered from a given EEG epoch
m_{ω_i}	the number of source signals corresponding to class ω_i
N	the total number of training samples
N_i	the number of training samples from the i^{th} class
n	the number of EEG channels

n_{ij}	the number of samples with a true label of class i being classified as class j
$\mathbf{p}(\mathbf{f})$	the vector of multi-class posterior probabilities given $\mathbf{f}$
$p_i(\mathbf{f})$	the multi-class posterior probability of belonging to class i given $\mathbf{f}$, i.e. $P(\omega_i\|\mathbf{f})$
$p^{ij}(\mathbf{f})$	the pairwise probability of belonging to class i knowing that $\mathbf{f}$ is from class i or class j
$\mathbf{Q}$	the matrix denoting a set of code vectors representing the class labels of the source signals from an EEG epoch
$\mathbf{q}_i$	the code vector outputted from the error correction algorithm representing the predicted label of the i^{th} sample
q_{ij}	the j^{th} element of the code vector $\mathbf{q}_i$, being either 0 or 1
$\mathbb{R}$	set of real numbers
$\mathbb{R}^d$	d-dimensional real Euclidean space
$\mathbb{R}^{n\times m}$	set of $n \times m$ real matrix
$\mathbf{S}$	the matrix denoting the source signals resulting from the EEG epoch $\mathbf{X}$ by ICA
$\tilde{\mathbf{S}}$	the matrix obtained from $\mathbf{S}$ by zeroing all artifactual source signals
$\mathbf{s}^0_{ecg}$	the time series of reference source signal accounting for cardiac artifacts
$\mathbf{s}^0_{eog}$	the time series of reference source signal accounting for ocular artifacts

$\mathbf{s}_i$	the time series of the i^{th} source signal
t	discrete time instant
u_{ω_i}	the upper bound for the number of source signals corresponding to class ω_i
var	mathematical variance operator
$\mathbf{w}^{ij}$	the parameters determining the optimal separating hyperplane in the SVM classifying class i and class j
$\mathbf{X}$	the matrix denoting an EEG epoch
$\tilde{\mathbf{X}}$	the matrix denoting the reconstructed artifact-free EEG epoch
$\mathbf{x}_i$	the EEG time series recorded from the i^{th} channel
$\mathbf{x}_i^0$	the i^{th} EEG time series in the reference dataset
y_i	the class label of the i^{th} sample

Acronyms

ACC	anterior cingulate cortex
ANOVA	analysis of variance
BA	Brodmann's area
BAcc	balanced accuracy
BEP	brain evoked potential
BSS	blind source separation
CFA	cardiac field artifact
CPS	cortical power spectrum
CPT	cold pressor test
DLPFC	dorsolateral prefrontal cortex
EA	the agreement expected by chance
ECG	electrocardiogram
EEG	electroencephalogram
EMG	electromyogram
EOG	electrooculogram
FastICA	a Newton-iteration based fast fixed-point ICA algorithm

fMRI	functional magnetic resonance imaging
GMM	Gaussian Mixture Models
HEP	heartbeat evoked potential
IASP	International Association for the Study of Pain
IC	independent component
ICA	independent component analysis
KL	Kullback-Leibler
KNN	K-Nearest Neighbors
LDF	Linear Discriminant Function
M1	primary motor cortex
MAPS	Multidimensional Affect and Pain Survey
MEG	magnetoencephalography
MNI	Montreal Neurological Institute
MPFC	medial prefrontal cortex
NRS	numerical rating scale
NUS-IRB	Institutional Review Broad of National University of Singapore
OA	overall agreement
PAF	peak alpha frequency
PAG	periaqueductal grey matter
PCA	principal component analysis
PCC	posterior cingulate cortex
PDF	probability density function

PET	positron emission tomography
PF	prefrontal cortex
PMA	premotor cortex
PWC_PSVM	the probabilistic multi-class SVM by pairwise coupling
RCI	the amount of uncertainty about the class of an input reduced by a classifier
ROI	region of interest
S1	primary somatosensory cortex
S2	secondary somatosensory cortex
SA	specific agreement
SEM	standard error of the mean
SEP	somatosensory evoked potential
sLORETA	standardized low resolution brain electromagnetic tomography
SMA	supplementary motor area
SNR	signal-to-noise ratio
SVM	Support Vector Machine
VAS	visual analogue scale
VRS	verbal rating scale

Chapter 1

Introduction

This thesis is mainly concerned with the measurement of human pain perception and gender differences in pain perception using electroencephalogram (EEG) methods. It also includes a novel automatic artifact removal method to handle various artifacts in EEG. This chapter presents the motivation and objectives of this research, followed by the outline of the thesis. The detailed background and literature review will be given in Chapter 2.

1.1 Motivation

Pain, defined by the International Association for the Study of Pain (IASP) as "an unpleasant sensory and emotional experience associated with actual or potential tissue damage, or described in terms of such damage" (Bonica, 1979), if insufficiently con-

trolled or inadequately treated, can seriously interfere with a person's normal functioning and impair quality of life.

Although the medical community has always been making great efforts to improve pain management, pain due to inadequate treatment or insufficient control is still widespread across all demographic groups (Deandrea *et al.*, 2008; Perron & Schonwetter, 2001; Rupp & Delaney, 2004). According to the estimation of the World Health Organization in 2008, about 80% of the world population suffers from moderate to severe pain due to either inadequate or even no access to treatment.

A major cause of the failures to adequate pain control/treatment is lack of accurate pain assessment methods (Rissacher *et al.*, 2007; Rupp & Delaney, 2004). In fact, the important roles of pain assessment are embodied in a variety of medical scenarios, such as to aid diagnosis, to determine the most effective analgesic drug and appropriate dose to control pain, to evaluate the relative effectiveness of different analgesic therapies (Noble *et al.*, 2005; Wall & Melzack, 1999). Clinically, pain assessment is mostly achieved via subjective self-report methods through the verbal or nonverbal communication between patients and health workers (e.g. multidimensional questionnaires using standardized descriptors and pain intensity rating scales) and/or behavioral analysis by the health workers (Noble *et al.*, 2005). However, the self-report methods suffer from the problems of being subject to the patients and not applicable in the situations when the patients are uncooperative and/or cannot formulate and express their pain experience (e.g. young children, patients with dementia, patients under anesthesia) (Caraceni *et al.*, 2002). Although behavioral analysis by health workers does not rely on the patients'

ability to do self-report, it has the disadvantage of being subject to the health workers doing the measurement. Besides, it is still subject to the patients who may exhibit few pain behaviors to avoid increasing pain.

In the past decades, various objective pain assessment methods have been proposed. The objective methods do not rely on the patients' ability to do self-report and are not subject to bias by the patients or by the health workers doing the measurement. Generally, the existing objective methods mainly include: a) performance measures derived from performance on laboratory tasks, and b) physiological variables, such as EEG measures, electromyogram (EMG) measures, autonomic indices (Johnson, 2008; Li *et al.*, 2008; Raj, 2000). Among the many objective measures, EEG measures show the greatest potential and advantages in its usefulness for pain assessment. First, pain is perceived in the brain. Many studies have shown that pain perception involves multiple brain areas by using functional imaging techniques like functional magnetic resonance imaging (fMRI), magnetoencephalography (MEG) and positron emission tomography (PET) (Adler *et al.*, 1997; Alkire *et al.*, 2004; Melzack & Casey, 1968; Mollet & Harrison, 2006; Ohara *et al.*, 2005; Talbot *et al.*, 1991; Torquati *et al.*, 2005). EEG, as a measurement of the brain's electrical activity, should be able to directly reflect pain experience felt. On the other hand, EEG has the practical advantages of being relatively inexpensive and easy to be administered as compared to the other functional imaging techniques like fMRI and PET (Jensen *et al.*, 2008; Rissacher *et al.*, 2007). Although EEG has relatively low spatial resolution, recent advances in EEG source localization techniques have enabled neuroimaging of underlying electrical sources within the brain using EEG

(Jones *et al.*, 2003b).

So far, there have been two lines of research on EEG measures of pain perception, one focusing on pain induced spontaneous EEG changes (Backonja *et al.*, 1991; Baltas *et al.*, 2002; Chang *et al.*, 2001a; Chen *et al.*, 1989b; Chen & Rappelsberger, 1994; Chen *et al.*, 1998; Croft *et al.*, 2002; Ferracuti *et al.*, 1994; Huber *et al.*, 2006; Nir *et al.*, 2010; Rissacher *et al.*, 2007; Veerasarn & Stohler, 1992) and the other into pain-related brain evoked potentials (BEPs) (Becker *et al.*, 1993, 2000; Bromm & Scharein, 1982; Carmon *et al.*, 1978; Chen, 1993; Chen *et al.*, 1979; Dowman *et al.*, 2008; Fernandes de Lima *et al.*, 1982; Granovsky *et al.*, 2008; Xu *et al.*, 1995; Zaslansky *et al.*, 1996a). However, there are still no EEG measures being widely accepted as pain indicators. The search for reliable EEG measures of pain perception is still ongoing. Spontaneous EEG activities represent endogenous patterns of neural activity and thus are able to capture endogenous brain activity associated with pain perception. However, the correlation between the spontaneous EEG measures and pain perception remains equivocal. It is difficult to determine whether the spontaneous EEG changes are related to pain perception itself or associated with general emotional/cognitive processes, and to what extent the EEG changes are related to pain perception itself (Chen, 1993; Croft *et al.*, 2002). The measurement of BEPs in response to external painful stimulation provides a valuable tool for investigating pain processing in the brain. In comparison to spontaneous EEG measures, BEPs in response to painful stimulation measure electrical activity time-locked to the painful stimuli and can provide the time course of brain response associated with the processing of the painful stimuli. However, likewise, none of the BEPs have been

concluded to be pain-specific. It is also questionable whether the BEPs in response to external stimulation can reveal endogenous brain activity associated with pain perception which is hardly time-locked to any external event (Chen, 1993). Moreover, it is debatable whether the phasic experimental pain induced by brief stimulation in BEP studies can faithfully simulate clinical pain (Nir *et al.*, 2010). Therefore, it is necessary to explore other prospective EEG measures which can represent pain perception better than the existing measures.

In addition to accurate pain assessment methods, a clear understanding on gender difference in pain perception also plays an important role in clinical pain management (Rupp & Delaney, 2004). More specifically, clinical pain management can greatly benefit from the incorporation of potential gender differences, for example, by establishing gender-specific diagnosis and treatment for pain disorders. In fact, a clear understanding of potential gender difference in pain perception can also sheds light on the development of reliable pain assessment methods.

In recent years, there has been increasing evidence on gender differences in pain perception. Not only higher prevalence of clinical pain but also higher sensitivity to various kinds of experimental pain modalities in terms of higher pain threshold, higher pain tolerance and/or higher pain ratings has been reported in females than in males (Fillingim *et al.*, 2009; Keogh, 2006). By using functional imaging techniques like fMRI and PET, a number of recent studies have revealed gender differences in hemodynamic responses to pain in several brain regions, which include the prefrontal cortex, cingulate cortex, thalamus, insula, amygdala as well as somatosensory cortices (Berman *et al.*, 2006;

Derbyshire *et al.*, 2002; Henderson *et al.*, 2008; Moulton *et al.*, 2006; Naliboff *et al.*, 2003; Paulson *et al.*, 1998; Straube *et al.*, 2009). However, the findings vary a bit across the studies (Fillingim *et al.*, 2009). Thus, further investigation on gender differences in pain-related brain activity is still desired. Moveover, very little evidence exists on the efficacy of incorporating such gender differences in clinical pain management, due to huge cost associated with functional imaging facilities like fMRI and PET. Therefore, it is of great interest and practical importance to investigate whether the gender differences in pain perception can also be measured by using EEG source localization method which is much more portable and affordable than fMRI and PET.

Last but not least, like all EEG studies, the present study also faces the challenging problem of EEG artifact removal. It is well known that EEG tends to be contaminated by various kinds of physiological artifacts, such as electrocardiogram (ECG) artifacts due to heart beat, electrooculogram (EOG) artifacts resulting from eye blinks or eye movements and EMG artifacts originating from muscle movements. These artifacts usually have much higher amplitudes (i.e. the magnitudes of voltage changes) than brain activities and seriously interfere with further interpretation of EEG. It is necessary to develop effective methods to remove the various artifacts from EEG before further investigation on reliable objective measures of pain perception and gender differences in pain perception using EEG.

1.2 Objectives

This thesis was mainly concerned with the measurement of human pain perception and gender differences in pain perception by using EEG methods. More specifically, the aims of the research were:

(1) to develop a novel artifact removal method for handling various artifacts in EEG;

(2) to propose a reliable EEG measure of human pain perception;

(3) to investigate gender differences in pain perception by EEG source localization.

This research is significant in that it serves as an essential step towards the development of an EEG-based pain measurement system. This work also provides evidence for the incorporation of gender differences and the establishment of gender-specific pain control/treatment strategies in clinical pain management. Besides, it also contributes to the whole EEG research community by developing an effective method to tackle the challenging problem of EEG artifact removal.

Due to the difficulty of involving patients with clinical pain, the present work is limited to healthy volunteers with pain induced by experimental pain models. It should be acknowledged that differences exist between experimental pain models and clinical pain. However, the relevance of experimental pain to clinical pain is well accepted (Geisser *et al.*, 2007). The findings from the present work can provide valuable insight, though not entirely applicable, to clinical pain. Though important, the validation of the findings on clinical pain is beyond the scope of this thesis.

1.3 Thesis Outline

This thesis is organized as follows:

Chapter 2 serves as both a reference and a guide for the researchers in this field, and defines the scientific context in which the problem to be addressed falls. It provides relevant background information on EEG and pain perception, as well as a detailed review of the past related work on EEG artifact removal, EEG measures of human pain perception and gender differences in pain perception.

Chapter 3 describes the general experimental methods used for data collection and pain induction.

Chapter 4 presents a novel automatic EEG artifact removal method, as well as the numerical experiments done to quantitatively and qualitatively evaluate the performance of the proposed artifact removal method.

Chapter 5 proposes an objective EEG measure of pain perception—the heartbeat evoked potential (HEP). Plausible explanations for the correlation between HEP and pain perception are discussed.

Chapter 6 presents the study of gender differences in pain perception by using EEG source localization method.

Chapter 7 summaries the contributions of this thesis and outlines directions for future research.

Chapter 2

Background and Literature Review

This chapter serves as both a reference and a guide that researchers in this field need. It provides background information on EEG and pain perception and gives a detailed review on the past efforts on EEG artifact removal, past related work on the measurement of pain perception using EEG and the existing evidence on gender differences in pain perception from functional imaging studies.

2.1 EEG

2.1.1 Neurophysiologic Basis of EEG

The EEG, first discovered by Hans Berger (1929), is a recording of the brain's electrical activity from electrodes placed on the surface of the scalp. The scalp EEG represents

the difference between two different electrodes in electrical potentials, which mainly result from extracellular ionic currents produced by postsynaptic potentials of pyramidal neurons in the cortical gray matter (Niedermeyer & Lopes da Silva, 1999; Olejniczak, 2006). The scalp EEG is a temporal and spatial summation of synchronous activations of a number of neurons. According to Olejniczak (2006), the synchronous activity of approximately 108 neurons in a cortical area of at least 6 cm^2 is required to generate measurable EEG.

The EEG can be typically described in terms of two types of activity: rhythmic activity and transients.

Spontaneous EEG Activity

The ongoing activity of spontaneous EEG, which reflects synchronous oscillatory processes involving many neurons, is rhythmic (Binnie *et al.*, 2002). According to Kubicki et al. (1979), the rhythmic activity can usually be further divided into the following 6 frequency bands: delta ($<$ 4 Hz), theta (4-7 Hz), alpha (8-12 Hz), beta1 (13-18 Hz), beta2(19-21 Hz) and beta3 (22-30 Hz). The delta activity is normally seen in babies or adults in slow wave sleep. The theta activity can normally be observed in young children as well as in older children and adults during drowsiness or arousal. The alpha rhythm is the strongest during relaxation with eyes closed and indicates a relaxed awareness without attention or concentration. The beta rhythm is associated with active thinking, active attention, focusing on the outside world or solving concrete problems. The high beta activity (beta2 and beta3) reflects alertness, agitation and general activation of mind

and body functions, as compared to a state of being alert but not agitated for beta1 activity. In addition to the above 6 rhythmic activities, there is also a faster brain wave — gamma (30-100 Hz). The gamma activity is generally thought to be associated with higher mental activity like perception and consciousness.

Brain Evoked Potential

The evoked activity, usually referred to as the BEP, which represents the brain's response to an internal or external stimulus, is a typical transient EEG phenomenon. The amplitude of BEP tends to be much smaller than the spontaneous activity, and thus time-locked signal averaging is usually performed to increase signal-to-noise ratio (SNR) (Misulis & Fakhoury, 2001).

2.1.2 Technological Basis of EEG Recording

Conventional scalp EEG is obtained by placing a number of electrodes or by wearing EEG cap on the scalp, with the electrode locations specified according to a specific configuration.

Electrode Configuration

A internationally recognized method to configure electrode locations is the international 10-20 system (Jasper, 1958). The standard electrode placement method not only ensures standardized reproducibility of EEG measurement on the same subject at different time

but also enables comparability of EEG measurements on different subjects.

The standard international 10-20 system covers 19 electrodes, with the actual distances between adjacent electrodes being either 10% or 20% of the total front-back or right-left distance of the skull. In recent years, there have been several extensions of the 10-20 system to achieve high-density EEG recordings, such as 10-10 and 10-5 systems which allow more than 300 electrode positions (Jurcak *et al.*, 2007).

Electrode Reference Montages

As mentioned earlier, scalp EEG measures the potential difference between two electrodes. The readings of EEG can be different when different referencing methods are used.

There are four common referencing methods (namely, montages): bipolar montage, unipolar (or referential) montage, average reference montage and Laplacian montage. In bipolar montage, the EEG signal from each channel represents the potential difference between two adjacent electrodes. In referential montage, each EEG channel represents the potential difference between an active electrode and a designated electrically inactive electrode (namely, reference electrode). The positions of the designated reference can be cephalic (e.g. a midline position on the scalp) or non-cephalic (such as neck-chest reference). For the average reference montage, the average of signals from all EEG electrodes is used as the common reference for each EEG channel, while for Laplacian montage, the EEG signal of each channel represents the potential difference between

an electrode and a weighted average of the surrounding electrodes (Nunez & Pilgreen, 1991).

Referential montage is often used in EEG studies as it provides an identical voltage baseline for all electrodes and it is believed to give a better approximation of the waveform shape in a truly reference-free recording (Fisch & Spehlmann, 1999). However, there is no ideal location which is electrically inactive for positioning the reference electrode. The "linked ears" reference (i.e. a physical or mathematical average of the electrodes attached to both earlobes) is often preferred due to its advantages of not capturing brain signals while minimizing non-cephalic artifact contamination like ECG artifact.

2.2 EEG Artifact Removal Methods

EEG recordings are usually contaminated with various kinds of artifacts, originating from either external non-physiological sources (such as power-line noise, electrode impedance changes) or physiological sources from the subject himself/herself, e.g. electrical activity generated by heartbeats (ECG artifacts), eye blinking and movements (EOG artifacts) and muscle movements (EMG artifacts) (Fatourechi *et al.*, 2007; Halder *et al.*, 2007; Jung *et al.*, 2000b). These artifacts typically have much higher amplitudes than true brain electrical signals and thus impose great difficulty in EEG interpretation (Urrestarazu *et al.*, 2004). Therefore, it is necessary to have the artifacts properly handled before further analysis of the EEG data.

Non-physiological artifacts can be easily handled or avoided by proper filtering, shield-

ing, etc. In comparison, physiological artifacts are hardly avoidable and much more challenging to handle. The simplest and commonest method to handle the artifacts is to reject the portions of contaminated EEG data by visual inspection or based on an automatic detection method (such as based on determined criterion threshold on the amplitude, variance or slope) (Croft & Barry, 2000; Fatourechi *et al.*, 2007). However, the rejection method has the problem of causing significant loss of valuable data and is not suitable for online applications (Millan *et al.*, 2002). A more preferable solution to handling the artifacts in EEG is to remove artifacts while keeping the brain activities of interest intact. This section presents a review of artifact removal techniques commonly used in the literature.

2.2.1 Linear Filtering

Linear filtering is often used to remove the artifacts in certain frequency bands in early clinical studies due to its simplicity (Gotman *et al.*, 1973; Zhou & Gotman, 2005). However, the linear filtering method is not applicable when the artifacts and the brain activities of interest lie in the same frequency or their frequency ranges overlap with each other.

2.2.2 Regression

A classical way to handle the artifacts in EEG is regression, which is based on the assumption that the EEG is a linear combination of true EEG activity and the artifact (Croft

& Barry, 2000; Elbert *et al.*, 1985; Gratton *et al.*, 1983). The regression based artifact removal methods can be performed in either time or frequency domain (Woestenburg *et al.*, 1983). The time-domain regression method assumes that the propagation of an artifact to the scalp is volume conducted, frequency independent and without any time delay. In comparison, the frequency-domain regression method considers the medium through which the artifact is conducted to scalp as a linear filter.

The regression based methods can effectively handle the kinds of artifacts which can be well represented by one or several reference signal(s). A typical kind of the artifacts are the EOG artifacts.

Equation (2.1) shows the model for removal of EOG artifact by the time-domain regression method.

$$EEG^{i}_{clean}(t) = EEG^{i}_{raw}(t) - \sum_{k=0}^{M} EOG_{ref}(t-k)\mathbf{c}^{i}_{p}(k), \tag{2.1}$$

where, $EEG^{i}_{raw}(t)$ refers to the raw EEG recording contaminated by EOG artifact from channel i, $EEG^{i}_{clean}(t)$ is the artifact-free EEG signal for channel i, $EOG_{ref}(t)$ represents a reference signal for the EOG artifact from an additional channel, and $\mathbf{c}^{i}_{p}(k),\ k = 0,\ \cdots,\ M$ is a series of propagation coefficients for the EOG artifact propagating from the reference channel to the i^{th} EEG channel estimated by least-squares regression analysis.

It is not difficult to see that, the effectiveness of the regression methods largely relies on the availability and the quality of reference signal(s). The regression methods are not

suitable for the removal of those artifacts without reliable reference signal(s) available, e.g. EMG artifacts (Barlow, 1986). Another problem associated with the regression method is the so-called bidirectional contamination. That is, the reference artifact channel(s) may also contain brain signals and thus the subtraction of artifact activity may inevitably cancel out a portion of relevant brain signals together with the EOG artifact.

2.2.3 Blind Source Separation based Methods

In recent years, there has been increasing interest in using blind source separation (BSS) based methods for the removal of various artifacts from EEG recordings (Castellanos & Makarov, 2006; Fitzgibbon *et al.*, 2007; Ille *et al.*, 2002; Joyce *et al.*, 2004; Jung *et al.*, 1998, 2000a; Lagerlund *et al.*, 1997; Lins *et al.*, 1993a,b; Makeig *et al.*, 1996; Urrestarazu *et al.*, 2004; Vigario *et al.*, 2000; Vigario, 1997; Wallstrom *et al.*, 2004). The BSS methods are based on the assumption that the measured EEG is a linear mixture of independent or uncorrelated source signals, ideally attributed to either brain activities or artifacts (Fatourechi *et al.*, 2007; Fitzgibbon *et al.*, 2007; Halder *et al.*, 2007; Joyce *et al.*, 2004; Jung *et al.*, 2000b; Lagerlund *et al.*, 1997; Wallstrom *et al.*, 2004).

The BSS based EEG artifact removal methods generally involve three steps: 1) decomposition of raw EEG signals into source signals by BSS techniques, 2) identification of source signals accounting for artifacts (namely, artifactual sources) from source signals attributed to brain activities (i.e. non-artifactual sources), and 3) reconstruction of artifact-free EEG signals by either subtracting the contribution of artifactual source signals from raw EEG signals or remixing all the non-artifactual sources. The first two,

i.e. EEG decomposition and artifact identification, are critical steps for the BSS based artifact removal methods.

EEG Decomposition

The BSS techniques most widely used for EEG decomposition mainly include principal component analysis (PCA) (Pearson, 1901) and independent component analysis (ICA) (Bell & Sejnowski, 1995; Comon, 1994; Hyvarinen *et al.*, 2001).

- **PCA**: PCA makes orthogonality assumption on the underlying sources, i.e. assuming that the source signals are uncorrelated (i.e. geometrically orthogonal) with each other (Fitzgibbon *et al.*, 2007; Joyce *et al.*, 2004). PCA has been shown to be effective in separating strong EOG artifacts from brain signals. However, it seems not very effective in the cases when the artifacts and brain signals have similar amplitudes (Fitzgibbon *et al.*, 2007; Joyce *et al.*, 2004). The orthogonality constraint of PCA is believed to be usually unrealistic for real-world sources.

- **ICA**: ICA assumes that the underlying source signals are statistically independent and decomposes multi-channel observations into temporally independent, spatially fixed components. Theoretically, ICA appears to be suitable for separation of artifactual sources from non-artifactual sources, as the multichannel EEG recordings from the scalp can be regarded as a linear mixture of cerebral activities and non-cerebral artifacts which are electrical signals generated by anatomically and physiologically separate processes (Joyce *et al.*, 2004; Jung *et al.*, 1998,

2000b; Vigario, 1997). The effectiveness of ICA in separating artifactual sources from non-artifactual sources has also been demonstrated on real-life EEG data. ICA has been shown to be able to isolate artifactual sources into a minority of (usually one or two) independent components (ICs) for the stereotyped artifacts which have stereotyped scalp projections, such as heartbeat, eye blinking, and muscle tension. It is shown to outperform PCA by preserving and recovering more brain activity (Jung *et al.*, 1998). Nowadays, the ICA-based methods have become the most popular methods used for EEG artifact removal.

Artifact Identification

In conventional BSS-based artifact removal methods (Lagerlund *et al.*, 1997; Urrestarazu *et al.*, 2004; Vigario *et al.*, 2000), artifactual sources are manually identified (usually by visual inspection), which is very time-consuming and unsuitable for online EEG based applications.

Recent years have seen many efforts to automate the artifact identification and removal processes (Delsanto *et al.*, 2003; Joyce *et al.*, 2004; LeVan *et al.*, 2006; Nicolaou & Nasuto, 2004; Shoker *et al.*, 2005). For example, Delsanto et al. (2003) and Joyce et al. (2004) attempted to automate the removal of EOG artifacts from EEG based on characteristic spatial or temporal patterns of ocular artifacts. Further, LeVan *et al.* (2006); Nicolaou & Nasuto (2004); Shoker *et al.* (2005) proposed a hybrid system combining ICA and a machine learning algorithm to simultaneously and automatically remove several types of artifacts (LeVan *et al.*, 2006; Nicolaou & Nasuto, 2004; Shoker *et al.*,

2005), which provides a promising solution to the automatic EEG artifact removal problem.

In general, the BSS-based artifact removal methods show many advantages over the other kind of methods, including that: 1) it provides a possibility to remove artifacts without affecting the EEG signals of interest (Iriarte *et al.*, 2003); 2) it does not rely on the availability of clean reference signal(s) for separating artifacts from EEG (Fatourechi *et al.*, 2007); 3) it is generally applicable to simultaneous removal of various kinds of EEG artifacts; 4) it normally preserves and recovers brain activity better than many other kinds of methods (Jung *et al.*, 1998, 2000b).

2.3 EEG Analysis Methods

This section provides a brief introduction of the EEG analysis methods relevant to the present studies: frequency analysis and EEG source localization.

2.3.1 Frequency Analysis

Frequency analysis includes cortical power spectrum analysis and coherence analysis.

Cortical Power Spectrum Analysis

In EEG research, cortical power spectrum (CPS) analysis is one of the most commonly used techniques for investigating spontaneous EEG activity changes in different cortical regions as a function of physiological and behavioral states. It estimates the auto-power spectrum of EEG signals recorded at different electrode sites by Fast Fourier Transform to quantitatively characterize EEG.

Coherence Analysis

Coherence analysis provides a useful tool to investigate cortico-cortical connectivity, by examining synchronous oscillations between the EEG signals recorded at different electrode sites. Mathematically, coherence is defined as the normalized cross-power spectrum between the EEG signals from two different channels.

Given two EEG time series recorded from two different channels, $\mathbf{x}_1$ and $\mathbf{x}_2$, the magnitude-squared coherence between the two signals is (Baltas *et al.*, 2002):

$$C_{\mathbf{x}_1\mathbf{x}_2}(\omega) = \frac{|G_{\mathbf{x}_1\mathbf{x}_2}(\omega)|^2}{G_{\mathbf{x}_1\mathbf{x}_1}(\omega)G_{\mathbf{x}_2\mathbf{x}_2}(\omega)}, \tag{2.2}$$

where $G_{\mathbf{x}_1\mathbf{x}_2}(\omega)$ is the cross-spectral density of $\mathbf{x}_1$ and $\mathbf{x}_2$ at frequency ω, $G_{\mathbf{x}_1\mathbf{x}_1}(\omega)$ and $G_{\mathbf{x}_2\mathbf{x}_2}(\omega)$ are the power spectral densities of $\mathbf{x}_1$ and $\mathbf{x}_2$ at frequency ω, respectively.

2.3.2 EEG Source Localization

EEG provides a useful tool for exploring brain activity and it has many advantages including being non-invasive, inexpensive and easy to administer, and having high time resolution within a millisecond. However, EEG has a major disadvantage of poor spatial resolution. EEG is measured on the scalp and represents the summated postsynaptic potentials generated by thousands of or millions of active neurons (Michel *et al.*, 2004; Mishra, 2009). Thus, it is unable to directly pinpoint exact neuronal sources in the brain by EEG.

Recent advances in EEG source localization techniques have enabled the localization of the neuronal electrical sources within the brain by solving the so-called EEG inverse problem (Grave de Peralta Menendez *et al.*, 2001; Grech *et al.*, 2008; Khemakhem *et al.*, 2009; Michel *et al.*, 2004; Pascual-Marqui, 1999). Although the EEG inverse problem is essentially an ill-posed problem with infinite number of solutions, it can be solved by introducing sufficient appropriate mathematical, biophysical, statistical, anatomical or functional constraints (Khemakhem *et al.*, 2009; Wendel *et al.*, 2009). Currently, many different EEG source localization methods have been proposed, ranging from single equivalent dipole estimation to three-dimensional (3D) distributed current density estimation (Grech *et al.*, 2008; Koles, 1998; Pascual-Marqui, 2002).

The EEG source localization techniques offer a more portable and affordable tool (as compared to the functional imaging techniques like fMRI and PET) for the investigation of underlying neuronal circuits in cognitive and clinical neuroscience (Michel *et al.*,

2004).

2.4 Pain Basics

2.4.1 Pain: Definition

Pain is one of the most common sensations that every human throughout history has felt in his/her life. However, as a complex mixture of emotions, experience and sensation varying across individuals, pain is very difficult to define and describe.

There are various definitions of pain in the literature.

- The American Academy of Pain Medicine: "Pain is an unpleasant sensation and emotional response to that sensation."
- The web version of the Encyclopedia Britannica: "Pain is a complex experience consisting of a physiological (bodily) response to a noxious stimulus followed by an affective (emotional) response to that event. Pain is a warning mechanism that helps to protect an organism by influencing it to withdraw from harmful stimuli. It is primarily associated with injury or the threat of injury, to bodily tissues."
- Sternbach (1968): "Pain is an abstract concept which refers to l) a personal, private, sensation of hurt; 2) a harmful stimulus which signals current or impending tissue damage; 3) a pattern of responses which operate to protect the organism from harm. These responses can be described in terms which reflect certain con-

cepts, i.e., in neurological, physiological, behavioral, and affective languages."

- Ranney (1996): "...pain is a perception in the same way that vision and hearing are. By this I mean that its significance is determined by the cerebral cortex in the light of other activity there. It involves sensitivity to chemical changes in the tissues and then interpretation that such changes are, or may be harmful. This perception is real, whether or not harm has occurred or is occurring. Cognition is involved in the formulation of this perception. There are emotional consequences, and behavioral responses to the cognitive and emotional aspects of pain."

While there is still no definition of pain universally accepted by the scientific community, the definition of pain given by IASP (Rollman, 1991) that "Pain is an unpleasant sensory and emotional experience associated with actual or potential tissue damage, or described in terms of such damage" (Bonica, 1979) has been officially and the most widely accepted one.

Overall, there are general agreements among different definitions of pain on that:

(1) Pain is a subjective and multidimensional experience which may not be linearly related to the degree of physical damage. Herein, it is necessary to make a clear differentiation between pain and nociception. Nociception refers to "the neural processes of encoding and processing noxious stimuli" (Loeser & Treede, 2008), i.e. the physiological event evoked by a nociceptive stimulus, while pain is the perceptual correlate to the nociceptive stimulus (Zhu & Lu, 2010). Nociception is neither a necessary nor a sufficient condition for pain.

(2) Pain has at least two dimensions—sensory dimension and affective dimension (Tracey & Mantyh, 2007). To be precise, the experience of pain is usually described along two main dimensions: the sensory-discriminative dimension and the affective-motivational dimension (Hofbauer *et al.*, 2001; Treede *et al.*, 1999). The sensory-discriminative dimension of pain is believed to comprise spatial, temporal and intensity properties of the stimulus (such as stimulus localization, intensity discrimination and quality discrimination), while the affective-motivational dimension of pain is believed to be associated with the unpleasantness of the stimulus and the behavioral, autonomic reactions that the stimulus evokes (Fernandez & Turk, 1992; Hofbauer *et al.*, 2001; Melzack & Casey, 1968; Treede *et al.*, 1999). The affective-motivational component of pain is highly influenced by the sensory-discriminative dimension of pain. The affective-motivational dimension of pain can also affect your body in a way that increases the sensory-discrminative component. According to Benedetti (1997), it is necessary to take into consideration both the sensory-discriminative and affective-motivational components of pain in studies on gender differences in pain perception.

2.4.2 Pain: Classification

Pain can be classified into different categories by different classification methods. According to the duration, pain can be divided into acute pain and chronic pain. Both acute and chronic pain have two components: the brief phasic pain and the longer diffuse tonic pain. Acute pain is of sudden onset and lasts for hours to days. The tonic condition of

acute pain disappears once the underlying cause is treated. In contrast, chronic pain has a long duration of months to years, and the tonic condition persists even after healing is completed (Brando & De Luca Vinhas, 2006).

By etiology, pain can be classified into somatogenic pain and psychogenic pain (see Fig. 2.1). Somatogenic pain arises from a perturbation of the body while psychogenic pain arises from a perturbation of the mind (Turk & Okifuji, 2001). Somatogenic pain can be further divided into nociceptive pain and neuropathic pain by physical cause. Nociceptive pain is caused by activation of nociceptors (defined by IASP as "a receptor preferentially sensitive to a noxious stimulus or to a stimulus which would become noxious if prolonged"), while neuropathic pain is initiated or caused by a primary lesion or dysfunction in the nervous system (Bonica, 1979). Nociceptive pain can be classified as somatic pain (caused by the activation of nociceptors in cutaneous or deep musculoskeletal tissues) and visceral pain (originating in the viscera and resulting from infiltration, compression, extension, or stretching of the thoracic, abdominal, or pelvic viscera). Nociceptive pain can also be classified according to the mode of noxious stimulation, such as thermal pain, electrical pain, mechanical pain and chemical pain.

2.4.3 Experimental Pain Induction Methods

There are mainly four methods for experimental pain induction, i.e. mechanical stimulation, thermal stimulation, electrical stimulation and chemical stimulation (Arendt-Nielsen & Lautenbacher, 2004; Wall & Melzack, 1999). These methods induce mechanical pain, thermal (heat/cold) pain, electrical pain and chemical pain, respectively.

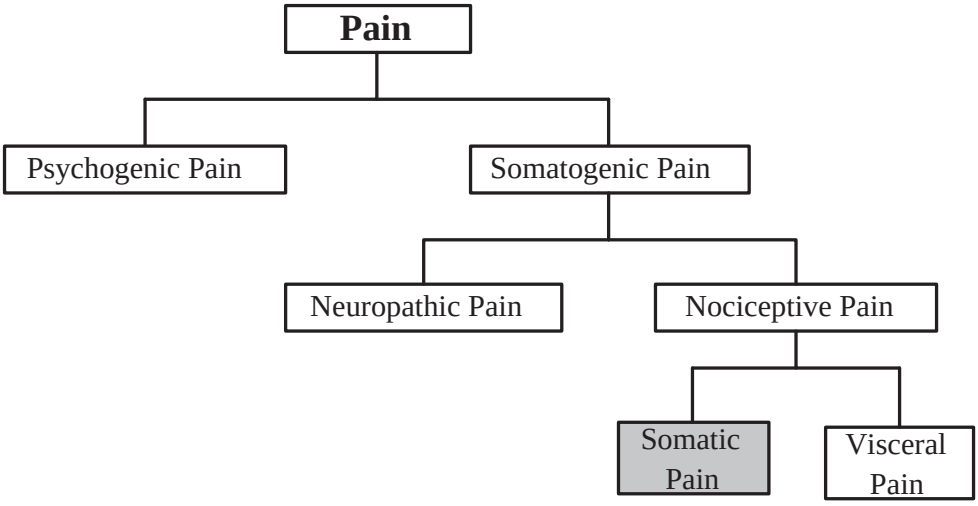

Figure 2.1: Classification of pain by etiology. The type of pain of interest in the present study is shown in the grayed box

Mechanical Stimulation

Mechanical painful stimulation is a most commonly used method for experimental pain induction. It can be achieved by deformation of the skin by the von Frey hairs or needles, distension of the oesophagus and colon, or application of pressure to a finger joint, muscles or/and deep tissue. Pressure pain stimulation is especially valuable for investigating musculoskeletal pain disorders due to the distinctive feature of being able to activate nociceptors located in deep tissues like muscles and tendons in addition to superficial tissues like skin (Arendt-Nielsen & Lautenbacher, 2004). A major disadvantage of this method is that it is difficult to control the stimulus magnitude due to the influence of tissue elasticity and stimulating area.

Thermal Stimulation

Thermal stimulation includes heat stimulation and cold stimulation.

(1) Heat stimulation: It induces heat pain. There are two forms of heat stimulation: contact stimulation by Peltier thermode or heat foil and radiant stimulation by argon, CO_2, Nd-YAG, Copper Vapour lasers etc.

(2) Cold stimulation: It induces cold pain. A classical method for cold stimulation is the cold pressor test (CPT) (Mitchell *et al.*, 2004; von Baeyer *et al.*, 2005; Walsh *et al.*, 1989), which involves hand or foot immersion in cold water. Although the CPT may also induce innocuous pressure sensations associated with limb immersion in the water in addition to cold pain, it is frequently used for pain induction in experimental pain research due to its low costs, simple administration and the similarity of resulting pain to that of certain clinical pain states (Arendt-Nielsen & Lautenbacher, 2004; Dowman *et al.*, 2008; Handwerker & Kobal, 1993). The innocuous pressure sensations associated with limb immersion in the water can be controlled by a proper designed control condition (Dowman *et al.*, 2008).

Electrical Stimulation

Electrical painful stimulation can be applied to skin, teeth, muscle and stomach or intestine, or directly to the neurons. A great advantage of electrical stimulation is that it is easy to control the amplitude and frequency of stimuli. However, this pain-induction method has the problem of concurrently stimulating all nerve fibres beside nociceptive

fibres and spreading current to adjacent structures. Moreover, the electrical method of pain induction tends to result in feelings of fear as well (Wall & Melzack, 1999).

Chemical Stimulation

Chemical pain can be induced by injection of algogenic substances (e.g. hypertonic saline) into the muscles or application of algogenic substances (e.g. capsaicin) into/onto the skin. Chemical stimulation may evoke a condition of central sensitization usually existing in the clinical condition of persistent pain (Wall & Melzack, 1999). However, this kind of pain-induction methods are usually difficult to be adequately standardized or precisely controlled.

2.5 Neurophysiology of Nociceptive Pain Perception

2.5.1 Nociceptive Pain Pathways

The perception of nociceptive pain involves four primary physiological processes: transduction, transmission, perception and modulation, as schematically shown in Fig. 2.2 (Almeida *et al.*, 2004; Brooks & Tracey, 2005; Caterina & Julius, 1999; Cesare & McNaughton, 1997; Price, 2000; Raja *et al.*, 1999; Schnitzler & Ploner, 2000; Willis & Westlund, 1997; Zhu & Lu, 2010).

(1) Transduction: The physical energy from a noxious stimulus (such as a mechani-

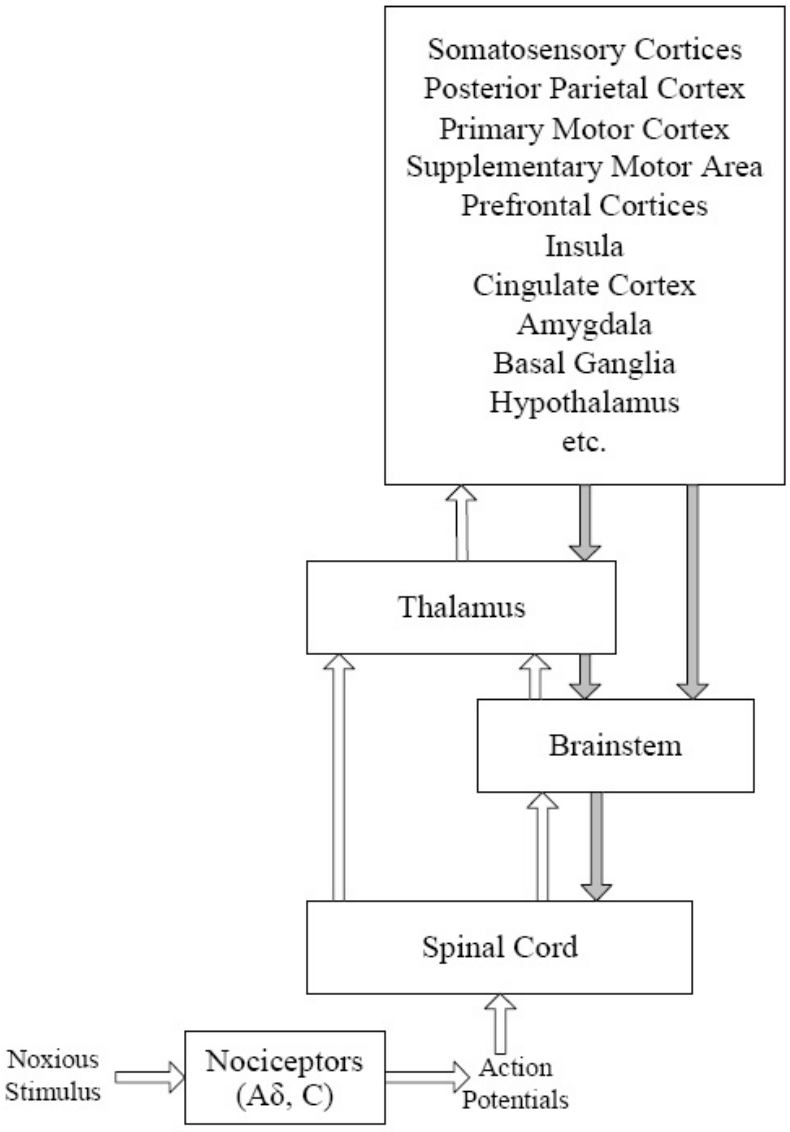

Figure 2.2: Schematic of nociceptive pain perception with ascending and descending pathways indicated by white and grey arrows, respectively. The schematic is modified from Brooks & Tracey (2005).

cal, thermal, electrical or chemical stimulus) is converted into neuronal action potentials by activation of nociceptors (defined by IASP as receptors preferentially sensitive to a noxious or potentially noxious stimulus (Bonica, 1979), including Aδ and C nerve fibres);

(2) Transmission: Transmission refers to the process that the generated action potentials are transmitted to and through the central nervous system (CNS) before the perception of pain. It includes three steps: (a) transmission of the impulses from nociceptors to the spinal cord; (b) processing within the dorsal horn of the spinal cord; and (c) transmission of the impulses from the spinal cord to the brain by several afferent/ascending nociceptive pathways, including the spinothalamic tract, the spinoreticular tract, the spinomesencephalic tract, the spinacervial tract, the spinohypothalamic tract and the second-order dorsal column tract (Almeida *et al.*, 2004).

(3) Perception: Pain sensation is elicited in the brain by the noxious inputs from the peripheral nervous system.

(4) Modulation: Nociceptive transmission from the spinal cord is modulated by descending input from brainstem.

2.5.2 The Pain Matrix

Numerous studies (Adler *et al.*, 1997; Alkire *et al.*, 2004; Melzack & Casey, 1968; Mollet & Harrison, 2006; Ohara *et al.*, 2005; Peyron *et al.*, 2000; Talbot *et al.*, 1991; Torquati *et al.*, 2005) have shown that multiple brain regions are involved in pain perception by using functional imaging techniques like fMRI, MEG and PET. The brain areas commonly reported to be activated or deactivated during pain perception (also referred to as the 'pain matrix') mainly include anterior and posterior cingulate cortex (i.e. ACC and

PCC), insula, prefrontal cortex (PF), primary (S1) and secondary somatosensory (S2) cortices, primary motor cortex (M1), supplementary motor area (SMA), premotor cortex (PMC), thalamus, basal ganglia (BG), cerebellum, amygdala, brainstem structures (mainly periaqueductal grey matter (PAG)) (Apkarian *et al.*, 2005; Jones *et al.*, 2003b; Leone *et al.*, 2006; Ohara *et al.*, 2005; Raij, 2005; Talbot *et al.*, 1991). Fig. 2.3 shows the most commonly reported brain regions involved in pain perception.

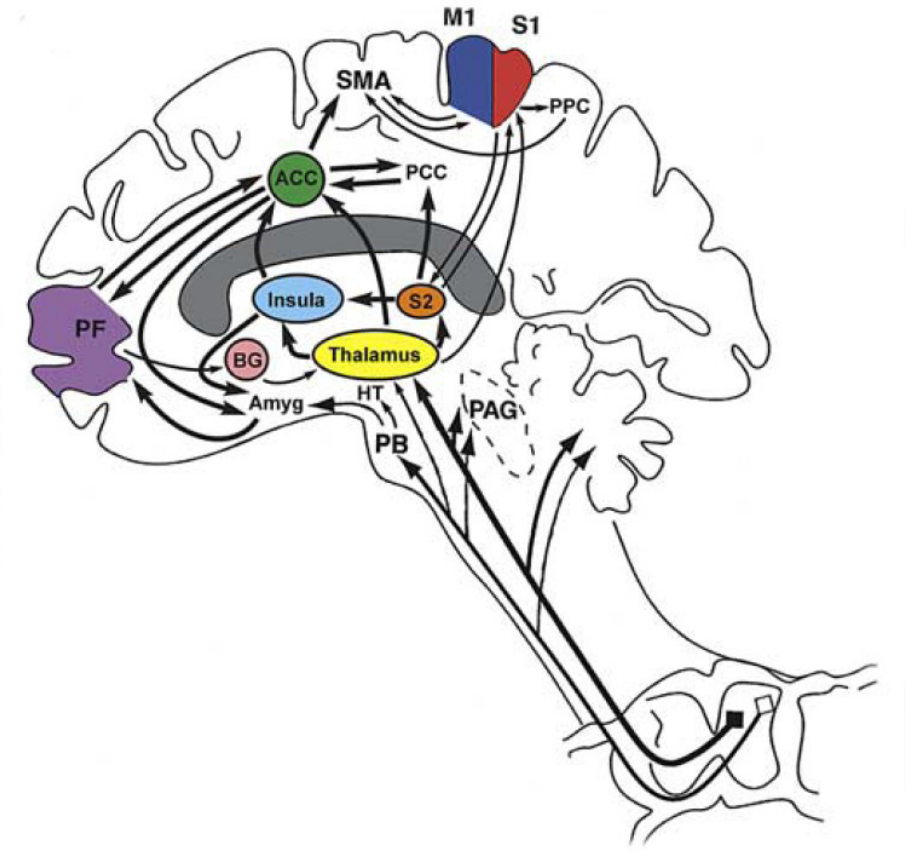

Figure 2.3: Schematic showing brain areas commonly reported to be involved in pain perception, their inter-connectivity and ascending pathways. Herein, ACC: anterior cingulate, AMYG: amygdala, HT: hypothalamus, M1: primary motor cortex, PAG: periaqueductal gray, PB: parabrachial nuclei, PCC: posterior cingulate, PF: prefrontal cortex, PPC: posterior parietal cortex, S1: primary somatosensory cortex, S2: secondary somatosensory cortex, SMA: supplementary motor ares. [Reprinted from Apkarian *et al.* (2005) with permission from Elsevier.]

The pain matrix can be further subdivided into a medial pain system and a lateral pain

system, based on that the projection sites to the cortex are from medial or lateral thalamic structures (Almeida *et al.*, 2004; Brooks & Tracey, 2005; Jones *et al.*, 2003b; Treede *et al.*, 1999). The lateral and medial pain system are believed to represent two groups of brain regions appearing to play different roles in pain perception.

(1) The lateral pain system: The lateral pain system is thought to be involved in the sensory-discriminative dimension of pain processing. It projects through lateral thalamic nuclei to the somatosensory cortices and results in mainly contralateral, discriminative nociception (Ray & Zbik, 2002). It is generally believed that S1 is associated with painful stimulus localization as well as intensity coding while S2 is involved in discrimination of stimulus intensity secondary to general somatosensory integration (Treede *et al.*, 1999).

(2) The medial pain system: The medial pain system is associated with the affective-motivational aspects of pain (Treede *et al.*, 1999). It projects through medial thalamic nuclei to the limbic and paralimbic regions (including the cingulate cortex, amygdala and hippocampus), and continue rostrally to the PF and motor cortices (including the M1, the SMA and the PMC) (Ray & Zbik, 2002). More specifically, the ACC is believed to be involved in encoding the emotional component and with attentional aspects of pain (attentional shifts and sustained attention to the painful area) (Almeida *et al.*, 2004). The amygdala could be associated with fear avoidance, while the hippocampus might create memories of the painful stimulus. The dorsolateral prefrontal cortex (DLPFC) is believed to mediate cognitive dimension of pain processing while the medial prefrontal cortex (MPFC) is prob-

ably associated with affective dimension of pain processing (Peyron *et al.*, 2000; Straube *et al.*, 2009). The motor related areas, including the M1, the SMA and the PMC, might be related to a withdrawal reaction, as a response to a painful stimulus. The medial pain system can be both ipsilateral and contralateral but non-discriminative.

The roles of the thalamus and the insula deserve much attention. The thalamus is of the central importance to the sensation of pain. All the information from the lateral spinothalamic tract is relayed through the thalamus. There is evidence (Green *et al.*, 2009; Smith, 2007) showing that the neural activities directly recorded from the thalamus and the PAG may offer an objective measure of perceived pain intensity. The insula lies between the lateral and medial pain cortex. It receives inputs from both the lateral and medical system, and it is associated with both sensory-discriminative and affective-motivational dimensions of pain (Brooks & Tracey, 2005; Treede *et al.*, 1999).

2.6 Pain Perception: Measurements

Pain measurement is a very important but especially difficult task. The challenges of pain measurement originate not only from the multidimensionality of pain but also from the subjectiveness of pain perception. It is now a known fact that there is usually no correspondence between the degree of pain experience (or pain perception) and the degree of injury (or nociception) (Bunketorp *et al.*, 2006; Fernandez & Turk, 1992; Kall *et al.*, 2008; Loeser & Treede, 2008; Melzack *et al.*, 2001; Price, 2000; Searle & Bennett,

2008).

Driven by the need to establish the efficacy of analgesics and other pain control/treatment methods, many efforts have been devoted to the investigation of accurate pain measurement methods and various methods have been proposed in the past decades. However, there is still no "gold standard" to objectively quantify pain perception. Overall, the existing methods for pain measurement can be broadly divided into several types: subjective self-report methods, behavioral measures, performance measures and physiological measures (Arendt-Nielsen & Lautenbacher, 2004; Chapman *et al.*, 1985; Fishbasin, 2003; Reading, 1983).

This section serves to provide the readers an overview of common pain measurement methods in experimental and clinical applications, with an emphasis on the review of subjective self-report methods. In human pain research, the self-report methods are often considered as benchmark methods against which prospective objective measures of pain perception are compared. The detailed review of EEG measures of pain perception, as the past work closely related to this study, will be given in the next section.

2.6.1 Subjective Self-Report Methods

Subjective self-report methods are the most commonly used methods for pain measurement in both experimental and clinical applications. This kind of methods are useful for those subjects or patients who are able to verbally or non-verbally report their pain experience. The self-report methods are usually achieved by rating of pain experience

on unidimensional rating scales or multidimensional pain scales (Chapman *et al.*, 1985; Fishbasin, 2003; Kall *et al.*, 2008).

Unidimensional Rating Scales

A unidimensional rating scale is a structured, categorized scale with clear defined limits, usually used for assessing acute pain (Chapman *et al.*, 1985; Fishbasin, 2003). Common unidimensinal pain rating scales include visual analogue scale (VAS), verbal rating scale (VRS), and numerical rating scale (NRS) (Chen *et al.*, 1998; Farrar *et al.*, 2001; Fishbasin, 2003; Williamson & Hoggart, 2005).

The VAS is presented as a 10-cm line anchored by two extremes of pain, 'no pain' and 'worst imaginable pain' (see Fig. 2.4a). The subjects or patients are required to rate their pain experience by indicating a position along a continuous line between the two end-points.

The VRS is the simplest rating scale to use. It usually describes pain using a list of adjectives: 'no pain', 'mild pain', 'moderate pain' and 'severe pain'.

The NRS is an 11, 21 or 101 point scale with the end points being the two extremes of pain, 'no pain' and 'worst imaginable pain'. The subjects or patients are required to choose a number between 0 and 10/20/100 to describe their pain experience. Fig. 2.4b shows a classical 11-point NRS.

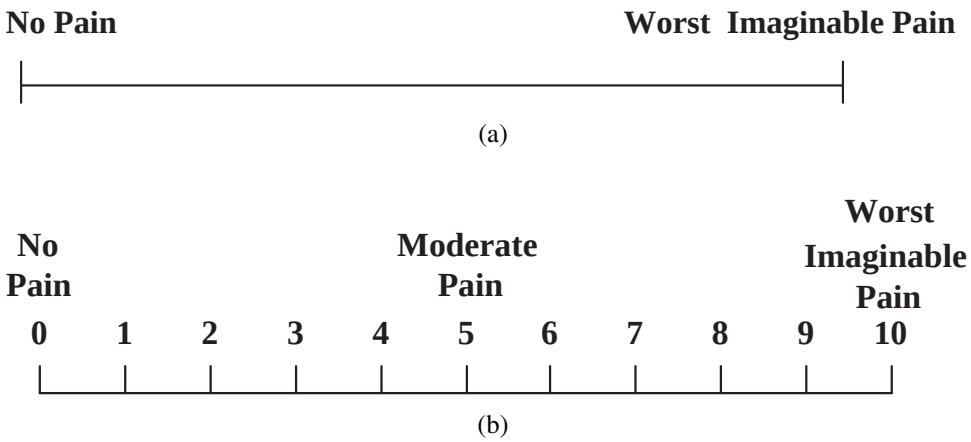

Figure 2.4: Common unidimensional pain rating scales: (a) visual analogue scale and (b) numerical rating scale.

Multidimensional Pain Scales

In contrast to unidimensional scales, multidimensional pain scales are often used for assessing chronic pain and in an attempt to address several domains including the sensory domain, the affective domain, the evaluative domain and the functional domain (Searle & Bennett, 2008). Common multidimensional pain scales include the McGill pain questionnaire, the memorial pain assessment card and the brief pain inventory (Melzack, 1975; Miaskowski, 2005).

The self-report methods have a major disadvantage of being subject to response bias or falsification (Reading, 1983). In addition, the self-report methods are not applicable to those individuals who are uncooperative and/or unable to do self-report (e.g. young children, patients with dementia, patients under anesthesia).

2.6.2 Behavioral Measures

Behavioral measures are based on the experimenter's or heath care worker's assessment of the degree of pain using a descriptive or numerical scoring system, by observation of subjects' or patients' pain behaviors (such as facial expression, moving in bed, bracing, rubbing an affected part, medication demand or intake, food intake, engagement in recreational activity) (Fishbasin, 2003). This technique has the disadvantage of being susceptible to the operator's experience and bias. Secondly, clinical patients likely exhibit few pain behaviors to avoid increasing pain. In such cases, measurement of pain by observation of pain behaviors is not reliable. Besides, there are cases when behavioral measures are not applicable due to the inability of patients to exhibit pain behaviors (e.g. patients under anesthesia).

2.6.3 Performance Measures

Performance measures are based on the measurement of perceptual ability derived from performance (e.g. activity level, frequency counts for certain behaviors, accuracy of judgements, reaction time and error rate) on laboratory tasks (Chapman *et al.*, 1985; Fishbasin, 2003). The major problem of performance measures is that they do not directly measure pain. The reliability of this kind of methods relies on the task used. A task, which itself also interferes with performance ability, may lead to useless or even misleading data for pain measurement.

2.6.4 Physiological Measures

Physiological measures are a class of promising objective pain assessment methods based on the measurement of physiological processes covarying with pain perception. The physiological measures do not rely on a subject's or patient's ability to self-report and are also not subject to the person whose pain is being measured or the person who is measuring the pain.

The existing physiological measures mainly include direct recording from the peripheral nerves, EMG measures, autonomic indices and EEG measures (Chapman *et al.*, 1985).

Direct Recording from Peripheral Nerves

The recording from peripheral nerves can be the electrical activity at the nociceptors or peripheral nerve trunks. This electrical activity is essentially a measure of the transduced stimulus intensity, which represents a better estimate of pain intensity as compared to direct measurement of the stimulus. However, the recording from peripheral nerves does not reflect the modulation processes occurring at the dorsal horn as well as higher brain centers and thus may not correlate well with pain experience.

EMG Measures

Enhanced muscle tension usually accompanies pain perception and thus measurement of EMG can provide a useful indicator of pain perception. However, there has been

evidence showing lack of correspondence between muscle tension and pain perception, and the causal link between muscle tension and pain is still not clear.

Autonomic Indices

Pain perception has also been reported to be usually accompanied by increases in skin conductance, blood pressure and heart rate. Thereby, a number of autonomic indices have been proposed for pain assessment, including pulse rate, skin conductance/resistance, skin temperature, and finger pulse volume. However, like EMG measures, exceptions to the normally observed changes in autonomic activity (i.e. increases in skin conductance, blood pressure and heart rate) have also been occasionally reported (Denise *et al.*, 2006; Tousignant-Laflamme *et al.*, 2005), and thus autonomic indices are also not always reliable.

EEG Measures

Among the many physiological measures, EEG measures deserve the most attention and have the greatest potential in its usefulness for reliable pain measurement. This is due to the fact that pain is perceived in the brain and thus EEG, as a measurement of the brain's electrical activity, should have a better correlation with pain experience than any other physiological measures.

2.7 Past Work on EEG Measures of Pain Perception

In the past decades, numerous studies have been conducted on searching for EEG measures of pain perception. The research can be divided into two lines, one focusing on the characterization of human pain by spontaneous EEG measures and the other into pain-related BEPs. The section presents a review of the past work most relevant to the present studies — laboratory studies on EEG measures of pain perception with healthy human volunteers.

2.7.1 Pain-induced Spontaneous EEG Changes

Two types of analytic methods have been mainly used to yield quantitative measures of spontaneous EEG for characterizing human pain perception: cortical power spectrum analysis and coherence analysis.

Pain-induced Cortical Power Spectrum Changes

There has been substantial evidence on the CPS changes in response to various kinds of painful stimulations by far. The earliest and most reported is the cold pain induced CPS changes. Back to the 1980s, Chen et al. (1989b) have reported significant increases in delta and beta activities during CPT. The heightened delta activity was believed to reflect the stress component of human pain responsivity, and the beta activity reflected the vigilance scanning of pain processes. Later, Backonja et al. (1991) found an initial

decrease in alpha activity followed by an alpha activity increase, in addition to increases in delta and beta activities by CPT. Being slightly different, Ferracuti et al.(1994) found a decrease in alpha activity and an increase in delta activity, but no significant changes in beta activity during CPT, while Chen and Rappelsberger (1994) reported a decrease in alpha activity and an increase in beta activity during cold pain stimulation. Subsequently, Chen et al. (1998) found increases in delta and theta activities but no significant changes in alpha and beta activities in response to cold pain. Chang et al. (2002) reported that cold pain induced CPS changes in all EEG frequency bands of interest, including increases in delta, theta and beta activities but a decrease in alpha activity. They proposed that alpha reduction could be related to the attention processing in nociceptive input, and the delta/theta/beta activation may be associated with the motivational modulation of the brain. Generally, these early studies reported varying cold pain induced CPS changes. According to Dowman et al. (2008), the major factors causing the varying findings of the early studies include that: a) the recording periods were too short to obtain stable EEG patterns for most of the studies; b) no-task control condition was used as the baseline in comparison to cold pain condition, leading to between- and within-subject variability in vigilance and/or arousal level; c) there was no standard criterion for handling EEG artifacts. They addressed these problems by using a) no-pain control conditions with proper control on vigilance and arousal, b) a long recording period of 10 mins, and c) proper methods to handle artifacts. Their results showed that a decrease of alpha activity over contralateral temporal scalp could be an EEG index of tonic pain perception.

Pain induced CPS changes have also be evidenced from the studies using other types of tonic experimental pain. Le Pera et al. (2000) reported decreases in delta, frontal beta1 (14-20 Hz) and contralateral parietal alpha1 (9-11 Hz) activities during hypertonic saline induced pain. Chang et al. (2003) showed that alpha1 (8-10.8 Hz) activity correlated negatively while beta2 (25-35 Hz) activity correlated positively with self-report of pain intensity during hypertonic saline induced pain. Chang et al. (2001a) found capsaicin pain induced decreases in alpha1 (8-10.5 Hz) and alpha2 (11-13.5 Hz) activities in posterior regions. Recently, Huber et al. (2006) showed that there were a generalized increase in the delta (2-4 Hz) activity, a left-sided temporal increase in the beta1 (12-16 Hz) activity, a left-biased fronto-temporal decrease in the theta (4-8 Hz) activity and a fronto-temporal decrease in the alpha1 (8-10 Hz) activity during heat pain. However, there was no evidence that these EEG changes were specific to tonic heat pain. More recently, Nir et al. (2010) reported a linear correlation between peak alpha frequency (PAF) and tonic heat pain.

In addition to tonic pain, CPS changes have also been reported in response to brief phasic pain. Bromm et al. (1989) found brief painful electrical stimuli induced increases in delta and theta activities. Arendt-Nielsen (1990) reported a significant power change in the low frequency band of 0.5-2.5 Hz at 1-2 s after brief laser stimulation. Croft et al. (2002) found a correlation between EEG gamma (32-100 Hz) activity over prefrontal scalp regions and subjective pain experience evoked by phasic electrical stimulation.

Pain-induced Cortical Connectivity Changes

Coherence analysis has greatly contributed to the understanding of cortical connectivity during pain perception. However, like findings on CPS changes, the results from coherence analysis also varied a bit across different studies. For example, Chen and Rappelsberger (1994) found increase of EEG coherence for alpha and beta2 (18.5-24 Hz) bands in central regions during cold pain as compared to no-task control condition. In a subsequent study, Chen et al. (1998) further compared EEG coherence during cold pain with that in non-painful cold condition. Different from the results in comparison to no-task control condition, there were higher coherence for delta and theta bands, lower coherence for beta1 (13-18 Hz) band but no significant coherence change for alpha band. More recently, Baltas et al. (2002) reported that as compared to no-pain condition, during laser induced heat pain, coherence significantly increased for almost all EEG channels, especially for beta band.

In summary, although pain induced brain activity in terms of CPS or coherence changes have been seen to vary a bit across studies, the existing evidence generally suggests that pain perception is associated with decreases in relative power of slower brain activities (mostly alpha and also theta in some studies) but increase in relative power of faster (beta) brain activity (Chen & Rappelsberger, 1994; Dowman *et al.*, 2008; Jensen *et al.*, 2008). The major barrier to use spontaneous EEG measures for pain assessment lies in that the equivocal causal link between the spontaneous EEG oscillations and pain perception. As the spontaneous EEG oscillations are not specific to painful stimulation, it is difficult to determine whether their changes during painful stimulation are related

to pain perception itself or associated with general emotional/cognitive processes, and to what extent the EEG changes are related to pain perception (Chen, 1993; Croft *et al.*, 2002). Moreover, spontaneous EEG are susceptible to artifacts, which may cause a misinterpretation of pain-related EEG features.

2.7.2 Pain-related Brain Evoked Potentials

Measurement of BEPs in response to painful stimulation has provided a valuable tool for the study of pain perception in the brain. Unlike spontaneous EEG oscillations, BEPs measure the electrical activity time-locked to painful stimulation and capture the time course of brain response associated with the processing of painful stimuli. Since Chatrian et al. (1975) firstly reported the correlation between BEPs and pain induced by electrical stimulation of tooth pulps, the BEPs in response to brief painful stimulation have gained great interest and been intensively studied. So far, various BEPs highly correlated with subjects' self-report of pain sensation and sensitive to the effect of analgesic drugs and their antagonists have been reported. Carmon et al. (1978) found a linear relationship between the amplitude of thermal pain evoked positive deflection at 372-391 ms and the magnitude of subjective pain sensation. Chen et al. (1979) reported that the peak-to-peak amplitude of the component at 175-260 ms in the painful dental stimulation evoked potentials was linearly correlated with subjective painfulness. By conducting principal component analysis on the cerebral potentials evoked by noxious and non-noxious mechanical and electrical stimulation, Bromm & Scharein (1982) detected two components which differed significantly between painful and non-painful

sensations. Fernendes de Lima et al. (1982) demonstrated an association between late midline tooth pulp evoked potentials and pain perception. Kakigi *et al.* (1989) found a correlation between the P320 component in the somatosensory evoked potential (SEP) following laser stimuli and subjective pain experience, and proposed that the P320 component could be generated by pain-specific cognition or perception. Becker et al. (1993) identified a pain component with the latency range of 200-550 ms in the somatosensory evoked potential (SEP) by painful electrical intracutaneous stimulation. More recently, Granovsky et al. (2008) showed a positive correlation between contact-heat pain evoked potentials and pain magnitude.

However, pain-specific BEPs are yet to be investigated (Bromm & Scharein, 1982; Fernandes de Lima *et al.*, 1982; Mouraux & Iannetti, 2009). Most of the reported pain-related BEPs have been shown to be likely also related to arousal or attentional reorientation. There is evidence that the pain-related component is often confounded with a P300 component in the pain evoked potentials (Becker *et al.*, 2000, 1993; Dowman, 2004; Zaslansky *et al.*, 1996b,a). Second, it is also questionable whether the BEPs in response to external stimulation can reveal endogenous brain activity associated with pain perception which is hardly time-locked to any external event (Chen, 1993). In addition, brief painful stimulation was used to induce pain in BEP studies, whereas it remains a debatable issue whether the induced phasic experimental pain can faithfully simulate clinical pain (Nir *et al.*, 2010).

2.8 Review of Gender Differences in Pain-Related Brain Activations

With the advances in functional imaging techniques such as fMRI, MEG and PET, researchers have been able to directly pinpoint pain-related brain activations within the human brain. In recent years, there has been increasing evidence on gender differences in pain-related brain activations from neuroimaging studies using fMRI, MEG and PET (Berman *et al.*, 2006; Derbyshire *et al.*, 2002; Moulton *et al.*, 2006; Naliboff *et al.*, 2003; Paulson *et al.*, 1998; Straube *et al.*, 2009).

Paulson et al. (1998) showed that, under equal heat stimuli, females had significantly stronger activation in the right, contralateral PF, the contralateral insula and thalamus. However, they were unable to determine whether the different activations in insula and thalamus were attributed to gender, perceived pain intensity or both factors, as they did not equalize perceived intensities. Unlike Paulson et al. (1998), Derbyshire et al. (2002) equalized pain experience. They found that females were more strongly activated in perigenual cingulate cortex while males were more activated in the left, contralateral, PF, S1, S2, parietal and insula cortices. These results suggested that males seemed to focus more on sensory processing in contrast to more on affect processing for females. Naliboff et al. (2003) investigated gender differences in central processing of experimental visceral pain on irritable bowel syndrome patients, and found that females had stronger activation in the ventromedial PF,the right ACC and the left amygdala, in contrast to the greater activation of the right DLPFC, the insula and the dorsal pons/PAG

for males. According to Naliboff et al. (2003), these results reflected that females had stronger affective and autonomic responses but decreased cognitive activity during visceral pain than males. Berman et al. (2006) examined gender differences in perception of experimental visceral pain on healthy subjects, and they obtained slightly different results from those of Naliboff et al. (2003) — stronger activation in the insular cortex for males but greater deactivation in the amygdala and the midcingulate for females. Moulton et al. (2006) found that males had stronger activations in the S1, the mid-ACC and the DLPFC under equivalent perception of contact heat pain than females. Recently, Henderson et al. (2008) reported that males had decreased activity in the DLPFC and increased activity in the cerebellar cortex, while females had increased activity in the midcingulate cortex and either decreased or increased (depending on whether the pain was subcutaneous or intramuscular) in the hippocampus, during hypertonic saline induced pain. They speculated that the observed gender differences in pain-related brain activations may be arisen from gender differences in the brain circuitry involved in processing affective component of pain experience. More recently, Straube et al. (2009) reported stronger activation of the pregenual MPFC for females but higher activation of the insular cortex for males during electrical painful stimulation.

In summary, the past studies generally suggest that females concentrate more on the affective dimension of pain by showing stronger pain-related activations in those emotion-based brain regions while males concentrate more on the sensory dimension of pain by showing stronger pain-related activations in sensory regions. However, results on gender differences in cerebral responses to pain vary a bit across the past functional imaging

studies, likely due to differences in the stimulus modality and experimental paradigm used (Fillingim *et al.*, 2009).

Chapter 3

General Experimental Methods

This chapter describes the general experimental methods used for EEG recording and pain induction. The experimental procedure and analysis methods specifically used to achieve each specific aim of the study will be given later in each corresponding chapter.

3.1 EEG Recording

3.1.1 Subjects

The subjects were recruited from the National University of Singapore and fulfilled the inclusion criteria of not being on any medication, no history of neurological, psychiatric and cardiovascular problems as well as pain disorders. The recruitment of human subjects for this study was approved by the Institutional Review Board of the National

University of Singapore (NUS-IRB). Informed consents were obtained prior to experiments and each subject was reimbursed with S$50 for his/her participation.

3.1.2 Experimental Setup and Recording Parameters

EEG were recorded using the Neuroscan NuAmps system (see Fig. 3.1) at a sampling rate of 250 Hz with a bandpass filtering of 0.5 - 100 Hz, from 30 electrodes arranged according to the extended 10-20 system (see Fig. 3.2) with a 32-Channel Quick-Cap (Compumedics Neuroscan, USA). The scalp EEG was referenced to the average of A1 and A2, with AFz serving as the ground electrode.

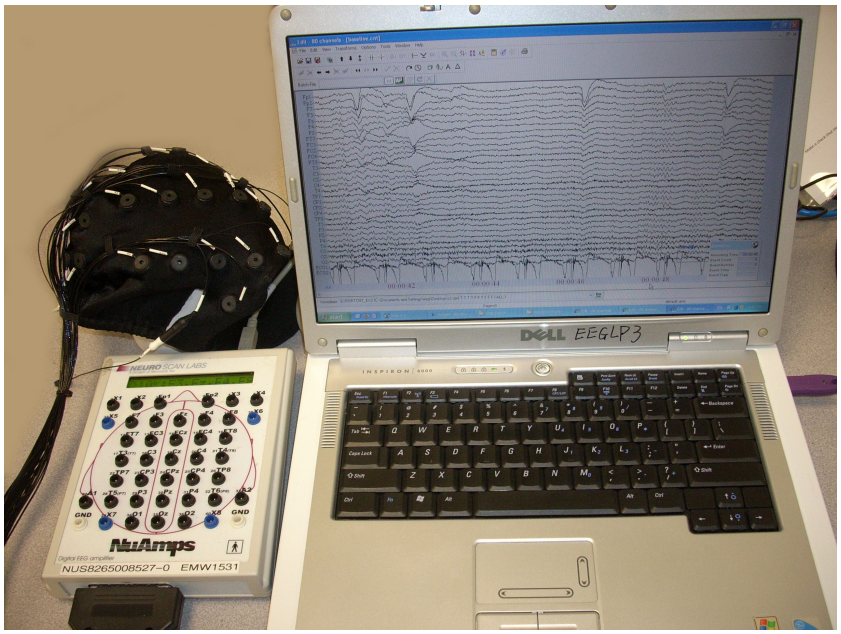

Figure 3.1: The Neuroscan NuAmps system used for EEG recording.

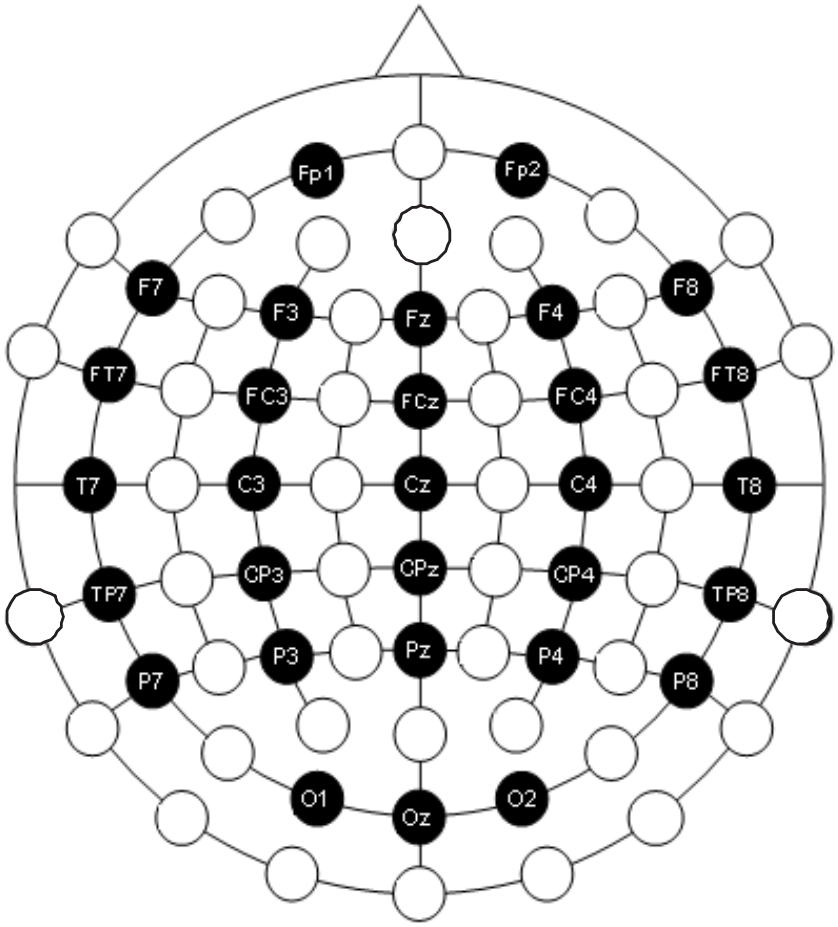

Figure 3.2: The electrode arrangement according to the extended 10-20 system.

3.2 Experimental Method for Pain Induction

The perception of different types of pain may be different and involve different brain networks (Apkarian *et al.*, 2005; Chen & Treede, 1985), and thus should be analyzed separately. The present study focused on a specific type of nociceptive pain—the somatic pain, as shown in the grayed box in Fig. 2.1. More specifically, the tonic cold pain induced by CPT was used to simulate acute clinical pain in the present study. It is believed that clinical pain is usually associated with the long-lasting and diffuse pain,

and thus the experimental tonic pain may simulate clinical pain more closely than phasic pain (Chen *et al.*, 1989a; Chen & Treede, 1985; Nir *et al.*, 2010).

The apparatus used for CPT, the administration of the test and the measurement of subjective pain experience strictly followed the guidelines for CPT in the literature (Mitchell *et al.*, 2004; von Baeyer *et al.*, 2005). Fig. 3.3 shows the apparatus used for CPT in the present study, which consisted of a heating circulator with open bath (JULABO model ED-19) and an immersion cooler (JULABO model FT200). This apparatus ensured that the water was continuously circulating at a specified temperature during the experiment.

Figure 3.3: The apparatus used for experimental cold pain induction, consisting of a heating circulator with open bath and an immersion cooler.

The present study followed the recommendation of von Baeyer et al. (2005) and used cold water maintained at a temperature of 10 ^{o}C for CPT, although a temperature of 0 to

7 ^{o}C were more commonly used for adults in the past works (Mitchell *et al.*, 2004). The use of 10 ^{o}C in this study was in an attempt to ensure that subjects could survive with hand immersion in the cold water for a long enough time to obtain representative EEG recordings.

The psychophysical responses of the subjects, including subjective self-report of pain intensity and unpleasantness ratings, were measured by using two separate 11-point numerical rating scales, as shown in Fig. 3.4a and Fig. 3.4b respectively.

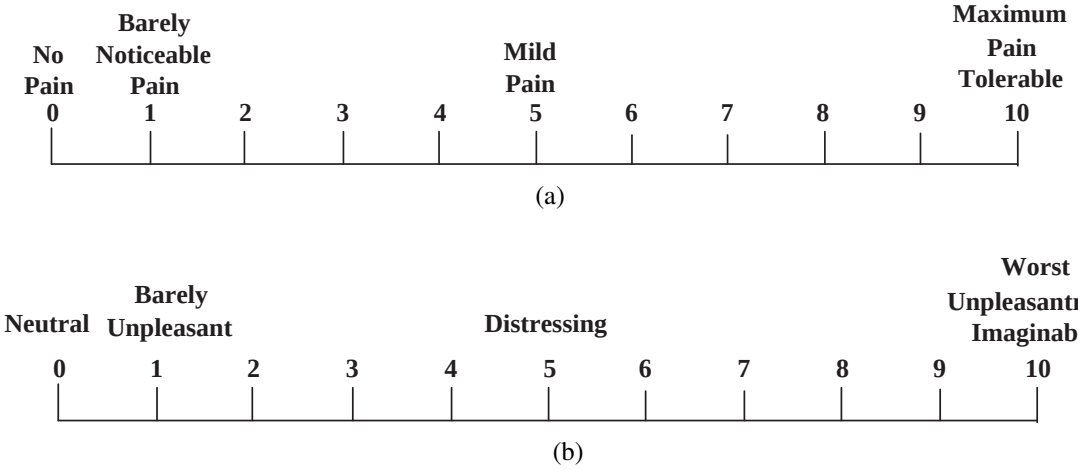

Figure 3.4: The pain rating scales used in the present study: (a) the numerical rating scale for pain intensity and (b) the numerical rating scale for pain unpleasantness.

Chapter 4

A Weighted Support-Vector-Machine Approach With Error Correction for Automatic EEG Artifact Removal

4.1 Introduction

EEG recordings are known to be contaminated by physiological artifacts from various sources, such as blinking and movements of the eyes, beating of the heart and movements of other muscle groups (Jung *et al.*, 2000b). These artifacts are mixed together with the brain signals, seriously interfering with the interpretation of EEG signals (Urrestarazu *et al.*, 2004). Therefore, it is necessary to remove the various artifacts from EEG before further EEG analysis.

There has been great interest in applying ICA (Comon, 1994; Hyvarinen *et al.*, 2001) to EEG artifact removal in recent years (Castellanos & Makarov, 2006; Jung *et al.*, 1998, 2000a; Makeig *et al.*, 1996; Urrestarazu *et al.*, 2004; Vigario *et al.*, 2000; Vigario, 1997; Wallstrom *et al.*, 2004). This is mainly motivated by the fact that ICA is effective in decomposing raw EEG recordings into electrical source signals originating from non-cerebral artifacts (namely, artifactual ICs) and electrical source signals accounting for true brain activations (namely, non-artifactual ICs) (see, e.g., Castellanos & Makarov 2006; Jung *et al.* 1998; Vigario *et al.* 2000). The ICA-based artifact removal methods have provided a possibility to simultaneously removing various artifacts in EEG while keeping brain signals of interest well preserved. However, in conventional ICA-based artifact removal methods (see, e.g., Makeig *et al.* 1996; Urrestarazu *et al.* 2004; Vigario *et al.* 2000), artifactual ICs are manually identified (usually by visual inspection) and removed. This process is very time-consuming and, hence, not suitable for real-time applications.

Recent effort towards automatic artifact removal includes the studies of Nicolaou & Nasuto (2004) and Shoker et al. (2005) where a standard support vector machine (SVM) (Boser *et al.*, 1992; Cortes & Vapnik, 1995; Cristianini & Shawe-Taylor, 2000; Vapnik, 1995), trained on equal number of artifactual and non-artifactual samples, is used for automatic identification of artifactual ICs. Such a combination of ICA and SVM (Boser *et al.*, 1992; Cortes & Vapnik, 1995; Cristianini & Shawe-Taylor, 2000; Vapnik, 1995) offers a promising approach for automatic artifact removal (Nicolaou & Nasuto, 2004; Shoker *et al.*, 2005). Unfortunately, unique properties of the problem at hand have not

been taken into consideration. First, the real data are extremely unbalanced–only a few of the ICs are artifactual ICs and the majority is non-artifactual ICs (see, e.g., Castellanos & Makarov, 2006; Joyce *et al.*, 2004; Jung *et al.*, 2001; Onton & Makeig, 2006; Romero *et al.*, 2003). It is well known in the machine learning community that the performance of a standard SVM, trained on balanced datasets, may perform poorly when the real data are unbalanced. Second, the number of artifactual ICs responsible for each type of artifact, decomposed from a given EEG epoch, is often small. This structural information of the underlying data can be very useful for improving the accuracy of automatic artifact identification. To the best of our knowledge, such structural information has however not been exploited in past literature.

In this chapter, a novel automatic EEG artifact removal method is presented. The proposed method exploits the above-mentioned unique properties by: 1) using a weighted version of SVM formulation (Osuna *et al.*, 1997) to handle the inherent unbalanced nature of component classification, and 2) imposing constraints on the number of artifactual ICs through a novel error correction algorithm. It is worth noting that the proposed formulation is conceptually different from past ICA-based artifact removal methods. It considers all the ICs derived from a given EEG epoch collectively while the past methods treat each IC independently. The advantages of the proposed method over a number of past methods in the literature are shown in a carefully controlled experiment using real-life EEG data with comparisons made to several benchmark methods. Results show that the proposed method is preferable to the other methods in the context of artifact removal by achieving a better tradeoff between removing artifacts and preserving inherent

brain activities.

4.2 Overview of the Proposed Automatic Artifact Removal Method

This section provides an overview of the proposed artifact removal system and establishes the necessary notations needed for subsequent sections. Like other ICA-based artifact removal systems in the literature, the proposed system (see Fig. 4.1) consists of four main modules: ICA, feature extractor, IC classifier and EEG reconstruction. The contribution of the present work is mainly on the new method used in the IC classifier, though the feature extractor also includes some new features.

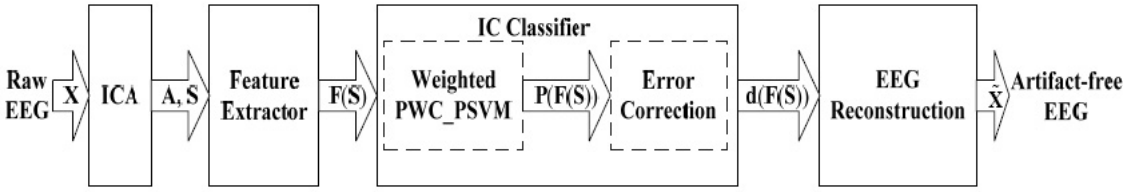

Figure 4.1: Block diagram of the proposed automatic artifact removal system. The system consists of four main modules: ICA, feature extractor, IC classifier and EEG reconstruction module. The novelty of the proposed IC classifier is explicitly shown. It has two sub-modules: a modified probabilistic multi-class SVM (denoted by weighted PWC_PSVM in the figure) to address the unbalanced nature of the data and an error correction block to handle the unique structural information of the data.

The continuous raw EEG recording is first segmented into epochs with a fixed length. The resulting EEG epochs are then fed, epoch by epoch, into the artifact removal system. Given a raw EEG epoch as the input, the output of the system is the reconstructed

artifact-free EEG epoch.

4.2.1 ICA Module

Consider a given n-channel raw EEG epoch, $\mathbf{X} = [\mathbf{x}_1\ \mathbf{x}_2\ \cdots\ \mathbf{x}_n]^T$ where $\mathbf{x}_i \in \mathbb{R}^l,\ i = 1,\ \ldots,\ n$, is the time series for the i^{th} EEG channel with a fixed length, l. The ICA module decomposes $\mathbf{X}$ into $m\ (\leq n)$ ICs, $\mathbf{S} = [\mathbf{s}_1\ \mathbf{s}_2\ \cdots\ \mathbf{s}_m]^T$ where $\mathbf{s}_i \in \mathbb{R}^l,\ i = 1,\ \ldots,\ m$, is the i^{th} IC, by solving (Hyvarinen, 1999):

$$\mathbf{X} = \mathbf{AS} \tag{4.1}$$

where, $\mathbf{A} = [\mathbf{a}_1\ \mathbf{a}_2\ \cdots\ \mathbf{a}_m]$ denote the mixing matrix with $\mathbf{a}_i \in \mathbb{R}^n$ containing the scalp distribution coefficients of $\mathbf{s}_i$.

There are many different algorithms based on different measures of independence for solving the ICA problem shown in Equation (4.1). A most commonly used measure of independence is mutual information or non-Gaussianity. The ICs, $\mathbf{s}_i \in \mathbb{R}^l,\ i = 1,\ \ldots,\ m$, can be estimated by minimizing the mutual information between them or maximizing their non-Gaussianity (Hyvarinen, 1999; Hyvarinen *et al.*, 2001).

While many implementations of ICA are available, the FastICA package (Gvert *et al.*, 2005) is used in the present study. The FastICA package implements a Newton-iteration based fast fixed-point optimization scheme and an objective function based on maximization of negentropy for ICA. The fast fixed-point algorithm has proven to be much

faster than conventional gradient descent methods. Details on the algorithm can be found in Hyvarinen et al. (2001).

4.2.2 Feature Extractor

The feature extractor generates a set of feature vectors from the $\mathbf{s}_i$'s needed for classification of the $\mathbf{s}_i$'s. Suppose d features are extracted from $\mathbf{s}_i$. Then, $\mathbf{f}(\mathbf{s}_i) = [f_1(\mathbf{s}_i)\ f_2(\mathbf{s}_i)\ \cdots\ f_d(\mathbf{s}_i)]^T$ denotes the feature vector extracted from $\mathbf{s}_i$ and $\mathbf{F}(\mathbf{S}) = [\mathbf{f}(\mathbf{s}_1)\ \mathbf{f}(\mathbf{s}_2)\ \cdots\ \mathbf{f}(\mathbf{s}_m)]^T$ denotes the set of feature vectors obtained from $\mathbf{S}$.

In the present study, six features are extracted from each IC. The definitions of the six features are given in Equation (4.2)-Equation (4.7). The first four features (as shown in Equation (4.2)-Equation (4.5)) are directly adopted from the literature (Shoker *et al.*, 2005) for characterizing EOG artifact. The last two (as shown in Equation (4.5)-Equation (4.7)) are new features proposed for characterizing ECG artifact.

Feature 1: The first feature is the ratio between the peak amplitude and the variance of $\mathbf{s}_i$, as given by (Shoker *et al.*, 2005)

$$f_1(\mathbf{s}_i) = \max(|\mathbf{s}_i|)/\sigma^2_{\mathbf{s}_i}, \tag{4.2}$$

where $\sigma_{\mathbf{s}_i}$ is the standard deviation of $\mathbf{s}_i$.

Feature 2: The second feature is the normalized skewness of $\mathbf{s}_i$, defined as (Shoker *et al.*,

2005)

$$f_2(\mathbf{s}_i) = \left| E\{\mathbf{s}_i^3\} / \sigma_{\mathbf{s}_i}^3 \right| \tag{4.3}$$

Feature 3: This feature measures the cross-correlation between $\mathbf{s}_i$ and an independent reference dataset containing eye-blinking dominated EEG channels (Fp1, Fp2, F3, F4, O1, O2), $\mathbf{x}_j^0,\ (j = 1,\ \cdots,\ 6)$, which is distinct from the training and testing datasets. It is calculated as (Shoker *et al.*, 2005)

$$f_3(\mathbf{s}_i) = \sum_{j=1}^{6} \max_{\tau} (\left| E\left\{\mathbf{x}_j^0(m)\mathbf{s}_i(m+\tau)\right\}\right|)/6. \tag{4.4}$$

Feature 4: This feature is the Kullback-Leibler (KL) distance between the probability density function (PDF) of $\mathbf{s}_i$ and that of a reference EOG IC which is separated from an EEG epoch distinct from the data used for training and testing, $\mathbf{s}_{eog}^0$. It is calculated as (Shoker *et al.*, 2005)

$$f_4(\mathbf{s}_i) = \int \mathbf{P}(\mathbf{s}_i) \ln(\mathbf{P}(\mathbf{s}_i)/\mathbf{P}(\mathbf{s}_{eog}^0)) d\mathbf{s}_i, \tag{4.5}$$

where $\mathbf{P}(\mathbf{s}_i)$ and $\mathbf{P}(\mathbf{s}_{eog}^0)$ are the PDF of $\mathbf{s}_i$ and $\mathbf{s}_{eog}^0$ respectively.

Feature 5: The fifth feature is the variance of scalp distribution of $\mathbf{s}_i$, given by

$$f_5(\mathbf{s}_i) = \mathrm{var}(\mathbf{a}_i / \left\|\mathbf{a}_i\right\|), \tag{4.6}$$

This feature is specially proposed for ECG ICs because empirical evidences have shown that their unique scalp distribution gives smaller variance compared to other types of ICs (Greco *et al.*, 2005).

Feature 6: The sixth feature gives the KL distance between the PDF of $\mathbf{s}_i$ and that of a reference ECG IC which is separated from an EEG epoch distinct from the data used for training and testing, $\mathbf{s}_{ecg}^0$. It is described as

$$f_4(\mathbf{s}_i) = \int \mathbf{P}(\mathbf{s}_i) \ln(\mathbf{P}(\mathbf{s}_i)/\mathbf{P}(\mathbf{s}_{ecg}^0)) d\mathbf{s}_i, \tag{4.7}$$

where $\mathbf{P}(\mathbf{s}_i)$ and $\mathbf{P}(\mathbf{s}_{ecg}^0)$ are the PDF of $\mathbf{s}_i$ and $\mathbf{s}_{ecg}^0$ respectively. This feature is proposed to account for distinct PDF of ECG ICs due to their unique composition of P wave, QRS complex and T wave.

It is worthy noting that features 3, 4 and 6 simply require reference EEG signals or ICs obtained from distinct EEG epochs that are not part of training and testing datasets, but not additional reference EEG channels that are generally required in many non-ICA based artifact removal methods.

4.2.3 IC Classifier

The proposed IC classifier has two sub-modules: a modified probabilistic multi-class SVM (denoted by weighted PWC_PSVM) and an error correction block, as shown in Fig. 4.1. The choice of SVM stems from its superior performance on many learning

problems and modification proposed in the present work to address the unbalanced nature of the data is a novel contribution. Justification to this choice is verified by experimental results compared with other classification approaches, like K-Nearest Neighbors (KNN), Gaussian Mixture Models (GMM) and Linear Discriminant Function (LDF).

The error correction block is another novel contribution of the present work. Suppose the $\mathbf{s}_i$'s are attributed to c different classes $\{\omega_1 \cdots \omega_c\}$, with ω_1 being the class of brain sources and the rest $c-1$ classes, i.e. $\omega_c, \cdots, \omega_c$, referring to different artifactual sources. Standard IC classifier in the literature (Nicolaou & Nasuto, 2004; Shoker *et al.*, 2005) classifies $\mathbf{s}_i$ into one of c classes, or the decision function $d(\mathbf{f}(\mathbf{s}_i))$ maps $\mathbf{f}(\mathbf{s}_i)$ into $\{\omega_1 \cdots \omega_c\}$. Such a setup considers $\mathbf{s}_i$, $i = 1, \ldots m$, independently and is the framework used in most works in the literature. However, it is difficult for such a setup to account for the unique structure of the underlying data. In contrast, the proposed classifier is able to accommodate the structural information with the error correction algorithm by considering the $\mathbf{s}_i$'s collectively and yielding all m predicted class labels via the decision function $\mathbf{d}(\mathbf{F}(\mathbf{S}))$.

The detailed account of the proposed weighted PWC_PSVM and the error correction algorithm will be given in Section 4.3.

4.2.4 EEG Reconstruction

The EEG reconstruction module reconstructs artifact-free EEG epoch by zeroing the contribution of all artifactual sources from raw EEG epoch. Suppose $\tilde{\mathbf{S}}$ is obtained from

S by zeroing all the identified artifactual ICs. The reconstructed artifact-free EEG epoch, denoted by $\tilde{\mathbf{X}}$, can be obtained as follows (Jung *et al.*, 2000b):

$$\tilde{\mathbf{X}} = \mathbf{A}\tilde{\mathbf{S}}. \tag{4.8}$$

4.3 The Proposed Weighted Support-Vector-Machine Approach With Error Correction

The proposed IC classifier is a combination of a modified probabilistic multi-class SVM and a novel error correction algorithm. It is our attempt to address the unique properties of the problem. Given m ICs decomposed from an EEG epoch, let m_{ω_j} be the number of ICs corresponding to class ω_j. The unique properties of the problem can be effected in terms of the following constraints:

$$m_{\omega_1} >> m_{\omega_2},\ m_{\omega_1} >> m_{\omega_3},\ \cdots,\ m_{\omega_1} >> m_{\omega_c} \tag{4.9}$$

and

$$l_{\omega_2} \leq m_{\omega_2} \leq u_{\omega_2},\ l_{\omega_3} \leq m_{\omega_3} \leq u_{\omega_3},\ \cdots,\ l_{\omega_c} \leq m_{\omega_c} \leq u_{\omega_c} \tag{4.10}$$

The constraints in Equation (4.9) represent the inherent unbalanced nature of the data, while those as in Equation (4.10) are the unique structural information that define the

upper and lower bounds, denoted by u_{ω_j} and l_{ω_j} respectively, with regards to the number of ICs belonging to each artifactual source. Optimal values of u_{ω_j} and l_{ω_j} depend on the bioelectrical nature of that artifact (for example, EOG artifacts can usually be modeled as a single dipole consisting of three spatial components each (Schlgl *et al.*, 2007)), and the protocol under which the EEG data are collected (e.g. the number of EEG channels used). Typically, they can be tuned by a data-driven approach. The details will be given in the description of the numerical experiments in Section 4.4.

4.3.1 The Modified Probabilistic Support Vector Machines

Multi-class SVM is typically built up from several standard binary SVMs (Duan & Keerthi, 2005; Hsu & Lin, 2002). The proposed probabilistic multi-class SVM is modified from a probabilistic multi-class SVM based on pairwise coupling strategy by Hastie and Tibshirani (1998), by replacing all the standard binary SVMs with weighted SVMs (Osuna *et al.*, 1997), to properly address the unbalanced learning problem at hand. It is hereafter referred as the weighted PWC_PSVM. The detailed implementation of the weighted PWC_PSVM is as follows. Consider a nominal c-class unbalanced classification problem with dataset D in the form of $\{\mathbf{f}_i, y_i\}_{i=1}^{N}$, where $\mathbf{f}_i \in \mathbb{R}^d$ is the i^{th} sample and $y_i \in \{\omega_1, \cdots, \omega_c\}$ is the corresponding class label and N is the total number of training samples. Let N_j denote the number of training samples belonging to class ω_j, and $D_{ij} := \{\mathbf{f}_k, y_k\}_{\mathbf{f}_k \in \omega_i \cup \omega_j}$ be the subset of D formed by the samples from class ω_i and ω_j.

Construction of Weighted Binary SVMs

In total, $c(c-1)/2$ weighted binary SVMs are constructed, each classifying a pair of classes. The weighted binary SVM classifying class ω_i and class ω_j is trained using D_{ij} by solving the following optimization problem (Osuna *et al.*, 1997):

$$\begin{aligned} \min_{\mathbf{w}^{ij},b^{ij},\xi^{ij}} \quad & \tfrac{1}{2}(\mathbf{w}^{ij})^T\mathbf{w}^{ij} + C_i^{ij}\sum_{\mathbf{f}_k\in\omega_i}\xi_k^{ij} + C_j^{ij}\sum_{\mathbf{f}_k\in\omega_j}\xi_k^{ij}, \\ \text{subject to} \quad & \mathbf{w}^{ij}\cdot\phi^{ij}(\mathbf{f}_k) + b^{ij} \geq 1-\xi_k^{ij}, \text{if } \mathbf{f}_k\in\omega_i, \\ & \mathbf{w}^{ij}\cdot\phi^{ij}(\mathbf{f}_k) + b^{ij} \leq -1+\xi_k^{ij}, \text{if } \mathbf{f}_k\in\omega_j, \\ & \xi_k^{ij} \geq 0, \forall k, \end{aligned} \tag{4.11}$$

where ϕ^{ij} is a nonlinear mapping function that maps feature vectors into a high (possibly infinite) dimensional Euclidean space $\mathscr{H}$; $\mathbf{w}^{ij}\in\mathscr{H}$, $b^{ij}\in\mathbb{R}$ are the parameters that determine the optimal separating hyperplane: $\mathbf{w}^{ij}\cdot\phi^{ij}(\mathbf{f})+b^{ij}=0$; $\xi_k^{ij}\in\mathbb{R}$ is the non-negative slack variable. Different regularization parameters, C_i^{ij} and C_j^{ij}, are introduced in Equation (4.11) for the classes ω_i and ω_j, respectively.

A useful choice (Eitrich & Lang, 2006; Markowetz, 2001) is to let

$$C_i^{ij}/C_j^{ij} = N_j/N_i. \tag{4.12}$$

Conceptually, this is to impose higher penalty on classification errors made on the sam-

ples from the minority class.

In practice, the following dual formulation (Boser *et al.*, 1992; Cortes & Vapnik, 1995; Cristianini & Shawe-Taylor, 2000; Vapnik, 1995) is used to find the numerical solution of Equation (4.12):

$$\begin{aligned} \max \quad & J(\alpha^{ij}) = \sum_{\mathbf{f}_k \in D_{ij}} \alpha_k^{ij} - \sum_{\mathbf{f}_k \in D_{ij}} \sum_{\mathbf{f}_r \in D_{ij}} \alpha_k^{ij} \alpha_r^{ij} y_k y_r K^{ij}(\mathbf{f}_k, \mathbf{f}_r), \\ \text{subject to} \quad & \sum_{\mathbf{f}_k \in D_{ij}} y_k \alpha_k^{ij} = 0 \text{ and} \\ & 0 \le \alpha_k^{ij} \le C_i^{ij}, \text{ if } \mathbf{f}_k \in \omega_i; \ 0 \le \alpha_k^{ij} \le C_j^{ij}, \text{ otherwise,} \end{aligned} \tag{4.13}$$

where α_k^{ij} is the non-negative Lagrangian multiplier for the k^{th} sample and $K^{ij}(\mathbf{f}_k, \mathbf{f}_r) = \phi^{ij}(\mathbf{f}_k) \cdot \phi^{ij}(\mathbf{f}_r)$ is the kernel function. With the solution of Equation (4.13), the output of the weighted binary SVM for a test sample $\mathbf{f}$ is given by

$$g^{ij}(\mathbf{f}) = \sum_{\mathbf{f}_k \in D_{ij}} \alpha_k^{ij} y_k K^{ij}(\mathbf{f}_k, \mathbf{f}) + b^{ij}. \tag{4.14}$$

Generating Pairwise Class Probabilities

Standard SVM classifies a sample $\mathbf{f}$ depending on the sign of $g^{ij}(\mathbf{f})$, or the half space in $\mathscr{H}$ into which $\phi^{ij}(\mathbf{f})$ falls. Such an approach, however, ignores the relative confidence in the classification, or the distance that $\phi^{ij}(\mathbf{f})$ is from the separating hyperplane. Platt (2000) proposes the use of the following sigmoid function to map $g^{ij}(\mathbf{f})$ into $p^{ij} \equiv$

$P(\omega_i|\mathbf{f},\ \mathbf{f} \in \omega_i \text{ or } \omega_j)$, the pairwise probability of belonging to class ω_i knowing that $\mathbf{f}$ is from class ω_i or ω_j:

$$p^{ij}(\mathbf{f}) = \frac{1}{1+\exp(A^{ij}g^{ij}(\mathbf{f})+B^{ij})}, \tag{4.15}$$

where the parameters A^{ij} and B^{ij} are determined from minimizing the negative log likelihood function, or

$$\min_{A^{ij},\ B^{ij}} \{ -\sum_{\mathbf{f}_k \in D_{ij}} [t_k \log(p^{ij}(\mathbf{f}_k)) + (1-t_k)\log(1-p^{ij}(\mathbf{f}_k))]\}, \tag{4.16}$$

where $t_k = (N_i+1)/(N_j+2)$ if $\mathbf{f}_k \in \omega_i$ and $t_k = 1/(N_j+2)$ if $\mathbf{f}_k \in \omega_j$. It is worth noting that a 5-fold cross-validation procedure is implicitly used in Equation (4.16) as suggested by Platt (2000). This cross-validation process removes the requirement of keeping a hold-out validation dataset for fitting the parameters A^{ij} and B^{ij}, which is especially useful when the number of training samples is small. Our implementation of Equation (4.16) includes the modifications suggested by Lin et al. (2007) for numerical stability. The choice of kernel function in Equation (4.13) is general and our study is done with the popular Gaussian kernel, $K^{ij}(\mathbf{f}_r,\mathbf{f}_s) = \exp(-\gamma^{ij}\|\mathbf{f}_r-\mathbf{f}_s\|^2)$ where γ^{ij} is the kernel parameter.

Estimating Multi-class Posterior Probability

Given the pairwise class probabilities, $p^{ij}(\mathbf{f})$ and $p^{ji}(\mathbf{f})(=1-p^{ij}(\mathbf{f}))$, $\forall i \neq j$, the multi-class posterior probability of belonging to ω_i given $\mathbf{f}$, denoted by $p_i(\mathbf{f}) \equiv P(\omega_i|\mathbf{f})$, $\forall i$,

can be estimated by solving the following optimization problem (Hastie & Tibshirani, 1998; Wu *et al.*, 2004):

$$\begin{aligned} \min_{p_i(\mathbf{f})} \quad & \sum_{i=1}^{c} \sum_{j:j\neq i} \left[p^{ji}(\mathbf{f})p_i(\mathbf{f}) - p^{ij}(\mathbf{f})p_j(\mathbf{f})\right]^2. \\ \text{subject to} \quad & \sum_{i=1}^{c} p_i(\mathbf{f}) = 1 \text{ and } p_i(\mathbf{f}) \geq 0. \end{aligned} \tag{4.17}$$

Let $\mathbf{p}(\mathbf{f}(\mathbf{s}_i)) = [p_1(\mathbf{f}(\mathbf{s}_i))\ p_2(\mathbf{f}(\mathbf{s}_i))\ \cdots\ p_c(\mathbf{f}(\mathbf{s}_i))]^T$, representing the vector of multi-class posterior probabilities as given by Equation (4.17) for the i^{th} IC derived from a given EEG epoch, $\mathbf{s}_i$. It will be used in the proposed error correction algorithm that is described in the next section.

4.3.2 Error Correction

Consider the classification of m feature vectors corresponding to m ICs from a given EEG epoch, $\mathbf{f}(\mathbf{s}_i),\ i = 1,\ \cdots,\ m$. Instead of simply using $d(\mathbf{f}(\mathbf{s}_i)) = \arg\max_k \{p_k(\mathbf{f}(\mathbf{s}_i))\}$ to classify each IC independently, the proposed IC classifier includes a novel error correction algorithm which is aimed to incorporate the structural information as given in Equation (4.10) by considering all the $\mathbf{s}_i$ ($i = 1,\ \cdots,\ m$) collectively and yielding all m predicted class labels simultaneously.

In loose terms, the proposed error correction algorithm is to find the m predicted class labels that satisfy the constraints as in Equation (4.10) and, at the same time, match the

$\mathbf{P}(\mathbf{F}(\mathbf{S})) = [\mathbf{p}(\mathbf{f}(\mathbf{s}_1))\ \mathbf{p}(\mathbf{f}(\mathbf{s}_2))\ \cdots\ \mathbf{p}(\mathbf{f}(\mathbf{s}_m))]$ as much as possible. Let $\mathbf{q}_i \in \mathbb{R}^c$ be the code vector representing the predicted class label of $\mathbf{s}_i$. This implies that, if the predicted class label of $\mathbf{s}_i$ is k, the k^{th} element q_{ik} is equal to one and all the other elements in $\mathbf{q}_i$ are zeros. The proposed error correction algorithm is implemented through the following mixed integer quadratic problem:

$$\begin{aligned} \min_{\mathbf{Q}} \quad & \sum_{i=1}^{m} \|\mathbf{q}_i - \mathbf{p}(\mathbf{f}(\mathbf{s}_i))\|, \\ \text{subject to} \quad & q_{ij} = 0 \text{ or } 1,\ \forall \text{i} = 1,\ \cdots,\ \text{m},\ \forall \text{j} = 1,\ \cdots,\ \text{c}, \\ & \sum_{j=1}^{c} q_{ij} = 1, \\ & l_{\omega_2} \leq \sum_{i=1}^{m} q_{i2} \leq u_{\omega_2},\ \cdots,\ l_{\omega_c} \leq \sum_{i=1}^{m} q_{ic} \leq u_{\omega_c}, \end{aligned} \tag{4.18}$$

where the optimization is over $\mathbf{Q} = [\mathbf{q}_1,\ \mathbf{q}_2,\ \cdots,\ \mathbf{q}_m]^T$. While various efficient solvers of Equation (4.18) are available, the present study uses the solver developed by Bemporad and Mignone (2001). With the solution of Equation (4.18), $\mathbf{Q}$, the $\mathbf{s}_i$'s ($i = 1,\ \cdots,\ m$) are simultaneously classified by

$$\mathbf{d}(\mathbf{F}(\mathbf{S})) = [\arg\max_k\{q_{1k}\}\ \arg\max_k\{q_{2k}\}\ \cdots\ \arg\max_k\{q_{mk}\}]^T. \tag{4.19}$$

4.4 Numerical Experiments

The numerical experiments were limited to the problem of automatic removal of ECG artifact and EOG artifact in real-life EEG. The proposed IC classifier was quantitatively compared to several benchmark methods in a stringent subject-wise cross-validation procedure. In addition, the reconstructed EEG epochs were reviewed by an independent EEG expert to qualitatively evaluate the performance of the proposed artifact removal method.

4.4.1 Data Preparation

Ten right-handed volunteers from the National University of Singapore were selected for EEG measurements. These subjects fulfilled the inclusion criteria of no history of cardiovascular disease, normal eye sight and with regular eye blinks. Informed consent was obtained and nominal monetary incentive was given for their participation. Multi-channel unipolar EEG data were recorded from 17 electrodes (excluding Fp1, Fp2) placed on the scalp according to the International 10-20 system (Jasper, 1958) using the PL-EEG Wavepoint System (Medtronic, Inc. Denmark), with sampling frequency of 167 Hz and a pass band of 0.02-35 Hz using a customized bandpass filter implemented in LabView (version 6.1, National Instruments, USA). Five minutes of EEG data were recorded from each subject with their eyes open and in resting state.

These EEG recordings were firstly segmented into 12-second epochs ($l = 2000$). Each EEG epoch was then decomposed into ICs by ICA. The ICs were manually labeled as

EEG IC (class ω_1), EOG IC (class ω_2) or ECG IC (class ω_3) by an EEG expert in a random order. These labels were regarded as "true" labels, against which the performance of IC classifiers was benchmarked.

The six features ($d = 6$) as defined in Section 4.2.2 were extracted from each IC and they were used as the chief information source, in place of the IC, for classification. Combining the resulting feature vectors with the "true" labels given by the EEG expert, a subject-wise data subset of 425 samples (25 epochs $\times$ 17 ICs), $D_k := \{\mathbf{f}_i,\ y_i\}_{i=1}^{425}$ ($k = 1,\ \cdots,\ 10$), was obtained for each subject.

4.4.2 Parameter Selection

For the proposed IC classifier, two groups of parameters need to be tuned: a) the hyper-parameters for each weighted SVM, i.e. the regularization parameters, C_i^{ij} and C_j^{ij}, and the kernel parameters, γ^{ij}; b) the lower and upper bounds for each type of artifactual ICs, i.e. u_{ω_j} and l_{ω_j}.

Tuning of Hyper-parameters for SVM

Since C_i^{ij} and C_j^{ij} are connected through Equation (4.12), only one of them needs to be tuned. In the experiments, $(C_i^{ij},\ \gamma^{ij})$ were jointly tuned by a 5-fold cross-validation (Muller *et al.*, 2001) using the model selection tool in the LIBSVM package (Chang & Lin, April 2007) on the following grids: $[2^{-5},\ \cdots,\ 2^{10}] \times [2^{-10},\ \cdots,\ 2^{3}]$ (step size$= 2^{0.5}$).

Tuning of Lower and Upper Bounds for Artifactual ICs

For both ECG and EOG artifacts, they can usually be modeled as a single dipole of three spatial components (Schlgl *et al.*, 2007). It is reasonable to believe that ICA may output three artifactual ICs corresponding to the three spatial components if high-density EEG recordings (such as 64-channel EEG) are used. However, the EEG data used in the present study were recorded from 17 locations in the standard 10-20 system and ICA tended to output less than three artifactual ICs for both ECG and EOG artifacts. In the present experiment, a simple grid-search, with both u_{ω_j} and l_{ω_j} ranging from 0 to 3 and a search step size of 1, was performed for ECG ICs and EOG ICs respectively to obtain optimal values for u_{ω_j} and l_{ω_j} that gave the highest balanced accuracy.

4.4.3 Quantitative Evaluation

Subject-Wise Cross Validation

Among the subsets $\{D_k\}_{k=1}^{10}$ from 10 subjects, samples from 9 subjects were used to form a training set D_{tra}, and the samples from the left-out subject were used to form a testing set D_{tes}. Practically, this resampling procedure resulted in 10 pairs of D_{tra} and D_{tes} in total. In the numerical experiments, for each pair of D_{tra} and D_{tes}, D_{tra} was used for tuning of parameters and training of SVM. The trained classifier was then tested on left-out dataset D_{tes}. The major advantages of such subject-wise cross-validation procedure include that: a) each testing set is independent of the training set and thus the test error simulates the classifier's generalization performance on other unseen subjects;

b) classifier performance obtained on multiple testing sets can be used for evaluating the significance in the comparison of two classifiers (Shen *et al.*, 2007).

Performance Measures

For a given testing set with c classes, let n_{ij} be the number of samples from ω_i (true label) being classified to ω_j by the classifier (predicted label). The following measures were used for evaluating the performance of the proposed IC classifier.

- **Balanced accuracy**: It is the average of accuracy on each class, i.e.

$$BAcc = \frac{1}{c}\sum_{i=1}^{c}\left(n_{ii}/\sum_{j=1}^{c} n_{ij}\right) \times 100\% \tag{4.20}$$

- **RCI**: It measures the amount of uncertainty about the class of an input reduced by a classifier (Sindhwani *et al.*, 2001), i.e.

$$RCI = (H_I - H_O)\big/H_I \times 100\%, \tag{4.21}$$

  where H_I and H_O denote the prior and posterior uncertainty about the class of an unseen input respectively. Here, $H_I = -\sum_{i=1}^{c}\left(p_i^{in}\log_2 p_i^{in}\right)$ and $H_O = \sum_{j=1}^{c}\left(p_j^{out}H_{O_j}\right)$, with $p_i^{in} = \sum_{j=1}^{c} n_{ij}/\sum_{i=1}^{c}\sum_{j=1}^{c} n_{ij}$, $p_j^{out} = \sum_{i=1}^{c} n_{ij}/\sum_{i=1}^{c}\sum_{j=1}^{c} n_{ij}$, $p_{ij} = n_{ij}/\sum_{i=1}^{c} n_{ij}$, and $H_{O_j} = -\sum_{i=1}^{c}\left(p_{ij}\log_2 p_{ij}\right)$. RCI has been shown to be a useful performance measure that captures a detailed picture of classifier performance while being immune to the effect of prior class probabilities (Sindhwani *et al.*, 2001).

- **Overall agreement**: It measures the portion of cases that two raters agree without distinguishing between agreements on different classes (Hripcsak & Heitjan, 2002), i.e.

$$OA = \sum_{i=1}^{c} n_{ii} / \sum_{i=1}^{c} \sum_{j=1}^{c} n_{ij}. \tag{4.22}$$

- **Specific agreement**: It measures the degree of agreement on each class (Hripcsak & Heitjan, 2002). Specific agreement on class ω_k is calculated as:

$$SA_{\omega_k} = 2n_{kk} / (\sum_{i=1}^{c} n_{ik} + \sum_{j=1}^{c} n_{kj}). \tag{4.23}$$

- **Cohen's kappa**: It is calculated as

$$kappa = (OA - EA) \big/ (1 - EA), \tag{4.24}$$

where OA refers to the overall agreement and EA is the agreement expected by chance: $EA = \sum_{k=1}^{c} (\sum_{i=1}^{c} n_{ik} \cdot \sum_{j=1}^{c} n_{kj}) / (\sum_{i=1}^{c} \sum_{j=1}^{c} n_{ij})^2$ (Cohen, 1960).

Other Methods for Comparison

The proposed IC classifier was compared to the following five benchmark methods:

(1) The weighted PWC_PSVM as given in Section 4.3.1;

(2) The standard SVM trained on under-sampled balanced dataset as used in the stud-

ies of Nicolaou & Nasuto (2004) and Shoker et al. (2005);

(3) GMM (with class conditional probability densities estimated by using the software package developed by Bouman (1997));

(4) KNN (K from 1 to 9 were tested and the best results obtained with K=5 were reported);

(5) LDF using the minimum-squared-error solution.

4.4.4 Qualitative Evaluation

An independent EEG expert was invited to qualitatively evaluate the performance of the proposed artifact removal system by examining each of the 250 raw EEG epochs and its corresponding reconstructed EEG epoch simultaneously. The evaluation of each epoch was based on three aspects: a) the removal of ECG artifact, b) the removal of EOG artifact and c) the preservation of inherent brain activities (hereafter referred as EEG preservation). The EEG expert was required to give detailed judgment on each of these three aspects.

For the evaluation of ECG or EOG removal, "*no improvement*" was used to indicate that almost no change was observed in the amount of artifacts before and after artifact removal; "*minor improvement*" indicated that artifacts were partially removed but still observed in the reconstructed EEG; a score of "*almost removed*" was given when almost no considered artifact was observed in the reconstructed EEG. For the evaluation of EEG preservation, "*major attenuation*" was used to indicate that inherent brain activities were

significantly attenuated; a score of "*minor attenuation*" was given when the amplitude of inherent brain activities was slightly reduced but still clearly visible; "*well preserved*" indicated that almost no change in brain activities was observed before and after artifact removal.

4.5 Results

4.5.1 Validation of the Unique Properties of the Learning Problem

The collected data as described in Section 4.4.1 showed that among the 17 ICs separated from each 12-second EEG epoch, there were only one ECG IC and no more than two EOG ICs. In total, 250 ECG ICs, 292 EOG ICs and 3,708 EEG ICs were separated from 250 EEG epochs from the ten subjects. Fig. 4.2a and Fig. 4.2b show a typical 12-second EEG epoch and the resulting ICs, respectively. As can be seen, only one EOG IC (marked by a square) and one ECG IC (marked by a circle) were separated from the EEG epoch. This verified the unique properties of the learning problem at hand: the uneven class distributions and the underlying structural information as given in Equation (4.9) and Equation (4.10), respectively. These properties were reaffirmed by the optimal values of u_{ω_j} and l_{ω_j} for EOG ICs and ECG ICs determined through grid-search, i.e. $u_{\omega_2} = 2,\ l_{\omega_2} = 1,\ u_{\omega_3} = l_{\omega_3} = 1$.

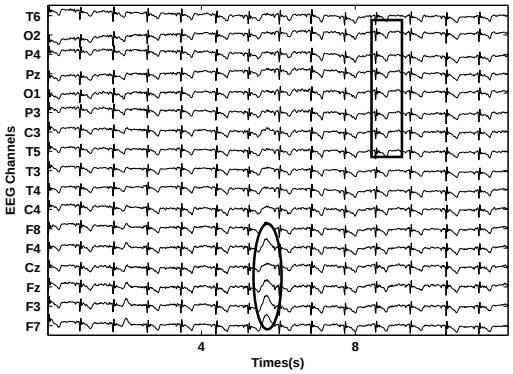

(a)

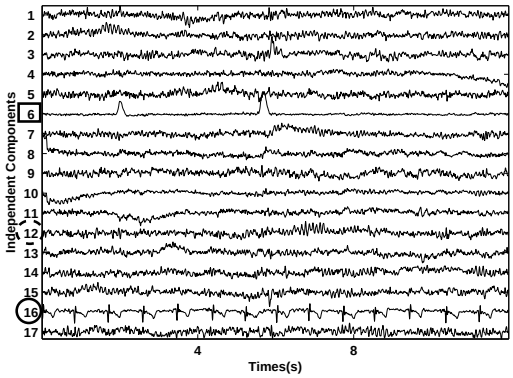

(b)

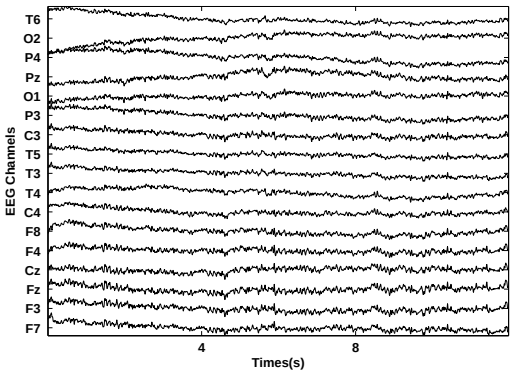

(c)

Figure 4.2: Typical example of (a) a 12-second EEG epoch (the waveforms marked by rectangular and ellipse are typical ECG and eye-blinking artifacts respectively), (b) its resultant ICs given by ICA (the IC marked by a square was "true" EOG IC and the one marked by a circle was "true" ECG IC labeled by the EEG expert. The IC marked by a dashed circle was a "true" EEG IC but misclassified as ECG IC by the weighted PWC_PSVM. This misclassification was corrected by the proposed error correction algorithm), and (c) the corresponding reconstructed EEG epoch after artifact removal by the proposed method.

4.5.2 Quantitative Comparison

Detailed classification results and performance measures of the proposed method and the benchmark methods are summarized in Table 4.1. The numbers shown are the averages over 10 test datasets corresponding to 10 pairs of D_{tra} and D_{tes}. The p-values (given in parentheses) were obtained in the paired t-test (Alpaydin, 2004; Box *et al.*, 1978) between the proposed method and each of the benchmark methods. Based on the results in Table 4.1, the proposed method appears to be superior to all the benchmark methods. Details are as follows.

Table 4.1: Performance comparison between the proposed method (i.e. weighted PWC_PSVM with error correction) and five benchmark methods (weighted PWC_PSVM, standard SVM, GMM, KNN and LDF). The number in parenthesis is the p-value obtained in the paired t-test between each of the benchmark methods and the proposed method. The symbols '+' and '-' indicate statistically significant wins or losses over the proposed method (p-value < 0.05). P: predicted label; T: true label.

Classifier	**Confusion Matrix**				**BAcc (%)**	**RCI (%)**	**Kappa**	**OA**	**SA**		
	P\T	ω_1	ω_2	ω_3					ω_1	ω_2	ω_3
Weighted PWC_PSVM With Error Correction	ω_1	3540	20	4	95.67	76.76	0.82	0.95	0.97	0.75	0.98
	ω_2	164	272	0							
	ω_3	4	0	246							
Weighted PWC_PSVM	ω_1	3474	20	2	95.35 (0.05)	70.33 (**0.00**$^-$)	0.78 (**0.01**$^-$)	0.94 (**0.01**$^-$)	0.95 (**0.01**$^-$)	0.74 (0.40)	0.88 (**0.01**$^-$)
	ω_2	171	272	0							
	ω_3	63	0	248							
Standard SVM	ω_1	3424	20	4	94.63 (**0.02**$^-$)	67.15 (**0.00**$^-$)	0.74 (**0.00**$^-$)	0.93 (**0.00**$^-$)	0.96 (**0.00**$^-$)	0.70 (**0.02**$^-$)	0.87 (**0.00**$^-$)
	ω_2	212	272	0							
	ω_3	72	0	246							
GMM	ω_1	3653	71	20	88.73 (**0.00**$^-$)	68.34 (**0.00**$^-$)	0.85 (0.23)	0.97 (**0.02**$^+$)	0.98 (**0.01**$^+$)	0.79 (0.40)	0.95 (**0.00**$^-$)
	ω_2	49	221	0							
	ω_3	6	0	230							
KNN(K=5)	ω_1	3661	69	27	87.87 (**0.00**$^-$)	66.46 (**0.00**$^-$)	0.85 (0.45)	0.97 (0.07)	0.98 (**0.04**$^+$)	0.82 (0.22)	0.90 (**0.01**$^-$)
	ω_2	28	221	0							
	ω_3	19	2	223							
LDF	ω_1	3691	129	197	58.71 (**0.00**$^-$)	29.08 (**0.00**$^-$)	0.53 (**0.00**$^-$)	0.92 (**0.00**$^-$)	0.96 (**0.00**$^-$)	0.70 (0.20)	0.34 (**0.00**$^-$)
	ω_2	12	162	0							
	ω_3	5	1	53							

Comparison Between the Proposed Method and the Modeling Approaches

As shown in Table 4.1, the proposed method achieved significantly higher balanced accuracy and RCI than the modeling approaches (including GMM, KNN and LDF). It performed well on all the three classes. In comparison, all the modeling approaches showed very good performance on EEG ICs; however, their performance on EOG and ECG ICs was not satisfying. In the context of artifact removal, the proposed method which achieved a better tradeoff among removing artifacts and preserving inherent brain activities is preferable. It worth noting that the insignificant wins or even loss of the proposed approach over the modeling approaches on Kappa, overall agreement and specific agreement can be attributed to that these performance measures are subject to the effect of prior class probabilities, and thus it would not be fair to solely use these measures for performance comparison.

Comparison Between the Proposed Method and the Standard SVM

As can be seen from Table 4.1, the proposed method showed significant wins over the standard SVM on all performance measures. The results given by the confusion matrices suggest that the better performance of the proposed method is mainly due to its higher accuracy on EEG ICs as compared to the standard SVM (3520/3708 vs. 3424/3708). One plausible reason is that the standard SVM as used in the studies of Nicolaou & Nasuto (2004) and Shoker et al.(2005) was trained on down-sampled balanced training data (with large portion of samples of EEG ICs being discarded). Such down-sampling causes loss of information and thus leads to suboptimal performance on the majority

class (Liu *et al.*, 2006).

Comparison Between the Weighted PWC_PSVM With Error Correction and the Weighted PWC_PSVM Without Error Correction

As shown in Table 4.1, the weighted PWC_PSVM with error correction showed significant wins over the weighted PWC_PSVM method without error correction on almost all performance measures. The confusion matrices show that the incorporation of error correction resulted in a large increase in the accuracy on EEG ICs (3540/3708 vs. 3474/3708) at a tiny cost of the accuracy on ECG ICs (246/250 vs. 248/250). It indicates the goodness of the proposed error correction algorithm in that it helps to achieve a better tradeoff between removing artifacts and preserving inherent brain activities. Consider a batch of ICs resulting from a given EEG epoch. The error correction algorithm prevents the number of ICs predicted as ECG/EOG ICs from either exceeding the corresponding upper limits or being less than the corresponding lower limits as given in Equation (4.10), by picking out appropriate number of most probable artifactual ICs (with largest posterior probability of belonging to the classes of ECG/EOG ICs). Fig. 4.2b shows a typical example when the weighted PWC_PSVM classified two ICs (marked by a circle and a dashed circle respectively) as ECG ICs but the IC marked by a dashed circle was actually an EEG IC. The proposed error correction algorithm corrected this error by incorporating the constraint on ECG ICs: $1 \leq m_{\omega_3} \leq 1$.

4.5.3 Review of Reconstructed EEG

The qualitative evaluation of the proposed artifact removal system by the independent EEG expert is given in Table 4.2. The amount of ECG artifacts was reduced in 98.4% of the epochs, with 98.0% indicated as ”almost removed” and 0.4 % indicated as ”minor improvement”. EOG artifacts were removed in 96.8% of the epochs, with 92.0% indicated as ”almost removed” and 4.8% indicated as ”minor improvement”. In 88.4% of the epochs, inherent brain activities were well preserved and in 10.8% of the epochs, brain activities were slightly attenuated. Only 0.8% of the epochs suffered from major attenuation in brain activities. Fig. 4.2c shows the reconstructed EEG epoch corresponding to the raw EEG epoch shown in Fig. 4.2a after artifact removal by the proposed method. The strong ECG and EOG artifacts in raw EEG epoch were barely seen in the reconstructed EEG epoch.

Table 4.2: Qualitative evaluation of the proposed method on artifact removal and EEG preservation by an independent EEG expert.

ECG Removal	*No improvement* 1.6%	*Minor improvement* 0.4%	*Almost removed* 98.0%
EOG Removal	*No improvement* 3.2%	*Minor improvement* 4.8%	*Almost removed* 92.0%
EEG Preservation	*Major attenuation* 0.8%	*Minor attenuation* 10.8%	*Well preserved* 88.4%

4.6 Discussion

A novel IC classifier which combines a modified probabilistic multi-class SVM and an error correction algorithm has been proposed in the present study. The proposed approach has been compared with several benchmark methods: the modified probabilistic multi-class SVM as described in Section 4.3.1 without error correction, the standard SVM used by Nicolaou & Nasuto (2004) and Shoker et al. (2005), GMM, KNN and LDF. In a stringent subject-wise cross-validation procedure, numerical experiments have shown that the proposed IC classifier is preferable to the benchmark methods in the context of artifact removal by achieving a better tradeoff between removing artifacts and preserving inherent brain activities. Moreover, qualitative review of the reconstructed EEG epochs by an independent expert has demonstrated that after artifact removal inherent brain activities are largely preserved. The superiority of the proposed approach can be attributed to the following reasons.

Firstly, the unbalanced nature of the underlying data as described in Equation (4.9) is properly addressed by using the modified probabilistic multi-class SVM. This multi-class SVM is modified from the probabilistic multi-class SVM proposed by Hastie and Tibshirani (1998), by replacing all standard binary SVMs with weighted SVMs. It uses real unbalanced data for training and compensates the bias of prior class probabilities by penalizing more on the classification errors produced by the samples from the minority class. As shown by experimental results, in comparison to the modeling approaches (GMM, KNN and LDF), the modified multi-class SVM achieved a better tradeoff among classification performance on each class by greatly increasing classification accuracy on

EOG ICs and ECG ICs at the cost of a minor decrease in classification accuracy on EEG ICs, making it preferable in the context of artifact removal where it is aimed to effectively remove artifacts while keeping inherent brain activities well preserved. The proposed method is also superior to the standard SVM used in the studies of Nicolaou & Nasuto (2004) and Shoker et al. (2005) which was trained on a balanced training set formed by down-sampling of the majority class. The down-sampling inevitably causes loss of information and thus leads to the suboptimal performance of the standard SVM on the majority class (Liu *et al.*, 2006).

Secondly, useful structural information of the underlying data is incorporated in decision making through the error correction algorithm. The structural information in the present study is the constraints on the number of ICs responsible for each type of artifact resulting from a given EEG epoch, as described in Equation (4.10). It is worth noting that this structural information is different from class priors: class priors can be directly included by many modeling methods (e.g. KNN, GMM); however, the constraints as of Equation (4.10) exist among the batch of ICs resulting from the same EEG epoch and thus can only be exploited by considering the batch of ICs collectively (as the proposed error correction algorithm does). Conventional classifiers, such as KNN, GMM and LDF, which consider each sample independently, are unable to incorporate such structural information. As shown by experimental results, a better tradeoff between removing artifacts and preserving brain activities is achieved by incorporating this structural information through the error correction algorithm. The proposed error correction algorithm is significant in both theoretical and practical aspects. It appears

generally useful for classification problems where similar structural information is contained in the test samples and thus simultaneous classification of several test samples is necessary.

Moreover, the use of a probabilistic SVM may also contribute to the superior performance of the proposed method. Given a test sample, $\mathbf{f}$, the decision of conventional SVM is based on the sign of standard SVM outputs, $g^{ij}(\mathbf{f})$ as in Equation (4.14), or the half space in $\mathscr{H}$ into which $\phi^{ij}(\mathbf{f})$ falls. Such an approach ignores the relative confidence in classification, or the distance that $\phi^{ij}(\mathbf{f})$ is from the separating hyperplane. In contrast, the probabilistic SVM is based on the calibrated confidence measures, i.e. the estimates of posterior probabilities. The superiority of probabilistic SVM over standard SVM has been recently demonstrated in a few studies in the domain of machine learning (see Duan & Keerthi, 2005; Platt, 2000; Shen *et al.*, 2007, 2008b), while its application in EEG signal processing remains rare (Shen *et al.*, 2008a).

The present study has been limited to the removal of ECG and eye-blinking artifacts. However, the idea of the proposed method can be generally extended to the removal of other types of stereotyped artifacts that have stereotyped scalp projections and can be isolated to one or more ICs by ICA (e.g. artifact due to muscle tension), provided suitable features are available. It should be acknowledged that possible discontinuities may be resulted in at the beginning and end of each reconstructed EEG epoch, although it appears minimal in our experiments. As a precaution, the segmentation should be retained in the review/use of reconstructed EEG to prevent the potential discontinuities from influencing EEG interpretation.

4.7 The MATLAB-based Graphical User Interface for Automatic Artifact Removal

A friendly graphical user interface (GUI) has been developed with MATLAB (version R2006a, The MathWorks, Inc.) for automatic removal of ECG and EOG artifacts using the proposed artifact removal method with the IC classifier trained offline (see Fig. 4.3). Given an raw EEG epoch contaminated with artifacts, an user can obtain the artifact-free

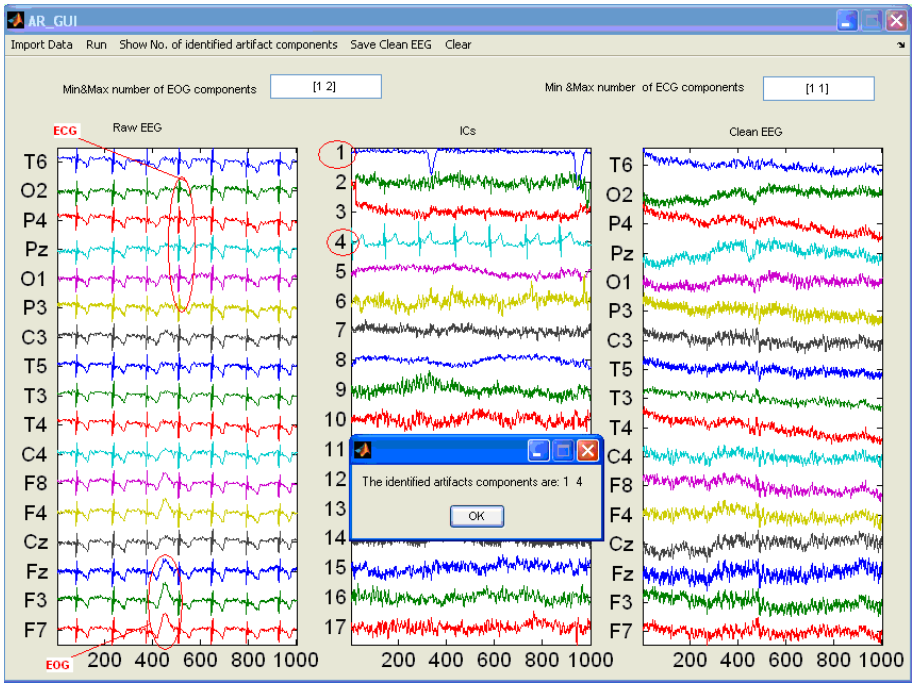

Figure 4.3: The MATLAB-based GUI for automatic EEG artifact removal. This figure shows a typical example with the input being a 12-second raw EEG segment contaminated EOG and ECG artifacts (marked with an ellipse). ICA resulted in one EOG IC and one ECG IC (marked by a circle). The proposed method correctly identified the two artifactual ICs, and thereby obtained artifact-free EEG.

EEG epoch by clicking ”Run”. The GUI allows the user to specify the upper and lower limits for the number of artifactual ICs responsible for ECG and EOG artifacts (i.e. u_{ω_j} and l_{ω_j}) according to the optimal values obtained from offline training. It displays the

raw EEG epoch, the separated ICs, the artifact-free EEG epoch as well as the predicted artifactual ICs.

4.8 Concluding Remarks

In this chapter, a novel automatic EEG artifact removal method has been presented. The proposed method takes into account the unique properties of the learning problem at hand by: 1) using weighted probabilistic SVM to handle the unbalanced data, and 2) implementing an error correction algorithm to accommodate useful structural information of the underlying data. Quantitative comparisons of the proposed method to several benchmark methods on real-life EEG data showed that the proposed method is preferable to the other methods in the context of artifact removal by achieving a better tradeoff between removing artifacts and preserving inherent brain activities. A qualitative review of the reconstructed EEG epochs also revealed that artifacts were greatly attenuated while brain activities were largely preserved. The proposed method appears to be well suited for automatic EEG artifact removal.

Chapter 5

Heartbeat Evoked Potential: A Promising Objective Measure of Pain Perception

5.1 Introduction

Pain, as an unpleasant sensory and emotional experience, if uncontrolled or under-treated, can seriously interfere with normal functioning and impair quality of life. In many cases, the failure to adequately treat pain is due to the lack of accurate pain assessment methods (Rissacher *et al.*, 2007), especially when subjective methods like self-report are not applicable due to patients' inability to formulate their pain experience (e.g. young children, patients with dementia, patients under anesthesia). Therefore, an

objective measure of pain perception, which does not rely on the patients' ability to do self-report and are not subject to the bias of the subjects, would be of great clinical significance.

A promising objective method for pain assessment is to measure the brain's electrical activity by EEG. Various EEG measures, in terms of spontaneous EEG oscillations or BEPs, have been reported to correlate with pain in the past decades. However, there is still no evidence showing that these EEG measures can be used as specific indicators of pain perception. Prospective EEG measures which can reliably reflect pain perception are yet to be explored.

Recently, some studies (Edwards *et al.*, 2008, 2002, 2001; Martins *et al.*, 2009; McIntyre *et al.*, 2006) have shown that nociceptive responding, pain-related evoked potential and/or pain rating can be modulated across the cardiac cycle. There is also emerging evidence that afferent signals from the heart can modulate pain perception through the neural pathways including the PAG, the thalamus, the hypothalamus, the amygdala and the prefrontal cortex (McCraty *et al.*, 2009). These seem to indicate close neuronal links between pain perception and central processing of cardiac-cycle related activities. Therefore, it is interesting to see whether the cardiac-cycle related brain activities, in particular, the HEP (Chen & Dworkin, 1982; Dirlich *et al.*, 1998; Jones *et al.*, 1986; Leopold & Schandry, 2001; McCraty *et al.*, 2009; Montoya *et al.*, 1993; Pollatos & Schandry, 2004; Riordan *et al.*, 1990; Schandry & Montoya, 1996; Schandry *et al.*, 1986), could lead to an objective and non-intrusive biomarker of pain perception.

Chen and Dworkin (1982) in their pilot work attempted to link the HEP with pain per-

ception. The study provides so far the only evidence of the relation between the HEP and pain. However, the study was performed on patients with chronic headache. It is known that the perception of acute pain and chronic pain involves different brain networks (Apkarian *et al.*, 2005) and that chronic pain may be associated with neuroplastic changes in the nervous system (Wilder-Smith *et al.*, 2002). Hence, acute and chronic pain may reflect differently.

The present study is the first attempt to investigate the correlation between acute pain perception and the HEP. In the study, ECG R-peak locked HEP is examined in three conditions: a) no-task control, b) no-pain control and c) cold pain induced by CPT. Comparisons are made not only between the HEP in pain and no-pain conditions but also between the HEP during the first and last 5 mins of cold pain condition. Results show that the HEP is significantly suppressed in the cold pain condition as compared to the control conditions, especially over the right hemisphere which is contralateral to the painful stimulation. A significant correlation is found between the HEP suppression and subjective pain ratings. These demonstrate the potential usefulness of HEP for pain assessment.

5.2 Methods

5.2.1 Subjects

Twenty-one healthy young adults (12 males and 9 females, ages: 25.2 ± 3.6 years) participated in the experiment. They were recruited from the National University of Singapore. All the subjects were right-handed, not on medication, without any history of neurological, psychiatric and cardiovascular problems. Each subject was given a detailed explanation of the experimental procedure and each signed a consent form prior to the experiment. The study was approved by the Institutional Review Board of the National University of Singapore (NUS-IRB, also referred to as the Research Ethics Committee in some countries), which requires all experiments to comply with the Declaration of Helsinki, the Belmont Report and all relevant laws and regulations in Singapore.

5.2.2 Experimental Procedure

In the experiment, each subject was comfortably seated in an upright chair in a brightly lit, sound attenuated and temperature controlled (24 to 26 ^{o}C) room, and participated with eyes open in three conditions: passive no-task control, no-pain control and cold pain induced by CPT (see Section 3.2 for details). The three conditions were presented in randomized order within a single session to remove potential confounds introduced by the task order, such as changes in anxiety levels due to adaptation to the experimental environment, the reaction to electrode application etc. The no-task control and no-pain

control conditions lasted for 5 mins while both the cold pain condition lasted for 10 mins.

In the no-task control condition, the subject was asked to relax and stay awake.

In the no-pain control condition, the subject was required to immerse his/her non-dominant hand in cool water maintained at a temperature of 25 ^{o}C and count backwards in 3's from a randomly determined 4-digit number throughout the test. This design was aimed to keep the subjects vigilant and focused on the experiment at constant level and control for innocuous pressure and cool sensation associated with hand immersion in the cool water.

In the cold pain condition, the subject was asked to immerse his/her non-dominant hand into cold water maintained at 10 ^{o}C . However, the subject was allowed to take the hand out of the water before the end of the 10-min recording block if the pain became unbearable. The subject was required to verbally rate the perceived pain intensity and unpleasantness on two 11-point numerical rating scales (NRSs) every minute. The NRSs for the perceived pain intensity/unpleasantness were as follows: 0=no pain/neutral, 1=barely noticeable pain/barely unpleasant, 5=mild pain/distressing and 10=maximum pain tolerable/worst unpleasantness imaginable, as shown in Fig. 3.4a and Fig. 3.4b respectively.

In the present study, both the no-task control condition and no-pain control condition were considered as baseline conditions in contrast to the cold pain condition. The no-task control was commonly used as the baseline condition in many neurophysiological studies (see e.g. Backonja *et al.*, 1991; Chang *et al.*, 2001b, 2002; Chen *et al.*, 1989b;

Chen & Rappelsberger, 1994). Following the work by Dowman et al. (2008), the no-pain control condition was also included because, though being arguable, the no-pain control condition may represent a better baseline condition than no-task control condition.

5.2.3 Data Acquisition

EEG and Lead-II ECG were simultaneously recorded using the Neuroscan NuAmps system (see Fig. 3.1) at a sampling rate of 250 Hz and with a bandpass filtering between 0.5 and 100 Hz, from 30 electrodes arranged according to the extended 10-20 system shown in Fig. 3.2 with a 32-Channel Quick-Cap (Compumedics Neuroscan, USA) and two surface ECG electrodes attached on the right arm and left leg respectively. The scalp EEG was referenced to the average of A1 and A2, with AFz serving as the ground electrode.

5.2.4 Data Preprocessing

EEG segments contaminated with strong muscle artifacts were manually rejected by visual inspection. The EEG data recorded during the periods when the subjects were verbally rating their pain intensity and unpleasantness (within the first 10 seconds of each minute in the cold pain condition) were also rejected. The eye-blinking and eye-movement artifacts were removed from the EEG using the novel ICA based method developed in the earlier work (Shao *et al.*, 2009) as given in Chapter 4. The Hjorth

method (Hjorth, 1975), which is believed to be able to substantially reduce the cardiac field artifact (CFA) (Montoya *et al.*, 1993; Pollatos *et al.*, 2005; Pollatos & Schandry, 2004), was used to reduce the possible effect of CFA on EEG data. The EEG signals were also filtered using a customized bandpass filter with a pass band of 0.5-15 Hz implemented in MATLAB (Version 7.2, The Mathworks). The R-peaks of ECG were detected with the package developed by Zhang et al. (2006) and used as the triggers for EEG averaging. Sweeps were defined as starting 100 ms before to 900 ms after each of the R-peaks.

5.2.5 Data Analysis

The averaged HEP for each subject and the grand average of the HEP across all subjects, were computed separately for the first and last 5 min of the cold pain condition (denoted by Cold Pain 1 and Cold Pain 2, respectively), the no-pain control condition and the no-task control condition. For the ease of analysis, the 30 EEG channels were grouped into 7 anatomical scalp sectors (left-frontal: Fp1, F7, F3; right-frontal: Fp2, F8, F4; left-central: FT7, FC3, C3, T3, CP3, TP7; right-central: FT8, FC4, C4, T4, CP4, TP8; left-parietal-occipital: T5, P3, O1; right-parietal-occipital: T6, P4, O2; midline: Fz, FCz, Cz, CPz, Pz, Oz). The division into left and right scalp sectors was to facilitate the investigation of potential laterality effects. Analysis of variance (ANOVA) was performed on the mean HEP magnitude over each scalp sector to investigate between-condition HEP differences, where the HEP magnitude was computed as the average of absolute values of HEP amplitudes over the time interval with prominent voltage deflec-

tion shown (i.e. 200-600 ms post ECG R-peak in the present study).

The potential influence of heart rate change on the HEP was examined by comparing for each subject the heart rate and the mean HEP magnitude over a scalp sector where significant differences between the HEP in the cold pain and control conditions were shown.

5.3 Results

5.3.1 Subjective Pain Ratings

Fig. 5.1 shows the mean ($\pm$standard error of the mean, SEM) of pain intensity and unpleasantness ratings given by the 21 subjects at 1-min interval during the cold pain condition. As can be seen, both the mean pain intensity and pain unpleasantness ratings steadily decreased within the first 6 minutes, and after 6 minutes the pain ratings became almost constant. This is slightly different from what was reported by most studies in the literature, that pain intensity ratings increased in the first several (usually < 4) minutes, and after that the pain ratings declined steadily (see e.g. Chang *et al.*, 2002) or became almost constant (see e.g. Dowman *et al.*, 2008).

The discrepancy between the subjective pain ratings obtained in the present study and those reported in the past studies is probably due to the use of cold water with higher temperatures for CPT. According to Eccleston (1995), for low temperature (0 ^{o}C) CPT, there is a growing pain intensity (first pain) which reaches its peak between 2 to 4 min-

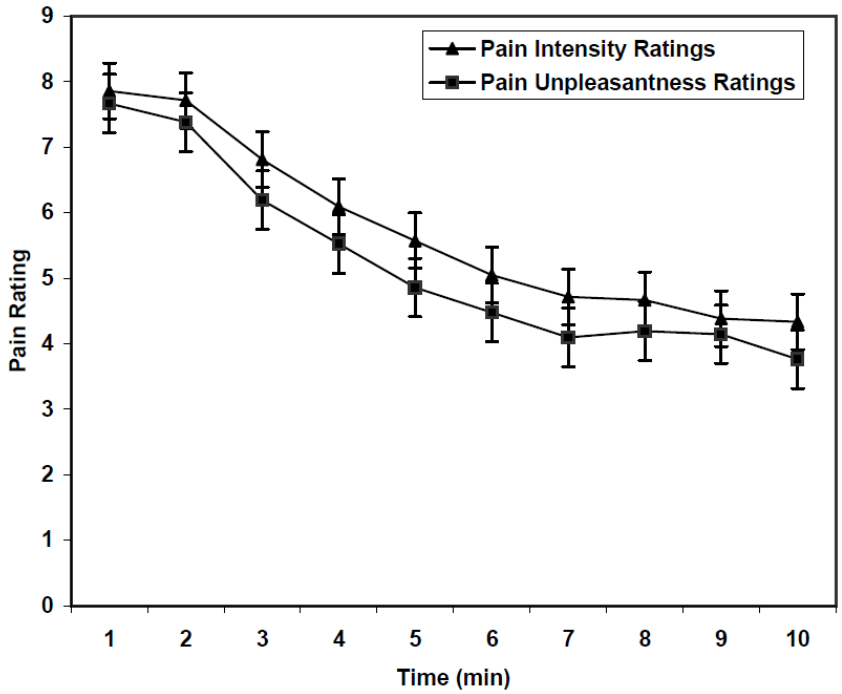

Figure 5.1: Mean (±SEM) pain intensity and unpleasantness ratings obtained at 1 min interval throughout the 10-min cold pain recording block. Pain intensity and unpleasantness were rated on two 11-point numerical rating scales, where 0=no pain/neutral, 1=barely noticeable pain/barely unpleasant, 5=mild pain/distressing, and 10=maximum pain tolerable/worst unpleasantness imaginable.

utes exposure. If the subject is still exposed to the cold water at this temperature, there will be a second sharp increase in pain intensity (i.e. second pain) without numbness. For warmer temperature CPT (3-7 ^{o}C), there tends to be a first pain of lower intensity and shorter duration, and there is no second pain. Thus, it is possible that for the CPT with even higher temperature (10 ^{o}C) used in the present study, the first pain is of even smaller intensity and shorter duration, probably within one minute. As in the present study, the first pain ratings were obtained from the subjects at the end of the first minute, the initial sharp increase in pain ratings resulting from the first pain was not captured.

5.3.2 HEP Morphology and Topography

Fig. 5.2 shows the across-subject grand averages of HEP over all EEG channels in the Cold Pain 1, no-pain control and no-task control conditions. From Fig. 5.2, prominent HEP can be observed in both no-task control and no-pain control conditions. The HEP appeared as a positive or negative deflection (depending on channel location) in the latency range of 200-600 ms post ECG R-peak, peaking at around 300 ms post ECG R-peak, mainly distributed over the frontal and central scalp regions. This can also be clearly seen from the scalp power maps of the across-subject grand averages of HEP in the three conditions at the latencies of 200 ms, 300 ms, 400 ms, 500 ms and 600 ms post ECG R-peak, as shown in Fig. 5.3.

5.3.3 HEP and Cold Pain Perception

Cold Pain vs. Control Conditions

The prominent HEP observed in both no-task and no-pain control conditions appeared to be largely suppressed in cold pain condition. Qualitatively, this can be seen from Fig. 5.2 and Fig. 5.3. The HEP suppression by cold pain can also be quantitatively evaluated by between-condition comparisons of the mean HEP magnitudes within the latency range of 200-600 ms (average over all channels within each sector and across all subjects), as shown in Table 5.1. Each value in Table 5.1 represents the mean HEP magnitude within the latency range of 200-600 ms for a specific scalp sector in a specific test condition. The symbol '*' indicates significant (p-value< 0.05) differences in the

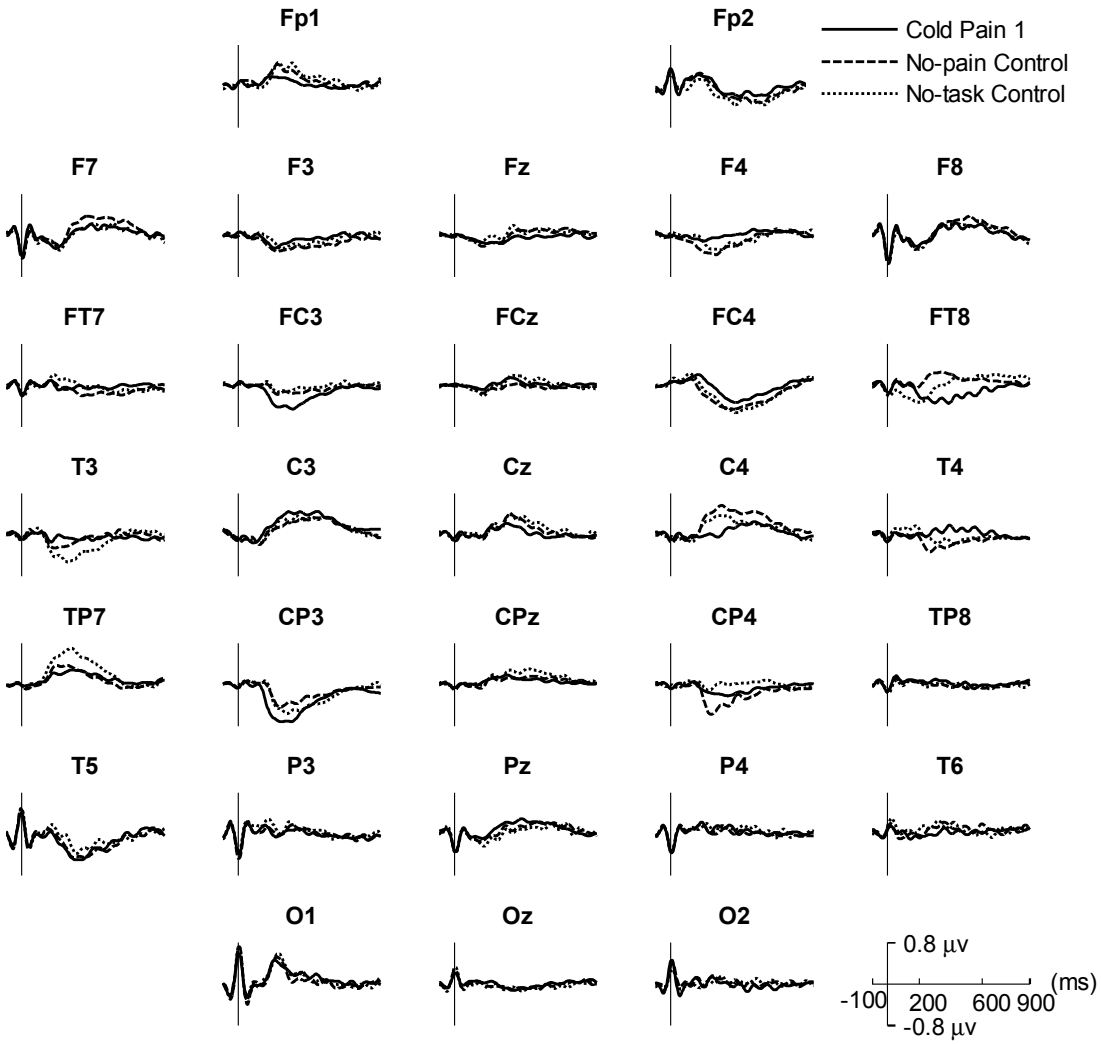

Figure 5.2: The across-subject grand averages of HEP in the Cold Pain 1, no-pain control and no-task control conditions.

mean HEP magnitude between the cold pain condition and either control condition. As can be seen from Table 5.1, there were significant HEP suppression between cold pain condition and either control condition over several scalp sectors. Especially for the right-frontal, right-central and midline scalp sectors, significant HEP magnitude decreases in comparison to both the no-task control and the no-pain control conditions were shown. That is to say, the HEP suppression was more evident over the right hemisphere which was contralateral to the painful stimulation. However, there was no significant difference

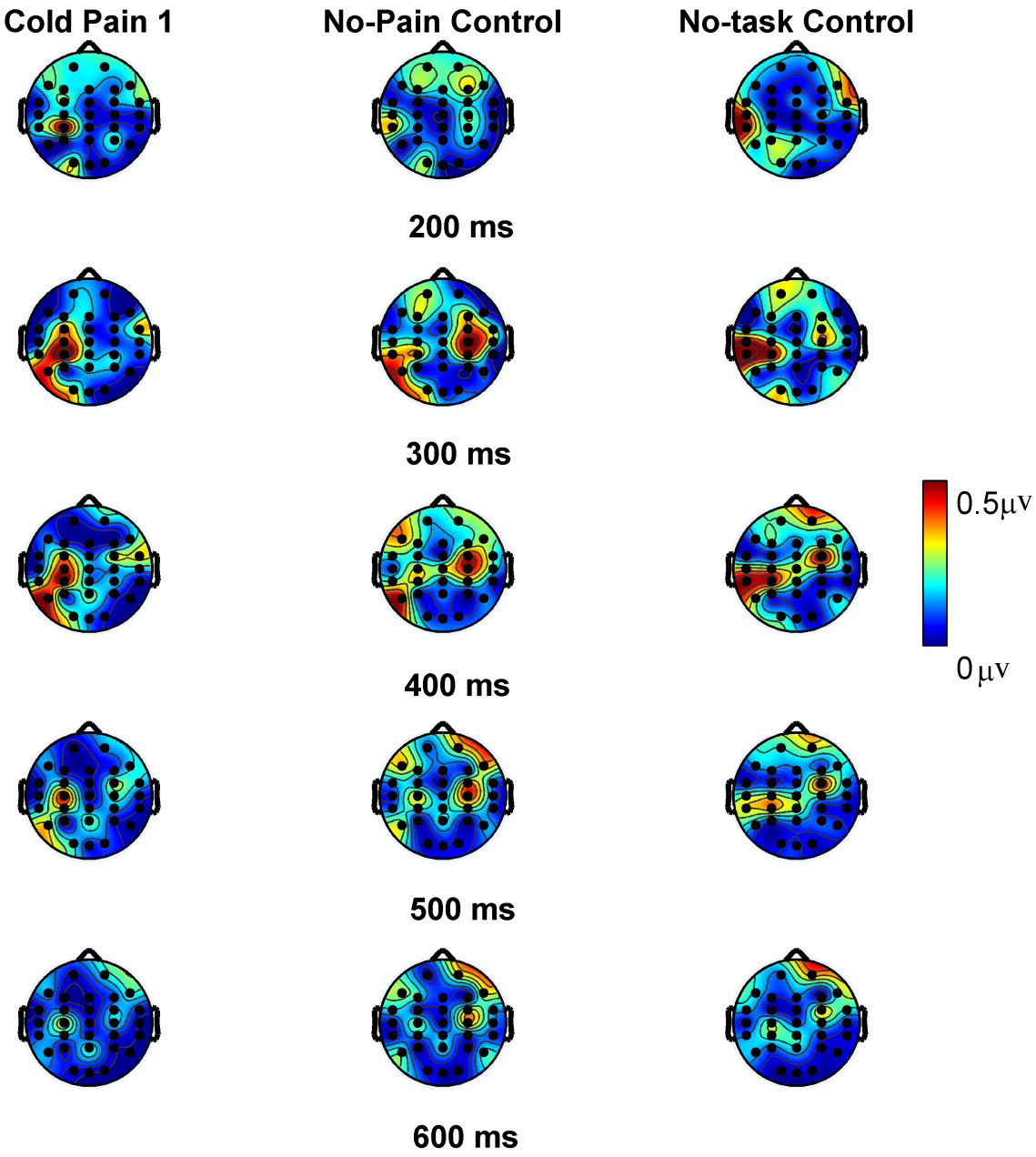

Figure 5.3: Scalp power maps of the across-subject grand averages of HEP in Cold Pain 1, no-pain control and no-task control conditions at the latencies of 200 ms, 300 ms, 400 ms, 500 ms and 600 ms post ECG R-peak.

between the mean HEP magnitudes in the two control conditions over all scalp sectors.

This implies that the HEP suppression may be specific to pain perception.

Table 5.1: Mean HEP magnitudes within the latency range of 200-600 ms (average over all channels within each sector and across all subjects) in Cold Pain 1, no-pain control, no-task control and Cold Pain 2 conditions. The symbol '*' indicates statistically significant higher HEP magnitude in no-pain control, no-task control or Cold Pain 2 conditions than that in Cold Pain 1 condition (p-value< 0.05).

Scalp Sectors	Mean HEP Magnitude(μV)			
	Cold Pain 1	No-Pain Control	No-task Control	Cold Pain 2
Left-frontal	0.48	0.65	0.72	0.51
Right-frontal	0.42	0.62*	0.66*	0.46
Left-central	0.51	0.59*	0.60	0.53
Right-central	0.40	0.66*	0.59*	0.41
Left-parietal-occipital	0.43	0.44	0.41	0.43
Right-parietal-occipital	0.28	0.33*	0.34	0.29
Midline	0.34	0.41*	0.41*	0.37*

In order to provide a clearer picture of the HEP suppression, means ($\pm$SEM) of percent decrease in the HEP magnitude across all subjects in Cold Pain 1 as compared to both control conditions (i.e. $[(control - cold pain)/control] \times 100\%$) were also computed for the three scalp sectors with significant HEP suppression shown. This is illustrated in Fig. 5.4.

HEP Magnitude and Subjective Pain Ratings

As can be seen from Table 5.1, the across-subject average of mean HEP magnitude in Cold Pain 1 was smaller over most of the scalp sectors as compared to that in Cold Pain 2. Especially for the midline scalp sector, statistically significant difference in mean HEP magnitude was shown, as indicated by "*" in Table 5.1. However, as can be seen from Fig. 5.1, the subjective pain ratings during Cold Pain 1 were higher than those during Cold Pain 2. This indicates a potential negative association between the HEP magnitude and subjective pain ratings, or a positive association between the HEP sup-

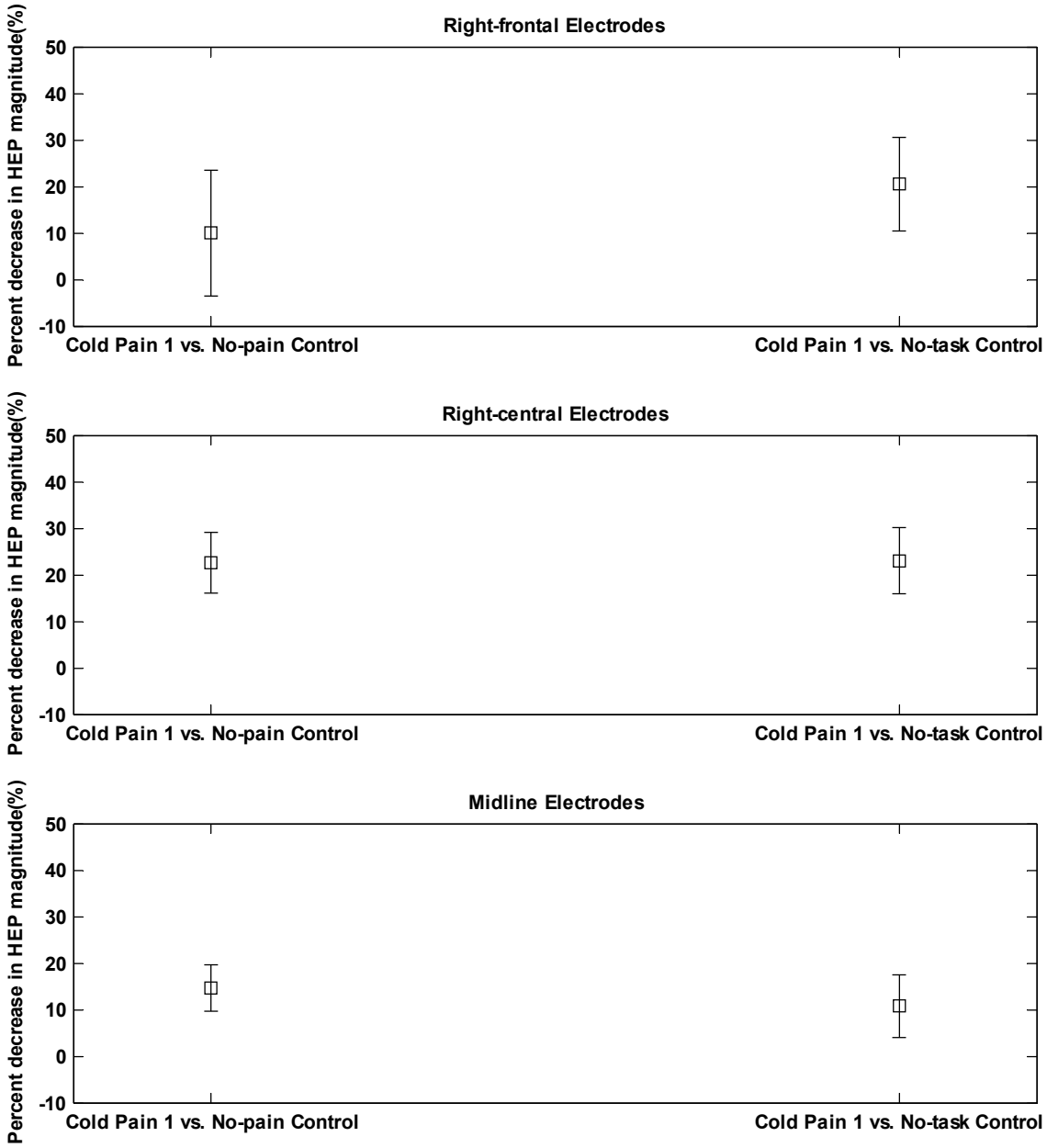

Figure 5.4: Means ($\pm$SEM) of percent decrease in the HEP magnitude across all subjects over the right-central, right-parietal-occipital and midline scalp regions in Cold Pain 1 in comparison to the two control conditions (computed as $[(control - coldpain)/control] \times 100\%$).

pression and subjective pain ratings. In order to further evaluate the correlation between HEP suppression and subjective pain rating (i.e. self-reports of pain intensity or unpleasantness), Pearson's correlation analysis was performed, for each scalp sector, by using

two sets of data: the standardized mean HEP magnitude and the normalized mean pain rating for each subject in a) Cold Pain 1 and b) Cold Pain 2. Herein, the standardized mean HEP magnitude was computed as the deviation in percentage from the average of mean HEP magnitudes over Cold Pain 1 and Cold Pain 2. The normalized mean pain rating was the mean of normalized pain ratings over Cold Pain 1 or Cold Pain 2, where the normalized pain ratings of a subject were the subject's pain ratings divided by the mean pain rating over the whole 10-min cold pain condition. The use of normalized pain ratings and standardized mean HEP magnitude was to reduce inter-subject variation in pain ratings and HEP magnitude. Significant negative correlations were found for both pain intensity ($r = -0.44$, p-value< 0.05) and pain unpleasantness ratings ($r = -0.50$, p-value< 0.05) to the mean HEP magnitude over the midline sector (see Fig. 5.5), but not over the other scalp sectors.

5.3.4 The Potential Effect of Heart Rate Change on the HEP

Cold pain tends to be accompanied by an increase in heart rate. In order to check for the potential effect of heart rate change on the HEP, comparison of the average heart rate and the mean HEP magnitudes over the right-central scalp sector was made between Cold Pain 1 and either control condition (Table 5.2) for each subject. In eight of the subjects (highlighted in bold), the average heart rates did not increase with Cold Pain 1 as compared to either control condition. However, these subjects still showed decreases in the mean HEP magnitude over the right-central scalp sector. This suggests that the HEP suppression in the cold pain condition is not accounted for by changes in the heart

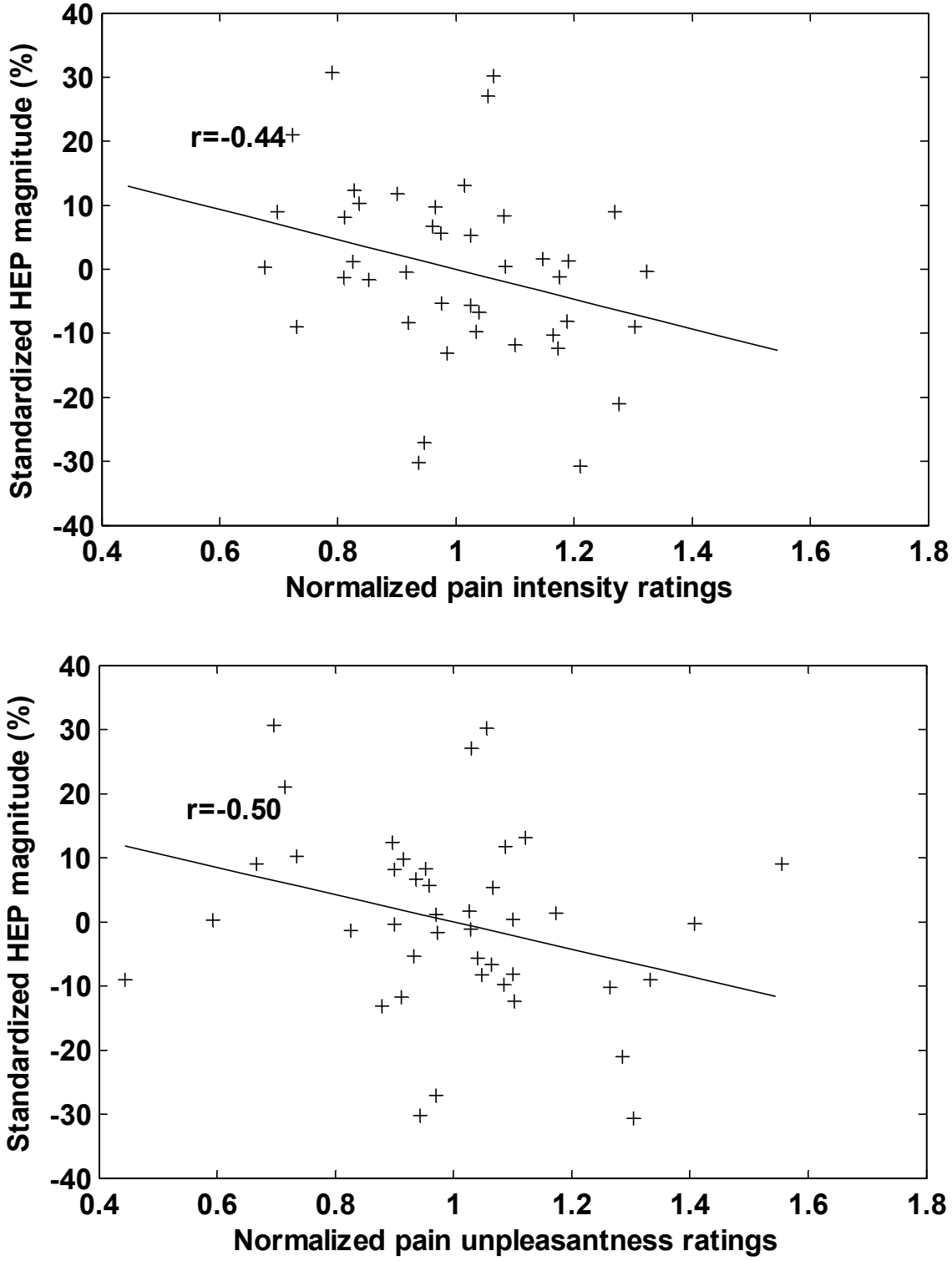

Figure 5.5: Correlation between the standardized mean HEP magnitude over the midline sector and the normalized mean pain intensity/unpleasantness ratings.

rate.

Table 5.2: The averaged heart rates and mean HEP magnitudes over right-central scalp sector for each subject in the Cold Pain 1, no-pain control control and no-task control conditions. The values highlighted in bold show the cases when the mean HEP magnitude decreased while the subject's averaged heart rate did not increase in cold pain condition as compared to either control condition. bpm: beats per minute.

Subject No.	Cold Pain 1		No-pain Control		No-task Control	
	Heart Rate (bpm)	Mean HEP Magnitude (μV)	Heart Rate (bpm)	Mean HEP Magnitude (μV)	Heart Rate (bpm)	Mean HEP Magnitude (μV)
1	73	0.42	66	0.88	65	0.75
2	68	0.65	62	2.51	60	1.74
3	**74**	**0.53**	**76**	**1.16**	**76**	**1.32**
4	86	0.29	73	0.26	76	0.50
5	**68**	**0.31**	**69**	1.28	**72**	**0.83**
6	64	0.20	55	0.16	58	0.26
7	**67**	**0.31**	**69**	**1.28**	**70**	**0.83**
8	56	1.34	54	1.90	57	0.94
9	**71**	**0.70**	**71**	**0.81**	**71**	**0.91**
10	**80**	**0.37**	**85**	**0.54**	**81**	**0.69**
11	**66**	**0.62**	67	0.54	**66**	**0.71**
12	**66**	**0.26**	65	0.43	**67**	**0.34**
13	71	0.39	65	0.40	64	0.52
14	74	0.13	64	0.18	64	0.14
15	72	0.21	71	0.29	71	0.29
16	70	0.13	68	0.14	68	0.11
17	**50**	**0.52**	**54**	**0.68**	**52**	**0.74**
18	61	0.33	59	0.33	55	0.32
19	92	0.20	80	0.28	72	0.47
20	79	0.47	71	0.37	66	0.30
21	68	0.16	67	0.17	65	0.16

5.4 Discussion

The present work examined the effect of acute tonic cold pain on the BEP accompanying cardio-afferent input (i.e. the HEP), through carefully controlled comparisons among cold pain, no-pain control and no-task control conditions. Prominent HEP was observed over the frontal and central scalp regions in both control conditions, as a deflection in the latency of 200-600 ms post ECG R-peak. The HEP was however significantly suppressed in the cold pain condition across several scalp regions.

5.4.1 The HEP

The HEP is believed to result from the central processing of cardio-afferent input, or the cardiac interoceptive process (Cameron, 2009; Dirlich *et al.*, 1998; Leopold & Schandry, 2001; Montoya *et al.*, 1993; Schandry & Montoya, 1996). The presence of HEP has been shown to be independent of subjects' conscious heartbeat perception (Schandry & Montoya, 1996). This is understandable, as afferent signals from the body (i.e. interoceptive impulses) continuously reach the brain, and consciously or unconsciously, the brain is continuously monitoring interoceptive afferent information (Cameron, 2009; Schandry & Montoya, 1996; Sviderskaya & Kovalev, 1996).

In the present study, the HEP was obtained without requiring subjects to perceive their heartbeats and thus it was associated with un/sub-conscious cardiac interoceptive process. The deflection in the latency range of 200-600 ms post ECG R-peak for the HEP may be explained by the time interval for the brain to process the cardiac afferent input.

According to McCraty *et al.* (2009), the period of 50-250 ms post ECG R-peak is the time interval for cardiac afferent signals to reach the lower brain areas, while the period of 250-600 ms post ECG R-peak is the time interval when the higher cognitive center is processing cardiac afferent information.

On the other hand, the scalp distribution of HEP, i.e. the dominance in frontal and central scalp regions, appears to suggest that the underlying networks for the HEP involves extensive functional regions of the brain. This is consistent with the evidence in the literature that extensive functional regions of the brain, including the prefrontal/frontal cortex, the insular cortex, the somatosensory cortex, the amygdala, the thalamus, the hypothalamus, and the cingulate cortex, are all involved in the interoceptive process (Cameron, 2001, 2009; Martins *et al.*, 2009).

5.4.2 HEP Suppression During Cold Pain Perception

It is interesting that the HEP was largely suppressed in the cold pain condition in comparison with both the no-task control and the no-pain control conditions. The between-condition comparisons of each subject's heart rate and HEP magnitude convincingly show that the HEP suppression in the cold pain condition is not accounted for by changes in the heart rate.

The comparison between the two control conditions showed no significant difference in the mean HEP magnitude. This suggests that the HEP suppression is also not accounted for by an effect of counting backwards or innocuous pressure sensation associated with

hand immersion in the water. During the no-task control condition, the brain was in the resting state which is known to activate the brain default mode network (DMN) and embody interoceptive processes (Buckner *et al.*, 2008; Nagai *et al.*, 2004; Uddin *et al.*, 2008). Thus, the un/sub-conscious cardiac interoceptive process which forms part of the functionality of DMN was active in the no-task condition. This may explain the prominent HEP shown in the no-task control condition. In comparison, under both the no-pain control and the cold pain conditions, the DMN was supposed to be largely deactivated with the attention-demanding mental calculation task or focused external attention and sensory processing demanded by pain (Buckner *et al.*, 2008; Eccleston, 1995; Eccleston & Crombez, 1999; Elomaa *et al.*, 2009; Nagai *et al.*, 2004; Uddin *et al.*, 2008). However, significant suppression of the HEP was only found in the cold pain condition but not in the no-pain control condition. This indicates that the network involved in un/subconscious cardiac interoceptive process is linked closely to the pain pathways but likely not so to the network involved in mental calculation.

A plausible explanation for this HEP suppression is the inhibition of un/subconscious cardiac interoceptive process by the perception of tonic cold pain. As stated earlier, the underlying networks for HEP (i.e. the un/subconscious cardiac interoceptive process) may include many brain regions. These regions have also been shown to be parts of the pain pathways (see Fig. 2.2) by many functional imaging studies (Adler *et al.*, 1997; Alkire *et al.*, 2004; Melzack & Casey, 1968; Mollet & Harrison, 2006; Ohara *et al.*, 2005; Talbot *et al.*, 1991; Torquati *et al.*, 2005). That is to say, the system involved in pain perception and the system involved in un/subconscious cardiac interoceptive

process are closely integrated. Thus, the two systems may interact with each other via overlapping neural networks, as is also supported by the behavioral evidence from the work by Martins et al. (2009) that pain ratings vary across the cardiac cycle. In the cold pain condition, the transmission and/or processing of pain signals could inhibit the processing of cardiac afferent input, resulting in a suppression of the HEP.

Moreover, it was found that the HEP magnitude was larger in the last 5 min of cold pain condition (with generally lower subjective pain ratings) than that in the first 5 min of cold pain condition (with higher pain ratings) over most scalp regions. That is, lower subjective pain ratings were accompanied by higher mean HEP magnitudes. Correlation analysis revealed a significant negative correlation between the mean HEP magnitude over the midline locations and subjective pain ratings.

These results indicate that the HEP could be an objective and non-intrusive measure of tonic pain perception. The HEP, as the BEP obtained by using the natural triggers—ECG R-peak, is believed to be able to reveal patterns of endogenous brain activity associated with pain perception. This may represent a major advantage of the HEP over the existing pain related BEPs which are triggered by external stimuli, in the usefulness as a measure of pain perception.

5.5 Concluding Remarks

This chapter presents a prospective objective and non-intrusive measure of pain perception–the HEP. In the chapter, the correlation between the HEP and pain perception has been

studied. The major findings of this study are as follows.

(1) The HEP appeared as a deflection in the latency range of 200-600 ms post ECG R-peak, being prominent mainly over frontal and central regions.

(2) The HEP was significantly suppressed in the cold pain condition as compared to no-task control and no-pain control conditions, especially over the right hemisphere which is contralateral to the painful stimulation. This HEP suppression seems to be specific to pain, as no significant difference was shown between the HEP magnitudes in the two control conditions.

(3) The HEP magnitude was smaller across several scalp sectors when the subjects reported higher pain ratings. Especially, the mean HEP magnitude over the midline region was found to have a significant negative correlation with subjective pain ratings.

Chapter 6

EEG Source Localization of Gender Differences in Pain Perception

6.1 Introduction

In recent years, there has been increasing evidence on gender differences in pain perception. Not only higher prevalence of clinical pain but also greater sensitivity to various kinds of experimental pain modalities (in terms of lower pain threshold, lower pain tolerance and/or higher pain ratings) has been reported in females than in males (Fillingim *et al.*, 2009; Keogh, 2006). These urge the necessity to investigate how males and females differ in pain perception. In fact, a clear understanding of potential gender differences in pain perception can not only be beneficial to clinical pain management by providing evidence for gender-specific diagnosis and treatment of pain disorders, but

also shed light on development of reliable pain measurement methods.

The variations in pain perception across genders have been related to various biological and psychosocial factors (Keogh, 2006). Some recent studies (Berman *et al.*, 2006; Derbyshire *et al.*, 2002; Henderson *et al.*, 2008; Moulton *et al.*, 2006; Naliboff *et al.*, 2003; Paulson *et al.*, 1998; Straube *et al.*, 2009) suggest that gender differences in pain perception, to a large extent, are associated with differences in the central processing of pain. By using functional neuroimaging techniques like fMRI and PET, the studies revealed significant between-gender differences in hemodynamic responses to painful stimulation in several brain regions, including the prefrontal cortex, cingulate cortex, thalamus, insula, amygdala as well as somatosensory cortices (Refer to Section 2.8 for details). It is generally shown that females seem to concentrate more on the affective dimension of pain with stronger pain-related activations in those emotion-based brain regions while males concentrate more on the sensory dimension of pain with stronger pain-related activations in sensory regions. However, results still vary a bit across different studies, likely due to differences in the stimulus modalities and experimental paradigms used (Fillingim *et al.*, 2009; Moulton *et al.*, 2006). Thus, gender differences in pain-related brain activities are yet to be further characterized. Moreover, very little evidence exists on the efficacy of incorporating such gender differences in clinical pain management, due to huge cost associated with functional imaging facilities like fMRI and PET. Therefore, it is of great interest and practical importance to investigate whether the gender differences in pain perception can also be measured by using EEG source localization method which is much more portable and affordable than fMRI and PET.

To date, there has been no report of gender differences in cerebral electrical activity associated with pain perception. However, there have been many reports of changes in EEG activity during various kinds of painful stimulations (see e.g. Backonja *et al.*, 1991; Chang *et al.*, 2001a; Chen *et al.*, 1998; Dowman *et al.*, 2008; Nir *et al.*, 2010). Pain is generally shown to induce decreases in the amplitudes of slower brain waves (mostly alpha and also theta in some studies) and increases in the amplitudes of faster waves (e.g. beta) (Dowman *et al.*, 2008; Jensen *et al.*, 2008).

The present study pioneers the use of EEG source localization with standardized low resolution brain electromagnetic tomography (sLORETA) (Fuchs *et al.*, 2002; Jurcak *et al.*, 2007; Pascual-Marqui, 2002) to investigate gender differences in cerebral responses to tonic cold pain in terms of electrical activity changes. In the study, it is hypothesized that there are stronger pain-related cerebral activations in emotion-based brain regions for females, and/or strong pain-related brain activations in sensory centers for males. It is explicitly designed to measure the psychophysical responses of subjects on both sensory and affective dimensions of pain, i.e. subjective ratings of pain intensity and pain unpleasantness. Results show that female subjects are significantly more activated in the ACC than male subjects during cold pain perception, suggesting that females concentrate more on the affective-motivational dimension of pain than males. This is in line with the hypothesis of the current study and the existing evidence.

6.2 Materials and Methods

6.2.1 Subjects

Twenty two healthy young adults (half males and half females, ages: 25.3 ± 3.3 years) participated in the study. All the subjects were right-handed, not on medication, without any history of neurological, psychiatric and/or cardiovascular problems. Each subject was given a detailed explanation of the experimental procedure and each signed a consent form prior to participating. The subjects were informed that if they feel any discomfort during the experiment, they could withdraw from the experiment. The study was approved by the NUS-IRB.

6.2.2 Experimental Procedure

In the experiment, each subject was comfortably seated in an upright chair in a brightly lit, sound attenuated, temperature controlled (24 to 26 ^{o}C) room, and participated with eyes open in two conditions in random order: no-pain control and cold pain induced by CPT (see Section 3.2 for details). Both the no-pain control condition and cold pain condition lasted for 10 mins, with a 5-min resting period in between.

Following the work by Dowman et al. (2008), in the no-pain control condition, the subject was required to immerse his/her non-dominant hand in warm water maintained at a temperature of 40 ^{o}C and count backwards in 3's from a randomly determined 4-digit number throughout the condition. According to Dowman et al. (2008), the no-pain

control condition can represent a better baseline condition than passive no-task control condition.

In the cold pain condition, the subject was asked to immerse his/her non-dominant hand into the cold water maintained at 10 ^{o}C. However, the subject was allowed to take the hand out of the water before the end of the 10-min recording block if the pain became unbearable. The subject was required to rate the perceived pain intensity and unpleasantness on two 11-point NRSs every minute. The NRSs for the perceived pain intensity/unpleasantness were as follows: 0=no pain/neutral, 1=barely noticeable pain/barely unpleasant, 5=mild pain/distressing and 10=maximum pain tolerable/worst unpleasantness imaginable, as shown in Fig. 3.4a and Fig. 3.4b respectively.

6.2.3 Data Acquisition

EEG data were recorded using Neuroscan NuAmps system (see Fig. 3.1) from 30 electrodes arranged according to the extended 10-20 system as shown in Fig. 3.2 with a 32-Channel Quick-Cap (Compumedics Neuroscan, USA), at a sampling rate of 250 Hz and with a band-pass filtering between 0.5 and 100 Hz. The scalp EEG was referenced to the average of A1 and A2, with AFz serving as the ground electrode.

6.2.4 Data Preprocessing

EEG segments contaminated with strong muscle artifacts were manually rejected by visual inspection. The eye-blinking and eye-movement artifacts were removed from

EEG using the novel ICA based method developed in the earlier work (Shao *et al.*, 2009) (Details on the method are given in Chapter 4).

6.2.5 sLORETA Source Localization Analysis

The sLORETA software (Fuchs *et al.*, 2002; Jurcak *et al.*, 2007; Pascual-Marqui, 2002) was used for source localization analysis in the present study. The sLORETA algorithm is a linear inverse algorithm which computes 3-D distribution of the cortical sources of scalp EEG data. It can be performed either in the time domain to estimate underlying sources at any time instant, or in the frequency domain to localize neuronal oscillators for different frequency bands. The computation is limited to cortical gray matter by using the digitized Talairach and probability atlas of the Brain Imaging Centre, Montreal Neurological Institute (MNI). The solution space is restricted to cortical gray matter, which is partitioned into 6239 voxels at 5 mm resolution. The sLORETA software reports MNI coordinates, but quantitative neuroanatomy is based on ”corrected” Talaiarch coordinates. The sLORETA algorithm has been shown to outperform several other linear inverse algorithms (Pascual-Marqui, 2002). Especially, it has been demonstrated to be a feasible method for analysis of pain-network activity in the brain (Nir *et al.*, 2008).

In the present study, EEG source analysis was performed in the frequency domain. The EEG data were firstly digitally filtered offline with a 1-30 Hz bandpass filter and segmented into 10-s epochs. Cross-spectra of the common averaged EEG segments were computed with the sLORETA software for the following 6 frequency bands: delta (1-3 Hz), theta (4-7 Hz), alpha (8-12 Hz), beta1 (13-18 Hz), beta2 (19-21 Hz) and beta3

(22-30 Hz). The EEG cross-spectra for each subject were then given as the input for sLORETA source analysis. The sLORETA solution was the spectral density of the estimated current density at each voxel. In order to reduce non-functional variability (Lorena *et al.*, 2007), subject-wise normalization was performed on the sLORETA solutions before statistical analysis (i.e. the total power across all frequency bands and across all 6239 voxels of the brain volume was normalized to 1).

6.2.6 Statistical Analysis

The differences in cortical electrical activity between the cold pain and no-pain control conditions were firstly evaluated, for male and female subjects separately, by voxel-by-voxel paired *t*-tests of the normalized and log-transformed sLORETA maps in each frequency band. Statistical significance was assessed by a nonparametric permutation test (Nichols & Holmes, 2002), with 5000 randomizations accounting for multiple comparisons. Voxels showing significantly (corrected p-value< 0.05) different electrical activities between the cold pain and no-pain control conditions for either males or females or both were combined into several regions of interest (ROIs) following the method of Babiloni *et al.* (2007). The responses to cold pain within each ROI were characterized by the average power changes in each frequency band over the whole ROI during the CP condition as compared to the NP condition.

The 10-min EEG recording during the cold pain condition for each subject was divided into three segments: 1-3 min, 4-7 min and 8-10 min. For each segment, the responses to cold pain within each ROI and the average pain intensity/unpleasantness ratings were

calculated. The correlation between the responses to cold pain within each ROI and the corresponding average pain ratings was evaluated in all subjects as a whole group by the Pearson test. The electrical activities that significantly correlated with pain ratings (Bonferroni corrected p-value< 0.05) were identified as pain-related brain activities.

After determining pain-related brain activities as described above, between-gender differences were then assessed by independent 2-sample t-tests of cold pain induced percentage changes in the power of these activities (calculated as [power of the brain activity under the cold pain condition / power of the brain activity under the no-pain control condition - 1] $\times$ 100%).

6.3 Results

6.3.1 Subjective Pain Ratings

Figs. 6.1a and 6.1b show the means ($\pm$SEM) of pain intensity and unpleasantness ratings given by the 2 groups of subjects (males vs. females) at 1-min interval during the 10-min cold pain condition, respectively. As can be seen, the mean pain intensity ratings given by females were slightly higher than those of males. However, the difference between them was not statistically significant (t-test, p-value> 0.05). The mean pain unpleasantness ratings of the two groups generally showed similar pattern to the mean pain intensity ratings. Likewise, there was no significant gender difference in pain unpleasantness ratings (t-test, p-value> 0.05).

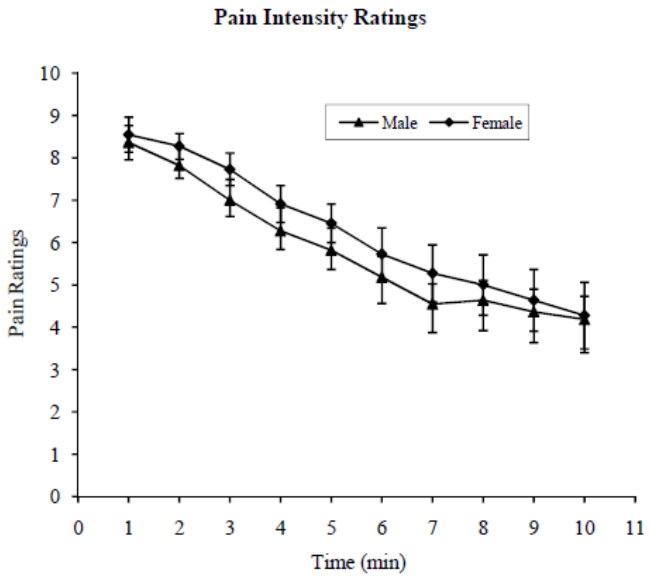

(a)

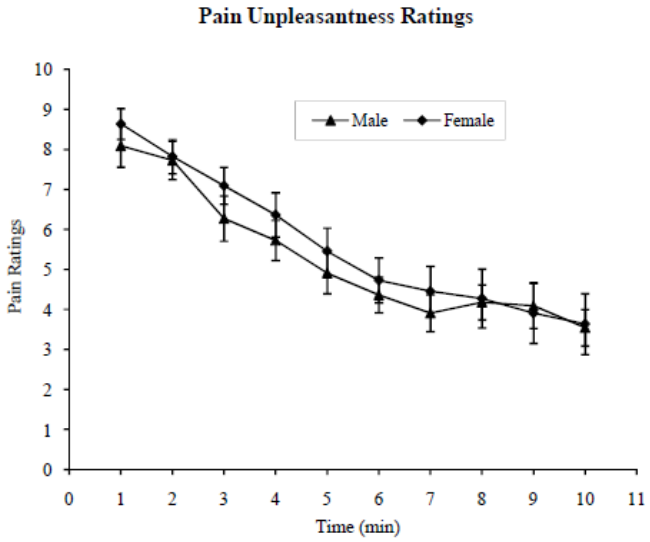

(b)

Figure 6.1: Mean (±SEM) of (a) pain intensity ratings and (b) pain unpleasantness ratings obtained at 1-min interval during the 10-min cold pain condition, separately for 11 male and 11 female subjects. Pain intensity and unpleasantness were rated on two 11-point numerical rating scales. There was no significant difference in either the pain intensity ratings or the pain unpleasantness ratings between males and females (t-test, p-value> 0.05).

6.3.2 Source Localization Analysis

Statistical analysis showed significant power changes in electrical activity over several frequency bands in multiple brain regions for both male and female subjects under the

cold pain condition, as compared to the no-pain control condition (Table 6.1). The male subjects showed significant decreases in theta, alpha and beta1 activities but significant increases in beta2 activity (Fig. 6.2). The female subjects showed significant decreases in alpha and beta1 activities but significant increases in beta2 activity (Fig. 6.3). The brain regions involved for either male or female subjects or both included the bilateral frontal (Brodmann areas, BA 4/6/8/9), parietal (BA 1/2/3/5/7/40) and limbic (BA 24/32/33), the left insula (BA 13) and temporal (BA 20/36/41) regions.

Table 6.1: Brain regions showing significant electrical activity differences between the cold pain and no-pain control conditions for male or female subjects or both.

Lobe	Gyrus	Brodmann areas	Male		Female	
			Side	Band	Side	Band
Frontal	Medial frontal gyrus	9	Left	Beta2	Right	Alpha
	Middle frontal gyrus	6/8/9	Right	Theta	Bilateral	Alpha, Beta1
	Superior frontal gyrus	8			Right	Alpha
	Precentral gyrus	4/6/9	Right	Beta1	Bilateral	Alpha, Beta1
Parietal	Postcentral gyrus	1/2/3/5	Left	Alpha	Right	Alpha
	Inferior parietal lobule	40	Right	Theta	Bilateral	Alpha, Beta2
	Superior parietal lobule	7	Right	Theta		
Temporal	Transverse temporal gyrus	41			Left	Beta2
	Fusiform gyrus	20	Left	Beta2		
Sub-lobar	Insula	13			Left	Beta2
Limbic	Cingulate cortex/gyrus	24/32/33			Bilateral	Alpha
	Uncus	20/36			Left	Alpha

The brain regions, mentioned above, with significant power changes between cold pain and no-pain control conditions were further combined into the following 10 ROIs: left/right prefrontal, left/right central, left/right parietal, left/right ACC, left insular and left temporal. Table 6.2 lists the Brodmann areas forming each of the ROI.

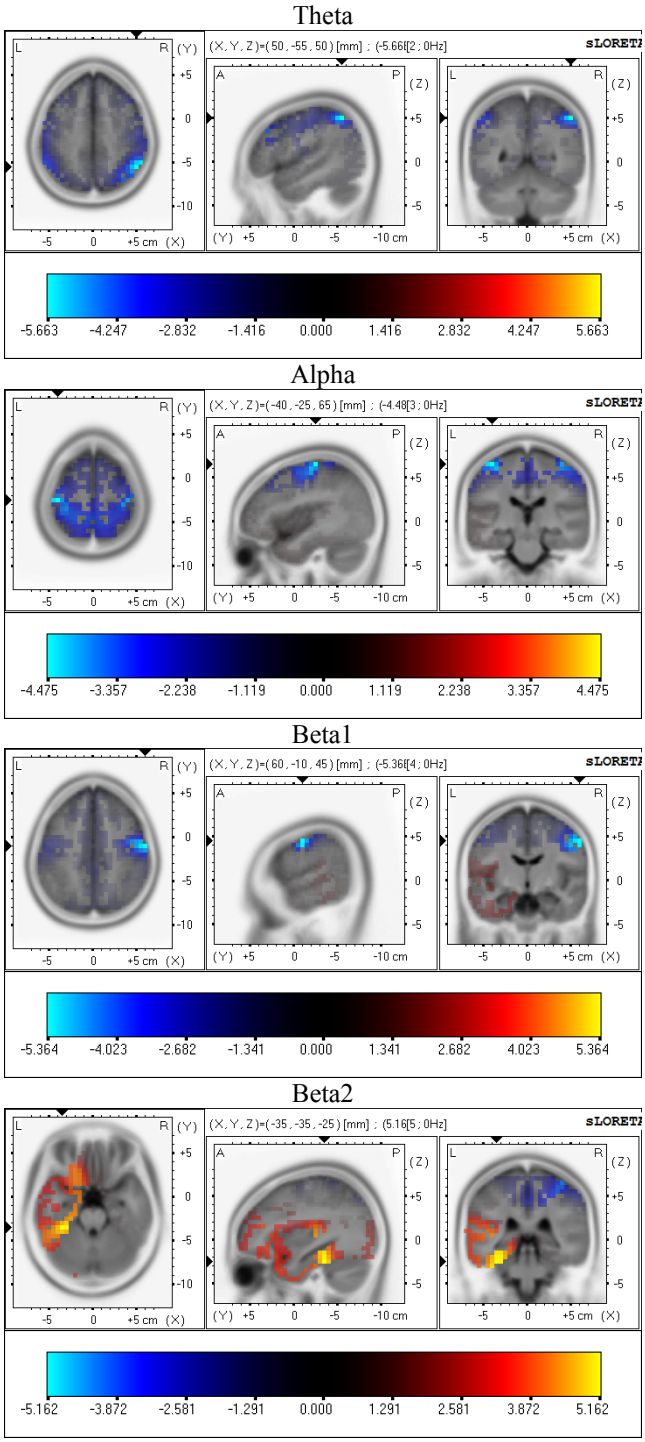

Figure 6.2: Coronal, sagittal and axial slices of the brain showing between-condition (cold pain vs. no-pain control) differences in theta, alpha, beta1 and beta2 activities for male subjects. The location of the maximal *t*-value is graphically indicated by black triangles on the coordinates axes.

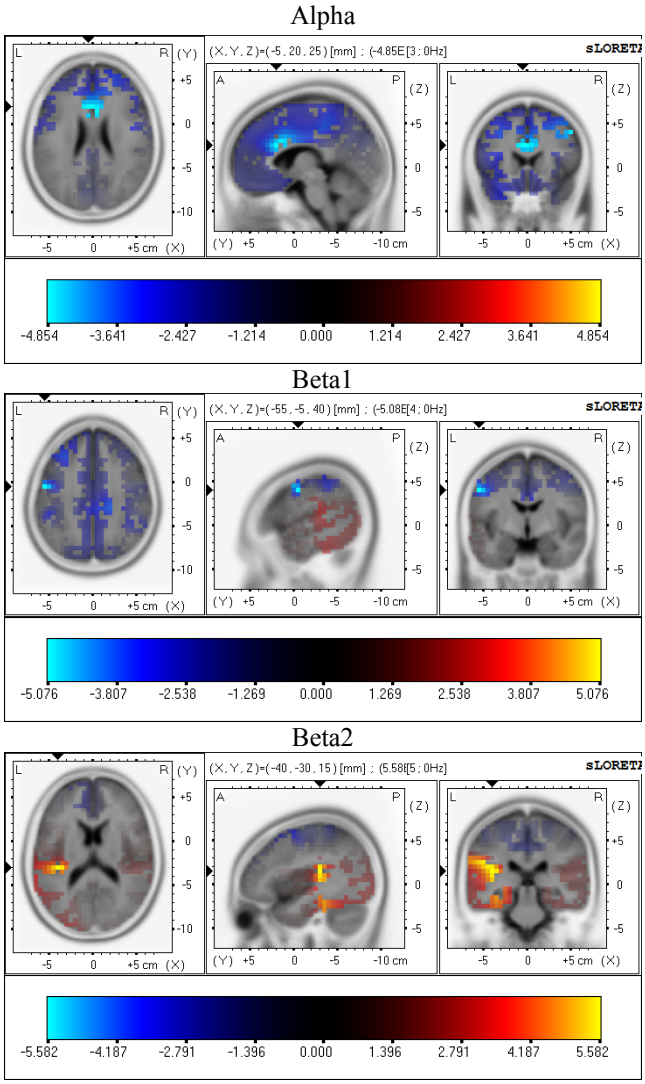

Figure 6.3: Coronal, sagittal and axial slices of the brain showing between-condition (cold pain vs. no-pain control) differences in alpha, beta1 and beta2 activities for female subjects. The location of the maximal *t*-value is graphically indicated by black triangles on the coordinates axes.

Table 6.2: Brodmann areas included in each of the ROIs in the present study.

ROI	Side	Brodmann areas
Prefrontal	Left/Right	8, 9
Central	Left/Right	1, 2, 3, 4, 6
Parietal	Left/Right	5, 7, 40
Temporal	Left	20, 36, 41
Insular	Left	13
ACC	Left/Right	24, 32, 33

The Pearson test showed that: a) the left/right central alpha activity significantly correlated with pain intensity ratings (the Bonferroni correlated p-value < 0.05; $r = -0.46$ and -0.37 for left and right central alpha activity, respectively); b) the left/right central, left prefrontal and left ACC alpha activity significantly correlated with pain unpleasantness ratings (the Bonferroni correlated p-value < 0.05; $r = -0.48, -0.40, -0.36$ and -0.36 for left central, right central, left prefrontal and left ACC alpha activity, respectively). Thus, the alpha activities in the four regions (i.e. left/right central, left prefrontal and left ACC) were identified as pain-related brain activities. Figs. 6.4a and 6.4b show scatterplots of the average power changes in these pain-related brain activities over 1-3 min, 4-7 min and 8-10 min of the cold pain condition in all subjects and the corresponding average pain intensity/unpleasantness ratings.

Between-gender comparison performed on the above pain-related brain activities showed that the cold pain induced percent decrease in the power of alpha activity in the left ACC was significantly more in the females than that in the males (independent t-test, p-value < 0.05). For the purpose of illustration, the statistical map comparing the cold pain induced power changes in alpha activity between male and female subjects (Female-Male) is shown in Fig. 6.5.

6.4 Discussion

The present study was the first attempt to investigate gender differences in cerebral responses to cold pain by EEG source localization analysis with sLORETA. The sLORETA

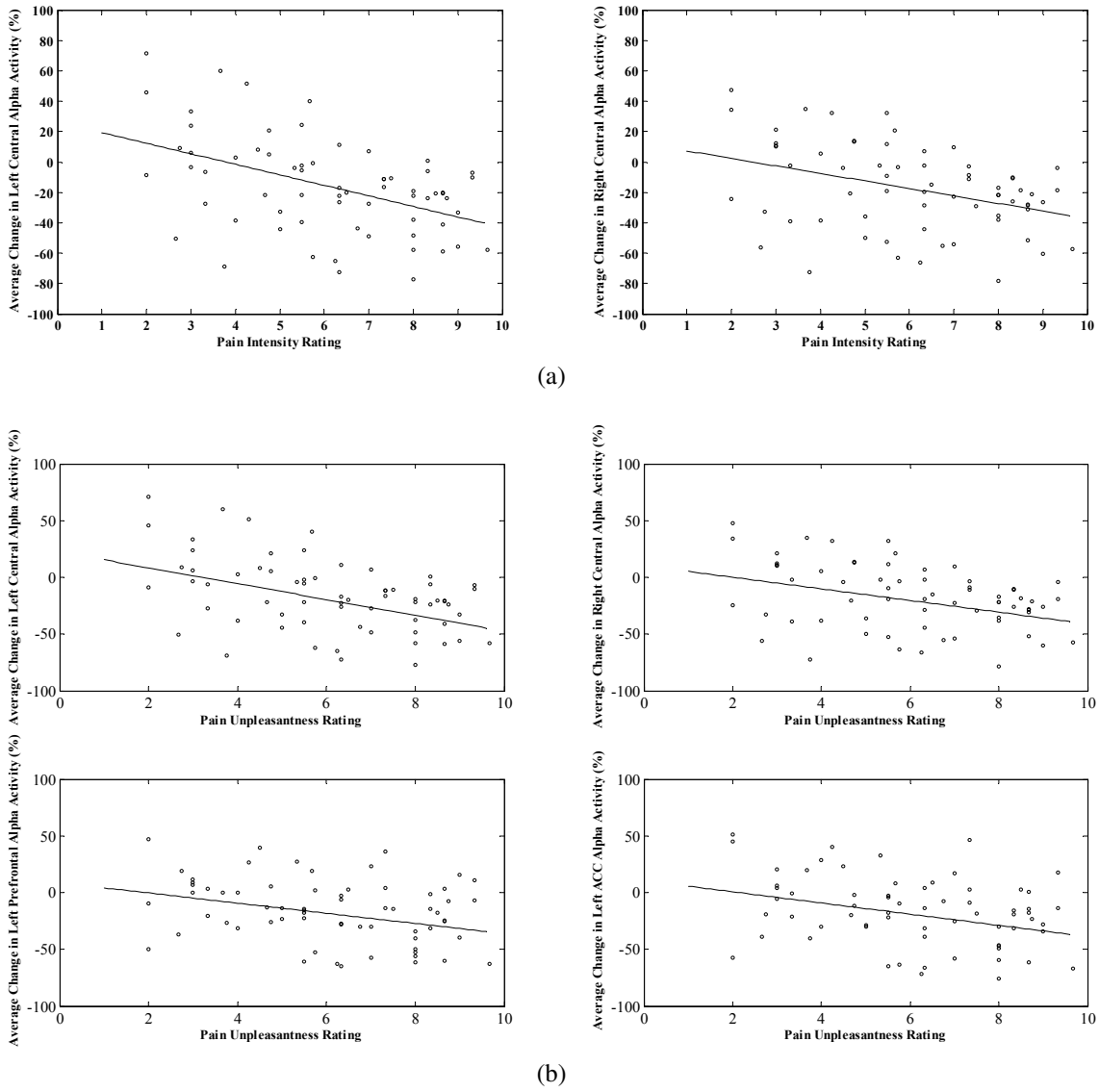

Figure 6.4: Scatterplots of the average power changes in pain-related brain activities and the corresponding average (a) pain intensity/(b) pain unpleasantness ratings over 1-3, 4-7 and 8-10 min of the cold pain condition in all subjects. The solid lines indicate the corresponding regression lines.

analysis revealed gender differences in pain-related cerebral activations in the ACC, which reaffirmed the existence of gender difference in central processing of pain.

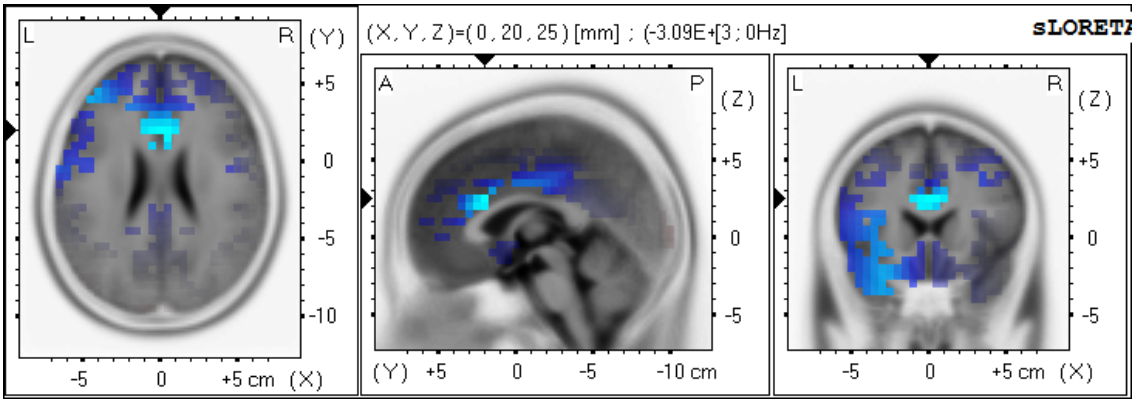

Figure 6.5: Coronal, sagittal and axial slices of the brain showing between-gender (female-male) difference in power changes in alpha activity by tonic cold pain. The location of the maximal *t*-value is graphically indicated by black triangles on the coordinates axes.

6.4.1 Gender Difference in Subjective Pain Ratings

There is a general consensus in the literature regarding significantly stronger sensitivity to experimental cold pain for females (Fillingim *et al.*, 2009). However, results on gender differences in continuous subjective pain ratings during experimental cold pain remain inconsistent. Considerable studies (see e.g. al'Absi *et al.*, 2004; Jackson *et al.*, 2005; Jones *et al.*, 2003a; Kim *et al.*, 2004a,b; Lowery *et al.*, 2003; Sarlani *et al.*, 2003; Weisenberg & Schwarzwald, 1995) have demonstrated significantly higher subjective pain intensity and/or pain unpleasantness ratings in females, while some other studies (see e.g. Mitchell *et al.*, 2006; Pud *et al.*, 2006; Zimmer *et al.*, 2003) have found no significant gender differences in pain ratings. The present study also found no significant differences in subjective pain intensity and unpleasantness ratings in the 10-min cold pain condition. However, the data did show a trend of higher sensitivity in females, as evidenced by the relatively higher mean pain ratings of female subjects than those of

male subjects. A plausible explanation for the statistical insignificance is that the size of psychophysical data is not large enough to reveal gender differences in the sensitivity to the tonic cold pain. It has been proposed by several past studies (Berkley, 1995; Henderson *et al.*, 2008; Riley Iii *et al.*, 1998) that gender differences in pain sensitivity tend to be very small if not nonexistent, and thus the number of subjects should be sufficiently large to reveal the differences.

6.4.2 Gender Difference in Cerebral Responses to Tonic Cold Pain

The sLORETA analysis showed that there was considerable overlap of cerebral responses to tonic cold pain between male and female subjects. Both genders showed decreased alpha and beta1 activities but increased beta2 activity during the cold pain condition as compared to the no-pain control condition. This is generally consistent with the findings of many past studies (Backonja *et al.*, 1991; Chang *et al.*, 2002; Chen *et al.*, 1989b; Chen & Rappelsberger, 1994; Chen *et al.*, 1998; Dowman *et al.*, 2008; Ferracuti *et al.*, 1994; Jensen *et al.*, 2008) that pain experience is associated with decreases in relative power of slower (mostly alpha and also theta in some studies) brain activities and increase in relative power of faster (beta) brain activity. The significant electrical activity changes were found for both male and female subjects in the prefrontal, somatosensory, motor and temporal regions. These regions have been shown to be involved in pain perception in many functional neuroimaging studies using MEG, fMRI or PET (Apkarian *et al.*, 2005; Brooks & Tracey, 2005; Jones *et al.*, 2003b; Leone *et al.*, 2006; Ohara *et al.*, 2005; Raij, 2005; Talbot *et al.*, 1991).

Interestingly, the current study revealed significantly greater decrease in alpha activity in the ACC by tonic cold pain for female subjects than for male subjects. It is generally believed that the activation of a cortical area is characterized by a decrease in alpha activity and an increase in gamma activity (25-100Hz) (Dowman *et al.*, 2008; Hari & Salmelin, 1997). Accordingly, the current result indicates that the female subjects were more activated by tonic cold pain in the ACC than the male subjects.

The ACC is believed to be involved in emotional component encoding and be associated with attention aspects of pain (attention shifts and sustained attention to the painful area) (Jones *et al.*, 2003b). It has been shown by some past PET and fMRI studies (Mertz *et al.*, 2000; Rainville *et al.*, 1997; Straube *et al.*, 2009) that affective reports of pain are correlated with activation in the ACC. It is worth noting that the present study also demonstrated a significant correlation between the alpha activity in the left ACC and pain unpleasantness ratings. Therefore, the stronger activation by tonic cold pain in the ACC for females suggests that females concentrate more on the affective component of pain. This is in agreement with the hypothesis of the present study. Although no significant gender difference is found in sensory and cognitive centers, this is consistent with the behaviorial evidence from the study of Kuhl and Clark (2004) that gender difference in pain experience seems to be more affective than sensory.

A potential limitation of the present study is that it did not control for the menstrual cycle phase of female subjects. However, a recent study (Rebecca *et al.*, 2010) has shown that the menstrual phase does not appear to influence gender difference in experimental pain sensitivity. On the other hand, it is not groundless that gender differences could exist

independent of hormonal variation across the menstrual cycle (Derbyshire *et al.*, 2002). Several past functional neuroimaging studies (Derbyshire *et al.*, 2002; Henderson *et al.*, 2008; Paulson *et al.*, 1998) have found gender differences in hemodynamic responses to pain, without control for the menstrual phase of female subjects as well.

6.5 Concluding Remarks

In this chapter, a pilot study of gender differences in cerebral responses to cold pain by EEG source localization via sLORETA has been presented. It has been shown that female subjects had significantly stronger pain-related activations than male subjects in the ACC. The activation in the ACC was found to be significantly correlated with subject's reports of pain unpleasantness. This suggests that females seem to concentrate more on the affective-motivational dimension of pain than males, which verifies the hypothesis of the present study and is generally consistent with the existing evidence.

Chapter 7

Conclusions and Recommendations

7.1 Conclusions

This work serves as an essential step towards the development of an objective and non-invasive pain measurement system. A ECG R-peak locked BEP — the HEP has been proposed as a prospective objective measure of acute pain perception. The HEP is found to be largely suppressed during tonic cold pain, which is likely due to the inhibition of cardiac interoceptive process through the overlapping neural pathways involved in both cardiac interoceptive process and pain perception. Furthermore, a significant correlation is shown between the HEP magnitude and subjective pain ratings. This explicitly demonstrates the potential use of HEP for indexing pain perception. As compared to the existing pain-related BEPs which are triggered by external stimuli, the HEP is triggered by an internal event — the heartbeat, and it may reveal patterns of endogenous brain

activity associated with pain perception.

Another contribution of the thesis is the investigation of gender differences in pain perception for the first time by EEG source localization. Stronger activation in the ACC has been revealed in females than in males, indicating gender differences in central processing of pain. That is, females seem to concentrate more on the affective dimension of pain. This is generally in line with the evidence from both behavioral and functional imaging studies using fMRI or PET. This study provides evidence for gender-specific pain diagnosis and treatment methods in clinical pain management. It also demonstrates the possibility of measuring gender differences in pain perception by using EEG source localization techniques which are more portable and affordable than fMRI and other functional imaging techniques.

Moreover, the present work contributes to the whole EEG research community by proposing a novel automatic EEG artifact removal method. This method provides a preferable solution to the challenging problem of automatic EEG artifact removal, by achieving a better tradeoff between removing artifacts and preserving inherent brain activities than the existing methods. The novelty mainly lies in the new method used for automatic artifact identification, which is essentially a combination of a weighted probabilistic multi-class SVM and an error correction algorithm. The weighted probabilistic multi-class SVM addresses the unbalanced nature of the learning problem at hand by compensating the bias of prior class probabilities by penalizing more on the classification errors produced by the samples from the minority class. The error correction algorithm incorporates the useful structural information of underlying data in decision making.

The idea of the error correction algorithm is generally useful for classification problems where similar structural information is contained in the test samples and thus simultaneous classification of several test samples is necessary.

7.2 Recommendations for Future Work

This thesis has demonstrated the potential usefulness of HEP in objective pain assessment, based on the association between the suppression of HEP and the level of pain experience. However, it should be acknowledged that further works on the causal link between pain perception and the HEP suppression are needed to establish the HEP as an pain indicator.

Firstly, besides heightened sympathetic activity (e.g. increased heart rate), the CPT may also lead to elevated blood pressure which triggers baroreceptor reflex. It has been demonstrated that the HEP suppression is not likely due to heart rate changes. However, the current study did not measure the blood pressure. Thus, it is not clear whether and how the changes of blood pressure would affect the HEP. Before this is addressed, a firm conclusion about the specificity of the observed HEP suppression to pain should not be made. Therefore, it would be necessary to include the measurement of blood pressure in future studies.

Secondly, this study examined the relation between HEP magnitude and subjective pain ratings by comparing HEP in the first and last 5 min of cold pain condition. However, the pain ratings were not constant but decreasing steadily in the first several minutes,

and for some subjects, the pain ratings in the first and last 5 minutes did not differ significantly. This could be a reason why significant HEP difference between the two periods was only found over the midline scalp sector. Thus, a pain-induction method whose nociceptive input can be readily controlled to induce distinct levels of pain would be preferable in future studies.

It should also be acknowledged that, the present study is limited to the test with cold pain stimulation applied to the non-dominant hand of right-handed subjects. It is found that the HEP was largely suppressed especially over the right hemisphere which is contralateral to the cold pain stimulation. That is, cold pain seems to have contralateral effects on the HEP. It will be interesting to test for this by using a fully controlled paradigm which includes pain stimulation of both left and right extremity in future studies.

Moreover, although some plausible explanations to the cold pain evoked HEP suppression have been posited, it is certainly necessary to further investigate the underlying neuronal sources of the HEP, preferably by using multi-modal neuroimaging techniques such as simultaneous EEG + ECG + fMRI measurement, so as to clearly elucidate the causal link between the HEP suppression and pain perception.

On the other hand, for the investigation of gender differences in cerebral responses to cold pain, the present study has not controlled the menstrual phase of the female subjects. Although it has been shown by a recent study (Rebecca *et al.*, 2010) that the menstrual phase does not appear to affect gender difference in experimental pain sensitivity, it would be more stringent and persuasive to have the menstrual phase controlled in future studies on gender differences in pain perception.

Publications From the Present Study

International Journal Articles:

- Shiyun Shao, Kaiquan Shen, Ke Yu, Einar P. V. Wilder-Smith, Xiaoping Li. Electroencephalogram Neuroimaging of Gender Differences in Cerebral Responses to Cold Pressor Pain. *European Journal of Pain*. Submitted for Publication.
- Shiyun Shao, Kaiquan Shen, Einar P. V. Wilder-Smith, Xiaoping Li. Effect of pain perception on the heartbeat evoked potential. *Clinical Neurophysiology*. In Press.
- Shiyun Shao, Kaiquan Shen, Chong Jin Ong, Einar P. V. Wilder-Smith and Xiaoping Li. Automatic EEG Artifact Removal: a Weighted Support-Vector-Machine Approach With Error Correction. *IEEE transactions on Biomedical Engineering*, Vol. 56, No. 2, 2009, pp. 336 - 344.
- Rohit Tyagi, Kaiquan Shen, Shiyun Shao, Xiaoping Li. A Novel Auditory Working-Memory Vigilance Task For Mental Fatigue Assessment. *Safety Science*, Vol. 47, No. 7, 2009, pp. 967-972.
- Kaiqaun Shen, Xiaoping Li, Chong Jin Ong, Shiyun Shao, and Einar P V Wilder-Smith. EEG-based Mental Fatigue Measurement using Multi-Class Support Vector Machines with Confidence Estimate. *Clinical Neurophysiology*, Vol. 119, No. 7, 2008, pp. 1524-1533.

Book Sections:

- Shiyun Shao, Kaiquan Shen, Wu Chun Ng, Wee Sin Tan, Einar P. V. Wilder-Smith, Xiaoping Li, and Chong Jin Ong. Electroencephalographic Study of Gender Difference in Brain's Response to Cold Pain. *Brain Topography and Multimodal Imaging*, Kyoto University Press, 2009, pp. 109-112.

- Kaiquan Shen, Shiyun Shao, Ee Min Ho, Wu Chun Ng, Ke Yu, Kenneth Kwok, Gounder Boopathi, and Xiaoping Li. Single-Trial ERP Detection for Rapid Image Triage. *Brain Topography and Multimodal Imaging*. Kyoto University Press, 2009, pp. 59-62.

International Conference Papers:

- Shiyun Shao, Kaiquan Shen, Einar P. V. Wilder-Smith, Chong Jin Ong, Xiaoping Li. The Heartbeat Evoked Potential: A Neural Correlate of Pain Perception? *Proceedings of the International Federation for Medical and Biological Engineering*, Vol. 31, No. 6, 2010, pp. 1578-1581.

- Shiyun Shao, Kaiquan Shen, Chong Jin Ong, Einar P. V. Wilder-Smith, Xiaoping Li. Automatic Identification and Removal of Artifacts in EEG using a Probabilistic Multi-class SVM Approach with Error Correction. *Proceedings of IEEE International Conference on Systems, Man, and Cybernetics*, Oct. 2008, pp. 1134-1139.

- Ke Yu, Kaiquan Shen, Shiyun Shao, Wu Chun Ng, Kenneth Kwok, Xiaoping Li, Single-Trial Event-Related Potential Based Rapid Image Triage System, *The 3rd International Forum on Systems and Mechatronics*, Singapore, Sep. 6-9, 2010.

- Ke Yu, Kaiquan Shen, Shiyun Shao, Kenneth Kwok and Xiaoping Li. Common Spatio-Temporal Patterns in Single-Trial Detection of Event-Related Potential for Rapid Image Triage. *The International Multi-Conference on Complexity, Informatics and Cybernetics*, USA, April 6-9, 2010.

Bibliography

Adler, L. J., Gyulai, F. E., Diehl, D. J., Mintun, M. A., Winter, P. M., & Firestone, L. L. 1997. Regional Brain Activity Changes Associated with Fentanyl Analgesia Elucidated by Positron Emission Tomography. *Anesthesia & Analgesia*, **84**(1), 120–126.

al'Absi, M., Wittmers, L. E., Ellestad, D., Nordehn, G., Kim, S. W., Kirschbaum, C., & Grant, J. E. 2004. Sex Differences in Pain and Hypothalamic-Pituitary-Adrenocortical Responses to Opioid Blockade. *Psychosom Med*, **66**(2), 198–206.

Alkire, M. T., White, N. S., Hsieh, R., & Haier, R. J. 2004. Dissociable Brain Activation Responses to 5-Hz Electrical Pain Stimulation: A High-field Functional Magnetic Resonance Imaging Study. *Anesthesiology*, **100**(4), 939–946.

Almeida, T. F., Roizenblatt, S., & Tufik, S. 2004. Afferent pain pathways: a neuroanatomical review. *Brain Research*, **1000**(1-2), 40–56.

Alpaydin, E. 2004. *Assessing and Comparing Classification Algorithms*. Introduction to Machine Learning. Cambridge, Massachusetts: MIT Press. Chap. 14, pages 327–350.

Apkarian, A. V., Bushnell, M. C., Treede, R. D., & Zubieta, J. K. 2005. Human brain mechanisms of pain perception and regulation in health and disease. *European Journal of Pain*, **9**(4), 463–484.

Arendt-Nielsen, L. 1990. Second pain event related potentials to argon laser stimuli: recording and quantification. *Journal of Neurology, Neurosurgery and Psychiatry*, **53**(5), 405–10.

Arendt-Nielsen, L., & Lautenbacher, S. 2004. *Pathophysiology of Pain Perception*. 1st edn. New York: Plenum. Chap. Assessment of Pain Perception, pages 25–40.

Babiloni, C., Cassetta, E., Binetti, G., Tombini, M., Del Percio, C., Ferreri, F., Ferri, R., Frisoni, G., Lanuzza, B., Nobili, F., Parisi, L., Rodriguez, G., Frigerio, L., Gurzi, M., Prestia, A., Vernieri, F., Eusebi, F., & Rossini, P. M. 2007. Resting EEG sources correlate with attentional span in mild cognitive impairment and Alzheimer's disease. *European Journal of Neuroscience*, **25**(12), 3742–57.

Backonja, M.and Howland, E. W., Wang, J., Smith, J., Salinsky, M., & Cleeland, C. S. 1991. Tonic changes in alpha power during immersion of the hand in cold water. *Electroencephalography and Clinical Neurophysiology*, **79**(3), 192–203.

Baltas, E., Bentley, D., Jones, A., Reoullas, M., Stergioulas, L. K., Xydeas, C. S., & Youell, P. 2002. An LVQ classifier of EEG coherence patterns for pain detection. *Pages 248–251 of: Proceedings of the international conference in communication systems, networks and digital signal processing*. Stafford, Sheffield: Sheffield Hallam University Press.

Barlow, J. S. 1986. Artifact processing (rejection and minimization) in EEG data processing. *Handb Electroencephalogr Clin Neurophysiol*, **2**, 15–62.

Becker, D. E., Yingling, C. D., & Fein, G. 1993. Identification of pain, intensity and P300 components in the pain evoked potential. *Electroencephalography and Clinical Neurophysiology/Evoked Potentials Section*, **88**(4), 290–301.

Becker, D. E., Haley, David W., Urena, V. M., & Yingling, C. D. 2000. Pain measurement with evoked potentials: combination of subjective ratings, randomized

intensities, and long interstimulus intervals produces a P300-like confound. *Pain*, **84**(1), 37–47.

Bell, A. J., & Sejnowski, T. J. 1995. An information-maximization approach to blind separation and blind deconvolution. *Neural Computation*, **7**(6), 1129–59.

Bemporad, A., & Mignone, D. 2001. *A Matlab function for solving Mixed Integer Quadratic Programs (Version 1.06)*.

Benedetti, F. 1997. The sensory and affective components of pain. *Behavioral and Brain Sciences*, **20**(03), 439–440.

Berger, H. 1929. Uber das elektrenkephalogramm des menschen (on the EEG in humans). *Arch. Psychiatr. Nervenkr.*, **87**, 527–570.

Berkley, K. J. 1995. From psychophysics to the clinic? *Pain Forum*, **4**(4), 225–227.

Berman, S. M., Naliboff, B. D., Suyenobu, B., Labus, J. S., Stains, J., Bueller, J. A., Ruby, K., & Mayer, E. A. 2006. Sex differences in regional brain response to aversive pelvic visceral stimuli. *Am J Physiol Regul Integr Comp Physiol*, **291**(2), R268–276.

Binnie, C., Boyd, S., Guerrini, R., & Rpessler, R. 2002. *Child and Adolescent Psychiatry*. 4th edn. Massachusetts: Blackwell Science. Chap. Clinical Neurophysiology, page 161.

Bonica, J. J. 1979. The need of a taxonomy. *Pain*, **6**(3), 247–8.

Boser, B. E., Guyon, I. M., & Vapnik, V. N. 1992. A Training algorithm for optimal margin classifiers. *Pages 144–152 of: Proceeding of the 5th Annual Workshop Comput. Learning Theory*. Pittsburgh, PA, USA: ACM, New York, NY, USA.

Bouman, C. A. 1997. *Cluster: An unsupervised algorithm for modeling Gaussian mixtures.*

Box, G. E. P., Hunter, W. G., & Hunter, J. S. 1978. *Statistics for Experimenters: An Introduction to Design, Data Analysis, and Model Building*. Wiley.

Brando, M. L., & De Luca Vinhas, M. C. 2006. *Neurobiology of Mental Disorders*. New York: Nova Science Publishers. Chap. Chronic Pain, pages 125–155.

Bromm, B., & Scharein, E. 1982. Principal component analysis of pain-related cerebral potentials to mechanical and electrical stimulation in man. *Electroencephalography and Clinical Neurophysiology*, **53**(1), 94–103.

Bromm, B., Meier, W., & Scharein, E. 1989. Pre-stimulus/post-stimulus relations in EEG spectra and their modulations by an opioid and an antidepressant. *Electroencephalography and Clinical Neurophysiology*, **73**(3), 188–197.

Brooks, J., & Tracey, I. 2005. From nociception to pain perception: imaging the spinal and supraspinal pathways. *Journal of Anatomy*, **207**(1), 19–33.

Buckner, R. L., Andrews-Hanna, Jessica R., & Schacter, D. L. 2008. The Brain's Default Network: Anatomy, Function, and Relevance to Disease. *Annals of the New York Academy of Sciences*, **1124**, 1–38. [1] doi:10.1196/annals.1440.011.

Bunketorp, L., Lindh, M., Carlsson, J., & Stener-Victorin, E. 2006. The perception of pain and pain-related cognitions in subacute whiplash-associated disorders: its influence on prolonged disability. *Disability and Rehabilitation*, **28**(5), 271–9.

Cameron, O. G. 2001. Interoception: The Inside Story–A Model for Psychosomatic Processes. *Psychosom Med*, **63**(5), 697–710.

Cameron, O. G. 2009. Visceral brain-body information transfer. *NeuroImage*, **47**(3), 787–794.

Caraceni, A., Cherny, N., Fainsinger, R., Kaasa, S., Poulain, P., Radbruch, L., & De Conno, F. 2002. Pain Measurement Tools and Methods in Clinical Research

in Palliative Care: Recommendations of an Expert Working Group of the European Association of Palliative Care. *Journal of Pain and Symptom Management*, **23**(3), 239–255.

Carmon, A., Dotan, Y., & Sarne, Y. 1978. Correlation of subjective pain experience with cerebral evoked responses to noxious thermal stimulations. *Experimental Brain Research*, **33**(3), 445–453.

Castellanos, N. P., & Makarov, V. A. 2006. Recovering EEG brain signals: Artifact suppression with wavelet enhanced independent component analysis. *Journal of Neuroscience Methods*, **158**(2), 300–312.

Caterina, M. J., & Julius, D. 1999. Sense and specificity: a molecular identity for nociceptors. *Current Opinion in Neurobiology*, **9**(5), 525–530.

Cesare, P., & McNaughton, P. 1997. Peripheral pain mechanisms. *Current Opinion in Neurobiology*, **7**(4), 493–499.

Chang, C., & Lin, C. April 2007. LIBSVM: a library for support vector machines (Version 2.84).

Chang, P. F.and Arendt-Nielsen, L., Graven-Nielsen, T., & Chen, A. C. N. 2003. Psychophysical and EEG responses to repeated experimental muscle pain in humans: Pain intensity encodes EEG activity. *Brain Research Bulletin*, **59**(6), 533–543.

Chang, P., Arendt-Nielsen, L., Graven-Nielsen, T., Svensson, P., & Chen, A. 2001a. Different EEG topographic effects of painful and non-painful intramuscular stimulation in man. *Experimental Brain Research*, **141**(2), 195–203.

Chang, P. F., Arendt-Nielsen, L., & Chen, A. C. N. 2001b. Dynamic changes and correlation between pain rating, skin temperature and EEG activities during tonic cold pain. *NeuroImage*, **13**(6, Supplement 1), 870.

Chang, P. F., Arendt-Nielsen, L., & Chen, A. C. N. 2002. Dynamic changes and spatial correlation of EEG activities during cold pressor test in man. *Brain Research Bulletin*, **57**(5), 667–675.

Chapman, C. R., Casey, K. L., Dubner, R., Foley, K. M., Gracely, R. H., & Reading, A. E. 1985. Pain measurement: an overview. *Pain*, **22**(1), 1–31.

Chatrian, G. E., Canfield, R. C., Knauss, T. A., & Eegt, E. L. 1975. Cerebral responses to electrical tooth pulp stimulation in man. An objective correlate of acute experimental pain. *Neurology*, **25**(8), 745–57.

Chen, A. C., & Treede, R. D. 1985. The McGill Pain Questionnaire in the assessment of phasic and tonic experimental pain: behavioral evaluation of the 'pain inhibiting pain' effect. *Pain*, **22**(1), 67–79.

Chen, A. C., Dworkin, S. F., Haug, J., & Gehrig, J. 1989a. Human pain responsivity in a tonic pain model: psychological determinants. *Pain*, **37**(2), 143–60.

Chen, A. C. N., & Dworkin, S. F. 1982. Human pain and evoked potential: possible assessment of headache with endogenous brain potentials triggered by the R wave of EKG in pain patients. *Adv. in Neural.*, **32**, 389–395.

Chen, A. C. N., & Rappelsberger, P. 1994. Brain and Human pain: Topographic EEG amplitude and coherence mapping. *Brain Topography*, **7**(2), 129–140.

Chen, A. C. N., Richard C., C., & Harkins, S. W. 1979. Brain evoked potentials are functional correlates of induced pain in man. *Pain*, **6**(3), 365–374.

Chen, A. C. N., Rappelsberger, P., & Filz, O. 1998. Topology of EEG Coherence Changes May Reflect Differential Neural Network Activation in Cold and Pain Perception. *Brain Topography*, **11**(2), 125–132.

Chen, Andrew C. N. 1993. Human brain measures of clinical pain: a review I. Topographic mappings. *Pain*, **54**(2), 115–132.

Chen, Andrew C. N., Dworkin, Samuel F., Haug, Joanna, & Gehrig, John. 1989b. Topographic brain measures of human pain and pain responsivity. *Pain*, **37**(2), 129–141.

Cohen, J. 1960. A Coefficient of Agreement for Nominal Scales. *Educational and Psychological Measurement*, **20**(1), 37–46.

Comon, P. 1994. Independent component analysis, A new concept? *Signal Processing*, **36**(3), 287–314.

Cortes, C., & Vapnik, V. 1995. Support-vector networks. *Machine Learning*, **20**(3), 273–297.

Cristianini, N., & Shawe-Taylor, J. 2000. *An Introduction to Support Vector Machines and other kernel-based learning methods*. New York: Cambridge University Press.

Croft, R. J., & Barry, R. J. 2000. Removal of ocular artifact from the EEG: a review. *Neurophysiologie Clinique/Clinical Neurophysiology*, **30**(1), 5–19.

Croft, R. J., Williams, J. D., Haenschel, C., & Gruzelier, J. H. 2002. Pain perception, hypnosis and 40 Hz oscillations. *International Journal of Psychophysiology*, **46**(2), 101–108.

Deandrea, S., Montanari, M., Moja, L., & Apolone, G. 2008. Prevalence of undertreatment in cancer pain. A review of published literature. *Annals of Oncology*, **19**(12), 1985–1991.

Delsanto, S., Lamberti, F., & Montrucchio, B. 2003. Automatic ocular artifact rejection based on independent component analysis and eyeblink detection. *Pages 309–312 of:* Lamberti, F. (ed), *First International IEEE EMBS Conference on Neural Engineering*.

Denise, H., Suzanne, B., Peter, L., Peter, D., Hanne, S., & Linda, J. 2006. Skin conductance as a measure of pain and stress in hospitalised infants. *Early Human Development*, **82**(9), 603–608.

Derbyshire, S. W. G., Nichols, T. E., Firestone, L., Townsend, D. W., & Jones, A. K. P. 2002. Gender differences in patterns of cerebral activation during equal experience of painful laser stimulation. *The Journal of Pain*, **3**(5), 401–411.

Dirlich, G., Dietl, T., Vogl, L., & Strian, F. 1998. Topography and morphology of heart action-related EEG potentials. *Electroencephalography and Clinical Neurophysiology/Evoked Potentials Section*, **108**(3), 299–305.

Dowman, R. 2004. The Pain-Evoked P2 Is Not a P3a Event-Related Potential. *Brain Topography*, **17**(1), 3–12.

Dowman, R., Rissacher, D., & Schuckers, S. 2008. EEG indices of tonic pain-related activity in the somatosensory cortices. *Clinical Neurophysiology*, **119**(5), 1201–1212.

Duan, K. B., & Keerthi, S. S. 2005. *Which Is the Best Multiclass SVM Method? An Empirical Study*. Pages 278–285.

Eccleston, C. 1995. The attentional control of pain: methodological and theoretical concerns. *Pain*, **63**(1), 3–10.

Eccleston, C., & Crombez, G. 1999. Pain demands attention: a cognitive-affective model of the interruptive function of pain. *Psychol Bull*, **125**(3), 356–66.

Edwards, L., Ring, C.and McIntyre, D., & Carroll, D. 2001. Modulation of the human nociceptive flexion reflex across the cardiac cycle. *Psychophysiology*, **38**(04), 712–718.

Edwards, L., McIntyre, D., Carroll, D., Ring, C., & Martin, U. 2002. The human nociceptive flexion reflex threshold is higher during systole than diastole. *Psychophysiology*, **39**(05), 678–681.

Edwards, L., Inui, K., Ring, C., Wang, X., & Kakigi, R. 2008. Pain-related evoked potentials are modulated across the cardiac cycle. *Pain*, **137**(3), 488–494.

Eitrich, T., & Lang, B. 2006. Efficient optimization of support vector machine learning parameters for unbalanced datasets. *Journal of Computational and Applied Mathematics*, **196**(2), 425–436.

Elbert, T., Lutzenberger, W., Rockstroh, B., & Birbaumer, N. 1985. Removal of ocular artifacts from the EEG–a biophysical approach to the EOG. *Electroencephalography and Clinical Neurophysiology*, **60**(5), 455–63.

Elomaa, M. M., de C. Williams, A. C., & Kalso, E. A. 2009. Attention management as a treatment for chronic pain. *European Journal of Pain*, **13**(10), 1062–1067.

Farrar, J. T., Young, J. P., LaMoreaux, L., Werth, J. L., & Poole, R. M. 2001. Clinical importance of changes in chronic pain intensity measured on an 11-point numerical pain rating scale. *Pain*, **94**(2), 149–158.

Fatourechi, M., Bashashati, A., Ward, R. K., & Birch, G. E. 2007. EMG and EOG artifacts in brain computer interface systems: A survey. *Clinical Neurophysiology*, **118**(3), 480–494.

Fernandes de Lima, V. M., Chatrian, G. E., Lettich, E., Canfield, R. C., Miller, R. C., & Soso, M. J. 1982. Electrical stimulation of tooth pulp in humans. I. Relationships among physical stimulus intensities, psychological magnitude estimates and cerebral evoked potentials. *Pain*, **14**(3), 207–32.

Fernandez, E., & Turk, D. C. 1992. Sensory and affective components of pain: separation and synthesis. *Psychol Bull*, **112**(2), 205–17.

Ferracuti, S., Seri, S., Mattia, D., & Cruccu, G. 1994. Quantitative EEG modifications during the cold water pressor test: hemispheric and hand differences. *International Journal of Psychophysiology*, **17**(3), 261–268.

Fillingim, R. B., King, C. D., Ribeiro-Dasilva, M. C., Rahim-Williams, B., & Riley Iii,

J. L. 2009. Sex, Gender, and Pain: A Review of Recent Clinical and Experimental Findings. *The Journal of Pain*, **10**(5), 447–485.

Fisch, B. J., & Spehlmann, R. 1999. *EEG primer: basic principles of digital and analog EEG*. 3rd edn. New York: Elsevier.

Fishbasin, D. A. 2003. *The Psychopharmacologic Treatment of Chronic Nonneuropathic Pain and its Associated Psychopathology*. 2nd edn. Philadelphia: Lippincott Williams & Wilkins.

Fitzgibbon, S. P., Powers, D. M. W., Pope, K. J., & Clark, C. R. 2007. Removal of EEG Noise and Artifact Using Blind Source Separation. *Journal of Clinical Neurophysiology*, **24**(3), 232–243.

Fuchs, M., Kastner, J., Wagner, M., Hawes, S., & Ebersole, J. S. 2002. A standardized boundary element method volume conductor model. *Clin Neurophysiol*, **113**(5), 702–12.

Geisser, M. E., Gracely, R. H., Giesecke, T., Petzke, F. W., Williams, D. A., & Clauw, D. J. 2007. The association between experimental and clinical pain measures among persons with fibromyalgia and chronic fatigue syndrome. *European Journal of Pain*, **11**(2), 202–207.

Gotman, J., Skuce, D. R., Thompson, C. J., Gloor, P., Ives, J. R., & Ray, W. F. 1973. Clinical applications of spectral analysis and extraction of features from electroencephalograms with slow waves in adult patients. *Electroencephalography and Clinical Neurophysiology*, **35**(3), 225–35.

Granovsky, Y., Granot, M., Nir, R. R., & Yarnitsky, D. 2008. Objective correlate of subjective pain perception by contact heat-evoked potentials. *The Journal of Pain*, **9**(1), 53–63.

Gratton, G., Coles, M. G., & Donchin, E. 1983. A new method for off-line removal of ocular artifact. *Electroencephalogr Clin Neurophysiol*, **55**(4), 468–84.

Grave de Peralta Menendez, R., Gonzalez Andino, S., Lantz, G., Michel, C. M., & Landis, T. 2001. Noninvasive localization of electromagnetic epileptic activity. I. Method descriptions and simulations. *Brain Topography*, **14**(2), 131–7.

Grech, R., Cassar, T., Muscat, J., Camilleri, K. P., Fabri, S. G., Zervakis, M., Xanthopoulos, P., Sakkalis, V., & Vanrumste, B. 2008. Review on solving the inverse problem in EEG source analysis. *J Neuroeng Rehabil*, **5**, 25.

Greco, A., Mammone, N., Morabito, F., & Versaci, M. 2005. Semi-automatic artifact rejection procedure based on kurtosis, renyi's entropy and independent component scalp maps. *Int. J. Biomed. Sci.*, **1**, 12–16.

Green, A. L., Wang, S., Stein, J. F., Pereira, E. A., Kringelbach, M. L., Liu, X., Brittain, J. S., & Aziz, T. Z. 2009. Neural signatures in patients with neuropathic pain. *Neurology*, **72**(6), 569–71.

Gvert, H., Hurri, J., Srel, J., & Hyvrinen, A. 2005. The FastICA package for MATLAB (Version 2.5).

Halder, S., Bensch, M., Mellinger, J., Bogdan, M., Kbler, A., Birbaumer, N., & Rosenstiel, W. 2007. Online Artifact Removal for Brain-Computer Interfaces Using Support Vector Machines and Blind Source Separation. *Computational Intelligence and Neuroscience*, **2007**.

Handwerker, H. O., & Kobal, G. 1993. Psychophysiology of experimentally induced pain. *Physiological Reviews*, **73**(3), 639–671.

Hari, Riitta, & Salmelin, Riitta. 1997. Human cortical oscillations: a neuromagnetic view through the skull. *Trends in Neurosciences*, **20**(1), 44–49.

Hastie, T., & Tibshirani, R. 1998. Classification by Pairwise Coupling. *The Annals of Statistics*, **26**(2), 451–471.

Henderson, L. A., Gandevia, S. C., & Macefield, V. G. 2008. Gender differences in brain activity evoked by muscle and cutaneous pain: a retrospective study of single-trial fMRI data. *NeuroImage*, **39**(4), 1867–76.

Hjorth, B. 1975. An on-line transformation of EEG scalp potentials into orthogonal source derivations. *Electroencephalography and Clinical Neurophysiology*, **39**(5), 526–530.

Hofbauer, R. K., Rainville, P., Duncan, G. H., & Bushnell, M. C. 2001. Cortical Representation of the Sensory Dimension of Pain. *J Neurophysiol*, **86**(1), 402–411.

Hripcsak, G., & Heitjan, D. F. 2002. Measuring agreement in medical informatics reliability studies. *Journal of Biomedical Informatics*, **35**(2), 99–110.

Hsu, C. W., & Lin, C. J. 2002. A comparison of methods for multiclass support vector machines. *Neural Networks, IEEE Transactions on*, **13**(2), 415–425.

Huber, M. T., Bartling, J., Pachur, D., Woikowsky-Biedau, S. V., & Lautenbacher, S. 2006. EEG responses to tonic heat pain. *Experimental Brain Research*, **173**(1), 14–24.

Hyvarinen, A. 1999. Fast and robust fixed-point algorithms for independent component analysis. *IEEE Trans Neural Netw*, **10**(3), 626–34.

Hyvarinen, A., Karhunen, J., & Oja, E. 2001. *Independent Component Analysis*. John Wiley & Sons.

Ille, N., Berg, P., & Scherg, M. 2002. Artifact Correction of the Ongoing EEG Using Spatial Filters Based on Artifact and Brain Signal Topographies. *Journal of Clinical Neurophysiology*, **19**(2), 113–124.

Iriarte, J., Urrestarazu, E., Valencia, M., Alegre, M., Malanda, A., Viteri, C., & Artieda, J. 2003. Independent Component Analysis as a Tool to Eliminate Artifacts in EEG: A Quantitative Study. *Journal of Clinical Neurophysiology*, **20**(4), 249–257.

Jackson, T., Iezzi, T., Chen, H., Ebnet, S., & Eglitis, K. 2005. Gender, interpersonal transactions, and the perception of pain: An experimental analysis. *The Journal of Pain*, **6**(4), 228–236.

Jasper, H. H. 1958. The ten-twenty electrode system of the International Federation. *Electroencephalography and Clinical Neurophysiology*, 371–375.

Jensen, M. P., Hakimian, S., Sherlin, L. H., & Fregni, F. 2008. New Insights Into Neuromodulatory Approaches for the Treatment of Pain. *The Journal of Pain*, **9**(3), 193–199.

Johnson, C. B. 2008. *New approaches to identifying and measuring pain*. OIE Technical series. Pages 131–144.

Jones, A., Zachariae, R., & Arendt-Nielsen, L. 2003a. Dispositional anxiety and the experience of pain: gender-specific effects. *European Journal of Pain*, **7**(5), 387–395.

Jones, A. K. P., Kulkarni, B., & Derbyshire, S. W. G. 2003b. Pain mechanisms and their disorders: Imaging in clinical neuroscience. *Br Med Bull*, **65**(1), 83–93.

Jones, G. E., Leonberger, T. F., Rouse, C. H., Caldwell, J. A., & Jones, K. R. 1986. Preliminary data exploring the presence of an evoked potential associated with cardiac visceral activity. *Psychophysiology*, **23**(4), 445.

Joyce, C. A., Gorodnitsky, I. F., & Kutas, M. 2004. Automatic removal of eye movement and blink artifacts from EEG data using blind component separation. *Psychophysiology*, **41**(2), 313–325.

Jung, T. P., Humphries, C., Lee, T. W., Makeig, S. A. Makeig S., McKeown, M. J., Iragui, V., & Sejnowski, T. J. 1998. Removing electroencephalographic artifacts: comparison between ICA and PCA. *Pages 63–72 of:* Humphries, C. (ed), *Neural Networks for Signal Processing VIII, 1998. Proceedings of the 1998 IEEE Signal Processing Society Workshop*.

Jung, T. P., Makeig, S., Westerfield, M., Townsend, J., Courchesne, E., & Sejnowski, T. J. 2000a. Removal of eye activity artifacts from visual event-related potentials in normal and clinical subjects. *Clinical Neurophysiology*, **111**(10), 1745–1758.

Jung, T. P., Makeig, S., Humphries, C., Lee, T. W., McKeown, M. J., Iragui, V., & Sejnowski, T. J. 2000b. Removing electroencephalographic artifacts by blind source separation. *Psychophysiology*, **37**(02), 163–178.

Jung, T. P., Makeig, S., Westerfield, M., Townsend, J., Courchesne, E., & Sejnowski, T. J. 2001. Analysis and Visualization of Single-Trial Event Related Potentials. *Human Brain Mapping*, **14**, 166–185.

Jurcak, V., Tsuzuki, D., & Dan, I. 2007. 10/20, 10/10, and 10/5 systems revisited: their validity as relative head-surface-based positioning systems. *NeuroImage*, **34**(4), 1600–11.

Kakigi, R., Shibasaki, H., & Ikeda, A. 1989. Pain-related somatosensory evoked potentials following CO2 laser stimulation in man. *Electroencephalography and Clinical Neurophysiology*, **74**(2), 139–46.

Kall, L. B., Kowalski, J., & Stener-Victorin, E. 2008. Assessing pain perception using the Painmatcher in patients with whiplash-associated disorders. *Journal of Rehabilitation Medicine*, **40**(3), 171–7.

Keogh, E. 2006. Sex and gender differences in pain: a selective review of biological and psychosocial factors. *The Journal of Men's Health & Gender*, **3**(3), 236–243.

Khemakhem, R.and Zouch, W., Ben Hamida, A., Taleb-Ahmed, A., & Feki, I. 2009. EEG Source Localization Using the Inverse Problem Methods. *International Journal of Computer Science and Network Security*, **9**(4).

Kim, H., Neubert, J. K., Rowan, J. S., Brahim, J. S., Iadarola, M. J., & Dionne, R. A. 2004a. Comparison of experimental and acute clinical pain responses in humans as pain phenotypes. *The Journal of Pain*, **5**(7), 377–384.

Kim, H., Neubert, J. K., San Miguel, A., Xu, K., Krishnaraju, R. K., Iadarola, M. J., Goldman, D., & Dionne, R. A. 2004b. Genetic influence on variability in human acute experimental pain sensitivity associated with gender, ethnicity and psychological temperament. *Pain*, **109**(3), 488–496.

Koles, Z. J. 1998. Trends in EEG source localization. *Electroencephalography and Clinical Neurophysiology*, **106**(2), 127–37.

Kubicki, S., Herrmann, W. M., Fichte, K., & Freund, G. 1979. Reflections on the topics: EEG frequency bands and regulation of vigilance. *Pharmakopsychiatrie Neuro-Psychopharmakologie*, **12**(2), 237–45.

Kuhl, J., & Clark, W. 2004. Pain and gender psychosocial: Gender differences in cold pressor pain are demonstrated by the Multidimensional Affect and Pain Survey (MAPS) factor scores. *The Journal of Pain*, **5**(3, Supplement 1), S100–S100.

Lagerlund, T. D., Sharbrough, F. W., & Busacker, N. E. 1997. Spatial filtering of multichannel electroencephalographic recordings through principal component analysis by singular value decomposition. *Journal of Clinical Neurophysiology*, **14**(1), 73–82.

Le Pera, D., Svensson, P., Valeriani, M., Watanabe, I., Arendt-Nielsen, L., & Chen, A. C. N. 2000. Long-lasting effect evoked by tonic muscle pain on parietal EEG activity in humans. *Clinical Neurophysiology*, **111**(12), 2130–2137.

Leone, M., Proietti Cecchini, A., Mea, E., Tullo, V., Curone, M., & Bussone, G. 2006. Neuroimaging and pain: a window on the autonomic nervous system. *Neurological Sciences*, **27**(0), s134–s137.

Leopold, C., & Schandry, R. 2001. The heartbeat-evoked brain potential in patients suffering from diabetic neuropathy and in healthy control persons. *Clinical Neurophysiology*, **112**(4), 674–682.

LeVan, P., Urrestarazu, E., & Gotman, J. 2006. A system for automatic artifact removal in ictal scalp EEG based on independent component analysis and Bayesian classification. *Clinical Neurophysiology*, **117**(4), 912–27.

Li, D., Puntillo, K., & Miaskowski, C. 2008. A Review of Objective Pain Measures for Use With Critical Care Adult Patients Unable to Self-Report. *The Journal of Pain*, **9**(1), 2–10.

Lin, H. T., Lin, C. J., & Weng, R. C. 2007. A note on Platt's probabilistic outputs for support vector machines. *Machine Learning*, **68**(3), 267–276.

Lins, O. G., Picton, T. W., Berg, P., & Scherg, M. 1993a. Ocular artifacts in EEG and event-related potentials I: Scalp topography. *Brain Topography*, **6**(1), 51–63.

Lins, O. G., Picton, T. W., Berg, P., & Scherg, M. 1993b. Ocular artifacts in recording EEGs and event-related potentials II: Source dipoles and source components. *Brain Topography*, **6**(1), 65–78.

Liu, Y., An, A., & Huang, X. 2006. Boosting Prediction Accuracy on Imbalanced Datasets with SVM Ensembles. 107–118.

Loeser, J. D., & Treede, R. D. 2008. The Kyoto protocol of IASP Basic Pain Terminology. *Pain*, **137**(3), 473–7.

Lorena, R. R. Gianotti, Gabriella, Knig, Dietrich, Lehmann, Pascal, L. Faber, Roberto, D. Pascual-Marqui, Kieko, Kochi, & Ursula, Schreiter-Gasser. 2007. Correlation between disease severity and brain electric LORETA tomography in Alzheimers disease. *Clinical neurophysiology*, **118**(1), 186–196.

Lowery, D., Fillingim, R. B., & Wright, R. A. 2003. Sex Differences and Incentive Effects on Perceptual and Cardiovascular Responses to Cold Pressor Pain. *Psychosom Med*, **65**(2), 284–291.

Makeig, S., Bell, A. J., Jung, T. P., & Sejnowski, T. J. 1996. Independent component analysis of electroencephalographic data. *Advances in neural information processing systems*, **8**, 145–151.

Markowetz, F. 2001. *Support vector machines in bioinformatics*. M.Phil. thesis.

Martins, A. Q., Ring, C., McIntyre, D., Edwards, L., & Martin, U. 2009. Effects of unpredictable stimulation on pain and nociception across the cardiac cycle. *Pain*, **147**(1-3), 84–90.

McCraty, R., Atkinson, M., Tomasino, D., & Trevor Bradley, R. 2009. The Coherent Heart: Heart-Brain Interactions, Psychophysiological Coherence, and the Emergence of System-Wide Order. *Integral Review*, **5**(2), 10–115.

McIntyre, D., Edwards, L., Ring, C., Parvin, B., & Carroll, D. 2006. Systolic inhibition of nociceptive responding is moderated by arousal. *Psychophysiology*, **43**(3), 314–319.

Melzack, R. 1975. The McGill Pain Questionnaire: major properties and scoring methods. *Pain*, **1**(3), 277–99.

Melzack, R., & Casey, K.L. 1968. *Sensory, motivational and central control determinants of pain*. Springfield: Thomas.

Melzack, R., Coderre, T. J., Katz, J., & Vaccarino, A. L. 2001. Central neuroplasticity and pathological pain. *Annals of the New York Academy of Sciences*, **933**, 157–74.

Mertz, H., Morgan, V., Tanner, G., Pickens, D., Price, R., Shyr, Y., & Kessler, R. 2000. Regional cerebral activation in irritable bowel syndrome and control subjects with painful and nonpainful rectal distention. *Gastroenterology*, **118**(5), 842–8.

Miaskowski, C. 2005. *Principles of Pain Assessment*. New York: McGraw-Hill.

Michel, C. M., Murray, M. M., Lantz, G., Gonzalez, S., Spinelli, L., & Grave de Peralta, R. 2004. EEG source imaging. *Clinical Neurophysiology*, **115**(10), 2195–222.

Millan, J., Franze, M., Mourino, J., Cincotti, F., & Babiloni, F. 2002. Relevant EEG features for the classification of spontaneous motor-related tasks. *Biological Cybernetics*, **86**(2), 89–95.

Mishra, P. S. 2009. *Biophysics*. 1st edn. New Delhi: VK (India) Enterprises.

Misulis, K. E., & Fakhoury, T. 2001. *Spehlmann's Evoked Potential Primer*. 3rd edn. Butterworth-heinemann.

Mitchell, L. A., MacDonald, R. A. R., & Brodie, E. E. 2004. Temperature and the cold pressor test. *The Journal of Pain*, **5**(4), 233–237.

Mitchell, L. A., MacDonald, R. A. R., & Brodie, E. E. 2006. A comparison of the effects of preferred music, arithmetic and humour on cold pressor pain. *European Journal of Pain*, **10**(4), 343–351.

Mollet, G., & Harrison, D. 2006. Emotion and Pain: A Functional Cerebral Systems Integration. *Neuropsychology Review*, **16**(3), 99–121.

Montoya, P., Schandry, R., & Muller, A. 1993. Heartbeat evoked potentials (HEP): topography and influence of cardiac awareness and focus of attention. *Electroen-*

cephalography and Clinical Neurophysiology/Evoked Potentials Section, **88**(3), 163–172.

Moulton, E. A., Keaser, M. L., Gullapalli, R. P., Maitra, R., & Greenspan, J. D. 2006. Sex differences in the cerebral BOLD signal response to painful heat stimuli. *Am J Physiol Regul Integr Comp Physiol*, **291**(2), R257–267.

Mouraux, A., & Iannetti, G. D. 2009. Nociceptive Laser-Evoked Brain Potentials Do Not Reflect Nociceptive-Specific Neural Activity. *J Neurophysiol*, **101**(6), 3258–3269.

Muller, K. R., Mika, S., Ratsch, G., Tsuda, K., & Scholkopf, B. 2001. An introduction to kernel-based learning algorithms. *IEEE Transactions on Neural Networks*, **12**(2), 181–201.

Nagai, Y., Critchley, H. D., Featherstone, E., Trimble, M. R., & Dolan, R. J. 2004. Activity in ventromedial prefrontal cortex covaries with sympathetic skin conductance level: a physiological account of a "default mode" of brain function. *NeuroImage*, **22**(1), 243–251.

Naliboff, B. D., Berman, S., Chang, L., Derbyshire, S. W. G., Suyenobu, B., Vogt, B. A., Mandelkern, M., & Mayer, E. A. 2003. Sex-related differences in IBS patients: central processing of visceral stimuli. *Gastroenterology*, **124**(7), 1738–1747.

Nichols, T. E., & Holmes, A. P. 2002. Nonparametric permutation tests for functional neuroimaging: a primer with examples. *Human Brain Mapping*, **15**(1), 1–25.

Nicolaou, N., & Nasuto, S. J. 2004. Temporal independent component analysis for automatic artifact removal from EEG. *Pages 5–8 of: Proceedings of the 2nd International Conference on Medical Signal and Information Processing*.

Niedermeyer, E., & Lopes da Silva, F. 1999. *Electroencephalography: Basic Principles, Clinical Applications, and Related Fields*. 4th edn. Baltimore: Williams & Wilkins.

Nir, R. R., Lev, R., Moont, R., Granovsky, Y., Sprecher, E., & Yarnitsky, D. 2008. Neurophysiology of the cortical pain network: revisiting the role of S1 in subjective pain perception via standardized low-resolution brain electromagnetic tomography (sLORETA). *J Pain*, **9**(11), 1058–69.

Nir, R. R., Sinai, A., Raz, E., Sprecher, E., & Yarnitsky, D. 2010. Pain assessment by continuous EEG: Association between subjective perception of tonic pain and peak frequency of alpha oscillations during stimulation and at rest. *Brain Research*, **1344**, 77–86.

Noble, B., Clark, D., Meldrum, M., ten Have, H., Seymour, J., Winslow, M., & Paz, S. 2005. The measurement of pain, 1945-2000. *Journal of Pain and Symptom Management*, **29**(1), 14–21.

Nunez, P. L., & Pilgreen, K. L. 1991. The spline-Laplacian in clinical neurophysiology: a method to improve EEG spatial resolution. *Journal of Clinical Neurophysiology*, **8**(4), 397–413.

Ohara, P. T., Vit, J. P., & Jasmin, L. 2005. Cortical modulation of pain. *Cellular and Molecular Life Sciences (CMLS)*, **62**(1), 44–52.

Olejniczak, P. 2006. Neurophysiologic basis of EEG. *Journal of Clinical Neurophysiology*, **23**(3), 186–9.

Onton, J., & Makeig, S. 2006. *Information-based modeling of event-related brain dynamics*. Elsevier. Chap. Progress in Brain Research book series, pages 99–120.

Osuna, E., Freund, R., & Girosi, F. 1997. *Support vector machines: Training and applications*. Tech. rept. MIT A. I. Lab.

Pascual-Marqui, R. D. 1999. Review of Methods for Solving the EEG Inverse Problem. *International Journal of Bioelectromagnetism*, **1**, 75–86.

Pascual-Marqui, R. D. 2002. Standardized low-resolution brain electromagnetic tomography (sLORETA): technical details. *Methods Find Exp Clin Pharmacol*, **24 Suppl D**, 5–12.

Paulson, P. E., Minoshima, S., Morrow, T. J., & Casey, K. L. 1998. Gender differences in pain perception and patterns of cerebral activation during noxious heat stimulation in humans. *Pain*, **76**(1-2), 223–229.

Pearson, K. 1901. On lines and planes of closest fit to systems of points in space. *Philosophical Magazine*, **2**(6), 559–572.

Perron, V., & Schonwetter, R. S. 2001. Assessment and management of pain in palliative care patients. *Cancer Control*, **8**(1), 15–24.

Peyron, R., Laurent, B., & Garcia-Larrea, L. 2000. Functional imaging of brain responses to pain. A review and meta-analysis (2000). *Neurophysiologie Clinique/Clinical Neurophysiology*, **30**(5), 263–288.

Platt, J. C. 2000. *Probabilistic Outputs for Support Vector Machines and Comparisons to Regularized Likelihood Methods*. Cambridge, MA: MIT Press.

Pollatos, O., & Schandry, R. 2004. Accuracy of heartbeat perception is reflected in the amplitude of the heartbeat-evoked brain potential. *Psychophysiology*, **41**(3), 476–482.

Pollatos, O., Kirsch, W., & Schandry, R. 2005. Brain structures involved in interoceptive awareness and cardioafferent signal processing: A dipole source localization study. *Human Brain Mapping*, **26**(1), 54–64.

Price, D. D. 2000. Psychological and neural mechanisms of the affective dimension of pain. *Science*, **288**(5472), 1769–1772.

Pud, D., Yarnitsky, D., Sprecher, E., Rogowski, Z., Adler, R., & Eisenberg, E. 2006. Can personality traits and gender predict the response to morphine? An experimental cold pain study. *European Journal of Pain*, **10**(2), 103–112.

Raij, T. 2005. *Pain processing in the human brainviews from magnetoencephalography and functional magnetic resonance imaging*. Ph.D. thesis.

Rainville, P., Duncan, G.H., Price, D. D., Carrier, B., & Bushnell, M. C. 1997. Pain Affect Encoded in Human Anterior Cingulate But Not Somatosensory Cortex. *Science*, **277**(5328), 968–971.

Raj, P. P. 2000. *Practical management of pain*. 3rd edn. St. Louis: Mosby, Inc.

Raja, S. N., Meyer, R. A., Ringkamp, M., & Campbell, J. N. 1999. *Peripheral neural mechanisms of nociception*. Textbook of pain. New York: Churchill Livingstone.

Ranney, D. 1996. Anatomy of Pain.

Ray, A. L., & Zbik, A. 2002. *Cognitive Behavioral Therapies and Beyond*. 3rd edn. Philadelphia: Lippincott Williams & Wilkins.

Reading, A. E. 1983. Pain measurement and experience. *Journal of Psychosomatic Research*, **27**(5), 415–420.

Rebecca, R. K., Beth, M., & Susan, S. G. 2010. Menstrual cycle phase does not influence gender differences in experimental pain sensitivity. *European journal of pain (London, England)*, **14**(1), 77–82.

Riley Iii, J. L., Robinson, M. E., Wise, E. A., Myers, C. D., & Fillingim, R. B. 1998. Sex differences in the perception of noxious experimental stimuli: a meta-analysis. *Pain*, **74**(2-3), 181–187.

Riordan, H., Squires, N. K., & Brener, J. 1990. Cardio-cortical potentials: electrophysiological evidence lot visceral perception. *Psychophysiology*, **27**(s4a), S59.

Rissacher, D., Dowman, R., & Schuckers, S. A. C. 2007. Identifying frequency-domain features for an EEG-based pain measurement system. *Pages 114–115 of:* Dowman, R. (ed), *NEBC '07, IEEE 33rd Annual Northeast*.

Rollman, G. B. 1991. *Pain responsiveness*. Lawrence Erlbaum Associates. Pages 91–114.

Romero, S., Mananas, M. A., Clos, S., Gimenez, S. A. Gimenez S., & Barbanoj, M. J. A. 2003. Reduction of EEG artifacts by ICA in different sleep stages. *Pages 2675–2678 of:* Mananas, M. A. (ed), *Engineering in Medicine and Biology Society, 2003. Proceedings of the 25th Annual International Conference of the IEEE*, vol. 3.

Rupp, T., & Delaney, K. A. 2004. Inadequate analgesia in emergency medicine. *Annals of Emergency Medicine*, **43**(4), 494–503.

Sarlani, E., Farooq, N., & Greenspan, J. D. 2003. Gender and laterality differences in thermosensation throughout the perceptible range. *Pain*, **106**(1-2), 9–18.

Schandry, R., & Montoya, P. 1996. Event-related brain potentials and the processing of cardiac activity. *Biological Psychology*, **42**(1-2), 75–85.

Schandry, R., Sparrer, B., & Weitkunat, R. 1986. From the heart to the brain: A study of heartbeat contingent scalp potentials. *International Journal of Neuroscience*, **30**(4), 261 – 275.

Schlgl, A., Keinrath, C., Zimmermann, D., Scherer, R., Leeb, R., & Pfurtscheller, G. 2007. A fully automated correction method of EOG artifacts in EEG recordings. *Clinical Neurophysiology*, **118**(1), 98–104.

Schnitzler, A., & Ploner, M. 2000. Neurophysiology and functional neuroanatomy of pain perception. *Journal of Clinical Neurophysiology*, **17**(6), 592–603.

Searle, R. D., & Bennett, M. I. 2008. Pain assessment. *Anaesthesia & Intensive Care Medicine*, **9**(1), 13–15.

Shao, S., Shen, K., Ong, C. J., Wilder-Smith, E. P.V., & Li, X. 2009. Automatic EEG Artifact Removal: A Weighted Support Vector Machine Approach With Error Correction. *Biomedical Engineering, IEEE Transactions on*, **56**(2), 336–344.

Shen, K., Ong, C. J., Li, X., Zheng, H., & Wilder-Smith, E. P. V. 2007. A Feature Selection Method for Multilevel Mental Fatigue EEG Classification. *Biomedical Engineering, IEEE Transactions on*, **54**(7), 1231–1237.

Shen, K., Li, X., Ong, C. J., & Shao, S.and Wilder-Smith, E. P. V. 2008a. EEG-based mental fatigue measurement using multi-class support vector machines with confidence estimate. *Clinical Neurophysiology*, **119**(7), 1524–1533.

Shen, K., Ong, C. J., Li, X., & Wilder-Smith, E. P. V. 2008b. Feature selection via sensitivity analysis of SVM probabilistic outputs. *Machine Learning*, **70**(1), 1–20.

Shoker, L., Sanei, S., & Chambers, J. 2005. Artifact removal from electroencephalograms using a hybrid BSS-SVM algorithm. *Signal Processing Letters, IEEE*, **12**(10), 721–724.

Sindhwani, V., Bhattacharya, P., & Rakshit, S. 2001. Information Theoretic Feature Crediting in Multiclass Support Vector Machines. *In: Proc. 1st SIAM Int. Conf. Data Mining*.

Smith, K. 2007. Brain waves reveal intensity of pain. *Nature*, **450**(7168), 329.

Sternbach, R. A. 1968. *Pain: A Psychophysiological Analysis*. New York: Academic Press.

Straube, T., Schmidt, S., Weiss, T., Mentzel, H. J., & Miltner, W. H. 2009. Sex differences in brain activation to anticipated and experienced pain in the medial prefrontal cortex. *Hum Brain Mapp*, **30**(2), 689–98.

Sviderskaya, N., & Kovalev, A. 1996. Effect of unconscious interoceptive afferentation on the spatial organization of electrical activity in the human cerebral cortex. *Neuroscience and Behavioral Physiology*, **26**(6), 532–538.

Talbot, J. D., Marrett, S., Evans, A. C., Meyer, E., Bushnell, M. C., & Duncan, G. H. 1991. Multiple Representations of Pain in Human Cerebral-Cortex. *Science*, **251**(4999), 1355–1358.

Torquati, K., Pizzella, V., Babiloni, C., Gratta, C. Del, Penna, S. Della, Ferretti, A., Franciotti, R., Rossini, P. M., & Romani, G. L. 2005. Nociceptive and non-nociceptive sub-regions in the human secondary somatosensory cortex: An MEG study using fMRI constraints. *NeuroImage*, **26**(1), 48–56.

Tousignant-Laflamme, Y., Rainville, P., & Marchand, S. 2005. Establishing a Link Between Heart Rate and Pain in Healthy Subjects: A Gender Effect. *The Journal of Pain*, **6**(6), 341–347.

Tracey, I., & Mantyh, P. W. 2007. The cerebral signature for pain perception and its modulation. *Neuron*, **55**(3), 377–91.

Treede, R. D., Kenshalo, D. R., Gracely, R. H., & Jones, A. K. P. 1999. The cortical representation of pain. *Pain*, **79**(2-3), 105–111.

Turk, D. C., & Okifuji, A . 2001. *Pain terms and taxonomies of pain*. 3rd edn. Bonica's management of pain. Philadelphia: Lippincott Williams & Wilkins.

Uddin, L. Q., Kelly, A. M. C., Biswal, B. B., Margulies, D. S., Shehzad, Z., Shaw, D., Ghaffari, M., Rotrosen, J., Adler, L. A., Castellanos, F. X., & Milham, M. P. 2008. Network homogeneity reveals decreased integrity of default-mode network in ADHD. *Journal of Neuroscience Methods*, **169**(1), 249–254. doi: DOI: 10.1016/j.jneumeth.2007.11.031.

Urrestarazu, E., Iriarte, J., Alegre, M., Valencia, M., Viteri, C., & Artieda, J. 2004. Independent Component Analysis Removing Artifacts in Ictal Recordings. *Epilepsia*, **45**, 1071–1078.

Vapnik, V. N. 1995. *The Vicinal Risk Minimization Principle and the SVMs*. 2nd edn. New York: Springer.

Veerasarn, P., & Stohler, C. S. 1992. The effect of experimental muscle pain on the background electrical brain activity. *Pain*, **49**(3), 349–360.

Vigario, R., Sarela, J., Jousmiki, V., Hamalainen, M. A. Hamalainen M., & Oja, E. A. 2000. Independent component approach to the analysis of EEG and MEG recordings. *Biomedical Engineering, IEEE Transactions on*, **47**(5), 589–593.

Vigario, R. N. 1997. Extraction of ocular artefacts from EEG using independent component analysis. *Electroencephalography and Clinical Neurophysiology*, **103**(3), 395–404.

von Baeyer, C. L., Piira, T., Chambers, C. T., Trapanotto, M., & Zeltzer, L. K. 2005. Guidelines for the cold pressor task as an experimental pain stimulus for use with children. *The Journal of Pain*, **6**(4), 218–27.

Wall, P. D., & Melzack, R. 1999. *Textbook of pain*. 4th edn. Edinburgh New York: Churchill Livingstone.

Wallstrom, G. L., Kass, R. E., Miller, A., Cohn, J. F., & Fox, N. A. 2004. Automatic correction of ocular artifacts in the EEG: a comparison of regression-based and component-based methods. *Int J Psychophysiol*, **53**(2), 105–19.

Walsh, N. E., Schoenfeld, L., Ramamurthy, S., & Hoffman, J. 1989. Normative model for cold pressor test. *Am J Phys Med Rehabil*, **68**(1), 6–11.

Weisenberg, M.and Tepper, I., & Schwarzwald, J. 1995. Humor as a cognitive technique for increasing pain tolerance. *Pain*, **63**(2), 207–212.

Wendel, K., Vaisanen, O., Malmivuo, J., Gencer, N. G., Vanrumste, B., Durka, P., Magjarevic, R., Supek, S., Pascu, M. L., Fontenelle, H., & Grave de Peralta Menendez, R. 2009. EEG/MEG source imaging: methods, challenges, and open issues. *Comput Intell Neurosci*, 656092.

Wilder-Smith, O. H. G., Tassonyi, E., & Arendt-Nielsen, L. 2002. Preoperative back pain is associated with diverse manifestations of central neuroplasticity. *Pain*, **97**(3), 189–194.

Williamson, A., & Hoggart, B. 2005. Pain: a review of three commonly used pain rating scales. *Journal of Clinical Nursing*, **14**(7), 798–804.

Willis, W. D., & Westlund, K. N. 1997. Neuroanatomy of the pain system and of the pathways that modulate pain. *J Clin Neurophysiol*, **14**(1), 2–31.

Woestenburg, J. C., Verbaten, M. N., & Slangen, J. L. 1983. The removal of the eye-movement artifact from the EEG by regression analysis in the frequency domain. *Biological Psychology*, **16**(1-2), 127–47.

Wu, T. F., Lin, C. J., & Weng, R. 2004. Probability Estimates for Multi-class Classification by Pairwise Coupling. *J. Mach. Learn. Res.*, **5**, 975–1005.

Xu, X., Kanda, M., Shindo, K., Fujiwara, N., Nagamine, T., Ikeda, A., Honda, M., Tachibana, N., Barrett, G.and Kaji, R., Kimura, J., & Shibasaki, H. 1995. Pain-related somatosensory evoked potentials following CO2 laser stimulation of foot in man. *Electroencephalography and Clinical Neurophysiology/Evoked Potentials Section*, **96**(1), 12–23.

Zaslansky, R., Sprecher, E., Tenke, C. E., Hemli, J. A., & Yarnitsky, D. 1996a. The P300 in pain evoked potentials. *Pain*, **66**(1), 39–49.

Zaslansky, R., Sprecher, E., Katz, Y., Rozenberg, B., Hemli, J. A., & Yarnitsky, D.

1996b. Pain-evoked potentials: what do they really measure? *Electroencephalography and Clinical Neurophysiology/Evoked Potentials Section*, **100**(5), 384–391.

Zhang, Q., Manriquez, A. I., Medigue, C., Papelier, Y., & Sorine, M. 2006. An Algorithm for Robust and Efficient Location of T-Wave Ends in Electrocardiograms. *Biomedical Engineering, IEEE Transactions on*, **53**(12), 2544–2552.

Zhou, W., & Gotman, J. 2005. Removing Eye-movement Artifacts from the EEG during the Intracarotid Amobarbital Procedure. *Epilepsia*, **46**(3).

Zhu, Y. J., & Lu, T. J. 2010. A multi-scale view of skin thermal pain: from nociception to pain sensation. *Philosophical Transactions. Series A, Mathematical, Physical, and Engineering Sciences*, **368**(1912), 521–59.

Zimmer, C., Basler, H. D., Vedder, H., & Lautenbacher, S. 2003. Sex differences in cortisol response to noxious stress. *Clin J Pain*, **19**(4), 233–9.